Check for updates

ADVANCING EARTH AND SPACE SCIENCE

Reviews of Geophysics

COMMISSIONED MANUSCRIPT
10.1029/2022RG000770

A. D. Fraser and P. Wongpan contributed equally to this work.

Key Points:

- Antarctic landfast ice is a crucial but often overlooked part of the Antarctic coastal environment
- Our review draws together the body of work which is wide-ranging but tends to lack coordination
- Observation programs need to be expanded and coordinated, and models need to incorporate realistic landfast ice

Correspondence to:
A. D. Fraser,
adfraser@utas.edu.au

Citation:
Fraser, A. D., Wongpan, P., Langhorne, P. J., Klekociuk, A. R., Kusahara, K., Lannuzel, D., et al. (2023). Antarctic landfast sea ice: A review of its physics, biogeochemistry and ecology. *Reviews of Geophysics*, *61*, e2022RG000770. https://doi.org/10.1029/2022RG000770

Received 20 OCT 2022
Accepted 18 MAY 2023

© 2023 The Authors.
This is an open access article under the terms of the Creative Commons Attribution-NonCommercial License, which permits use, distribution and reproduction in any medium, provided the original work is properly cited and is not used for commercial purposes.

Antarctic Landfast Sea Ice: A Review of Its Physics, Biogeochemistry and Ecology

A. D. Fraser[1], P. Wongpan[1], P. J. Langhorne[2], A. R. Klekociuk[1,3], K. Kusahara[4], D. Lannuzel[5,6], R. A. Massom[1,3,6], K. M. Meiners[1,3,6], K. M. Swadling[1,5], D. P. Atwater[1,5], G. M. Brett[7], M. Corkill[5], L. A. Dalman[1,5], S. Fiddes[1], A. Granata[8], L. Guglielmo[9], P. Heil[1,3], G. H. Leonard[10], A. R. Mahoney[11], A. McMinn[5], P. van der Merwe[5], C. K. Weldrick[1], and B. Wienecke[3]

[1]Australian Antarctic Program Partnership, Institute for Marine and Antarctic Studies, University of Tasmania, Nipaluna/Hobart, TAS, Australia, [2]Department of Physics, University of Otago, Dunedin, New Zealand, [3]Australian Antarctic Division, Department of Climate Change, Energy, the Environment and Water, Kingston, TAS, Australia, [4]Japan Agency for Marine-Earth Science and Technology, Yokohama, Japan, [5]Institute for Marine and Antarctic Studies, University of Tasmania, Hobart, TAS, Australia, [6]ARC Australian Centre for Excellence in Antarctic Science, University of Tasmania, Hobart, TAS, Australia, [7]Gateway Antarctica, University of Canterbury, Christchurch, New Zealand, [8]Department of Chemical, Biological, Pharmaceutical and Environmental Sciences, University of Messina, Messina, Italy, [9]Stazione Zoologica Anton Dohrn, Naples, Italy, [10]National School of Surveying, University of Otago, Dunedin, New Zealand, [11]Geophysical Institute, University of Alaska Fairbanks, Fairbanks, AK, USA

Abstract Antarctic landfast sea ice (fast ice) is stationary sea ice that is attached to the coast, grounded icebergs, ice shelves, or other protrusions on the continental shelf. Fast ice forms in narrow (generally up to 200 km wide) bands, and ranges in thickness from centimeters to tens of meters. In most regions, it forms in autumn, persists through the winter and melts in spring/summer, but can remain throughout the summer in particular locations, becoming multi-year ice. Despite its relatively limited extent (comprising between about 4% and 13% of overall sea ice), its presence, variability and seasonality are drivers of a wide range of physical, biological and biogeochemical processes, with both local and far-ranging ramifications for the Earth system. Antarctic fast ice has, until quite recently, been overlooked in studies, likely due to insufficient knowledge of its distribution, leading to its reputation as a "missing piece of the Antarctic puzzle." This review presents a synthesis of current knowledge of the physical, biogeochemical and biological aspects of fast ice, based on the sub-domains of: fast ice growth, properties and seasonality; remote-sensing and distribution; interactions with the atmosphere and the ocean; biogeochemical interactions; its role in primary production; and fast ice as a habitat for grazers. Finally, we consider the potential state of Antarctic fast ice at the end of the 21st Century, underpinned by Coupled Model Intercomparison Project model projections. This review also gives recommendations for targeted future work to increase our understanding of this critically-important element of the global cryosphere.

Plain Language Summary Landfast ice (known more simply as fast ice) is sea ice that doesn't move horizontally, unlike pack ice. It can cover extensive regions of the Southern Ocean, and ranges in thickness up to several tens of meters. In many regions it melts or breaks out each summer, but can survive the melt season in others regions. Antarctic fast ice is critically important for a wide variety of coastal processes, and has far-reaching consequences for the Earth system, however our knowledge of it is limited. This first review of Antarctic fast ice provides a synthesis of the current state of knowledge, including its baseline properties and its major roles in key glaciological, oceanographic, atmospheric, biogeochemical and biological interactions and processes, highlighting its crucial and far-reaching importance. Antarctic fast ice is likely to reduce by the end of the 21st Century, in terms of its season length, thickness and possibly extent, but projections are highly uncertain due to a current lack of inclusion of fast ice in climate models. Observations of fast ice, including both ground- and satellite-based, should be coordinated and expanded to allow deeper understanding of this important part of the global cryosphere and Antarctic coastal environment.

1. Introduction and Motivation

Antarctic landfast sea ice ("fast ice") is sea ice that is fastened to icebergs grounded on the continental shelf, or fastened to the coastline itself (including ice shelf margins), for a specified minimum duration; 2 to 3 weeks is

a common criterion (Mahoney et al., 2007). Fast ice occurs on parts of the Antarctic continental shelf in narrow (generally up to 200 km wide) bands. In most regions, it forms in autumn and melts in spring/summer, but can remain throughout the summer melt season in certain locations, forming multi-year fast ice. Its presence, seasonality and variability have been acknowledged as key drivers of a wide range of physical, biological, and biogeochemical processes, with both local and far-ranging ramifications for the Earth system.

Fast ice also occurs in Arctic regions, where the primary attachment mechanisms are (a) by becoming landlocked within lagoons or coastal inlets; or (b) when parts of the sea ice directly contact the sea bed, thereby stabilizing the ice against advection due to winds, currents, and stresses within the ice field (Mahoney, 2018). In contrast to the Antarctic, where grounded icebergs are the primary attachment mechanism in most areas (Li et al., 2020; Massom, Hill, et al., 2001), iceberg-associated grounding is only common in isolated areas of the Arctic (C. Wang et al., 2020) due to the limited distribution of icebergs from Greenland's ice shelves and tidewater glaciers. Arctic fast ice is well-studied, with a breadth of indigenous knowledge (Eicken, 2010), extensive and regular in situ observations (e.g., Howell et al., 2016), coastal radar installations that monitor its dynamics (Mahoney et al., 2007), as well as a range of techniques to study its extent, trends, stability and other properties from satellite remote-sensing (e.g., Dammann et al., 2019; Mahoney et al., 2007; Segal et al., 2020; Selyuzhenok & Demchev, 2021; Y. Yu et al., 2014). Much less is known about its Antarctic counterpart, due in large part to its geographic isolation.

The existing literature focusing on Antarctic fast ice has highlighted its crucial roles in the fields of (a) glaciology, where it provides mechanical stability to vulnerable ice shelves and tongues (e.g., Massom et al., 2018) and responds rapidly to environmental forcing (e.g., Leonard et al., 2021); (b) physical oceanography, where it controls coastal polynya size and associated production of dense water (Fraser et al., 2019), modulates dissipation and transfer of tidal and wind energy (Inall et al., 2021), modifies on-shelf circulation (Kusahara et al., 2021), and is thought to influence rates of the globally-important Antarctic bottom water formation (Ohshima et al., 2013); (c) biogeochemistry, where it forms a seasonal reservoir of limiting nutrients, with the potential for ocean fertilization as it breaks up and drifts offshore (Grotti et al., 2005); and (d) ecosystems, where it provides a key substrate for early-season primary production (Meiners et al., 2018) fueling coastal marine food webs (and underpinning key ecosystem processes; Bluhm et al., 2017).

Despite its demonstrated importance, no recent study has synthesized this knowledge on a circum-Antarctic scale. Indeed, many of the key references in the field are regional in scope, and highlight marked regional variability in fast-ice distribution, trends (Fraser et al., 2021) and formation mechanisms (Giles et al., 2008). A comprehensive and up-to-date review of the importance and roles of Antarctic fast ice in the Earth system is a major aim of this work, in addition to considering the future of Antarctic fast ice throughout the 21st Century, and identifying priority areas for further research.

1.1. Historical Observations of Antarctic Fast-Ice Distribution

Perhaps the first detailed account of Antarctic fast-ice distribution (as well as factors influencing formation and breakup, covered in Section 4 here) is that of Wright and Priestley (1922), from the famed British Antarctic (*Terra Nova*) Expedition (1910–1913), where the fast-ice distribution of Victoria Land (western flank of the Ross Sea; ~165°E) was accurately mapped, and that of King Edward VII Land (eastern flank of the Ross Sea; ~140°W) was commented on for the first time. Their account also contained mention of multi-year fast ice, deformed and level fast ice, and the role of "stranded" (here referred to as "grounded") icebergs in stabilizing fast ice.

Early accounts of East Antarctic fast ice occur throughout the Soviet/Russian literature, but only brief details of these accounts are translated into English. Lutsenko and Timokhov (1977) describe the distribution of coastal polynyas and fast ice across East Antarctica, based on 1970–1972 satellite data, drawing particular attention to the fast ice occurring off Cape Darnley (~70°E). The role of grounded icebergs in stabilizing this fast ice feature (and others) was also recognized around this time (Fedotov et al., 1998; Lutsenko & Timokhov, 1977). Fedotov et al. (1998) also emphasize the role of sheltered embayments in harboring fast ice, and remark that level fast ice is predominant over rough fast ice, in agreement with more recent work (Giles et al., 2008), although both studies are limited in their spatio-temporal coverage. Fast-ice roughness is now thought to be determined by coastal configuration (Porter-Smith et al., 2021) and the degree to which (generally westward-advecting) pack ice can intercept dynamical barriers, such as glacier tongues and grounded icebergs (Fraser et al., 2012).

19449208, 2023, 2, Downloaded from https://agupubs.onlinelibrary.wiley.com/doi/10.1029/2022RG000770 by University of Adelaide Alumni, Wiley Online Library on [16/08/2023]. See the Terms and Conditions (https://onlinelibrary.wiley.com/terms-and-conditions) on Wiley Online Library for rules of use; OA articles are governed by the applicable Creative Commons License

Fedotov et al. (1998), reporting in English on the earlier work of Kozlovsky et al. (1977), remark in some detail on the distribution of fast ice around East Antarctica, based on a limited number of satellite images. They assert that November is the month of maximum fast ice extent, although more recent work indicates that maximum extent occurs in late September to mid-October, in most years (Fraser et al., 2012, 2021). Their estimate of maximum circum-Antarctic fast-ice extent for that time is 550,000 km^2, broadly in line with recent estimates (~601,000 km^2 on average; Fraser et al., 2021). We note, however, the existence of Argon spy satellite images showing a lack of wintertime fast ice near Dumont d'Urville Station (140°E) during 1963 (Massom et al., 2009), a region of persistent extensive wintertime fast ice since 2000 (Fraser et al., 2012), indicating that fast ice may have been less extensive in the past. Murphy et al. (1995) also suggest lower fast ice extent around the South Orkney Islands (45.5°W, 60.58°S) during the 1940s and 1950s, further indicating that present-day fast-ice extent may not be representative of conditions throughout the 20th Century.

1.2. Review Scope and Approach

No single previous publication has provided a broad synthesis of the state of our knowledge of Antarctic fast ice, and the important roles that it plays in the Earth system, although elements of wide-ranging reviews exist in the following publications:

- The aforementioned Fedotov et al. (1998) paper contained a synthesis of the earlier Soviet Antarctic fast-ice work, but as detailed, was limited in its temporal coverage;
- Massom, Eicken, et al. (2001) contains a section on snow on fast ice, but the section is brief due to limited observations at the time;
- Section 5.9.3 of Lubin and Massom (2006) contains an introduction to fast ice in both hemispheres, but the focus of this work is on various techniques for its remote-sensing (covered briefly in this review), rather than a synthesis of knowledge;
- a portion of the review of Antarctic sea-ice change and variability by Massom and Stammerjohn (2010) is dedicated to fast ice, however considerable new knowledge has been gained in the 13 years since its publication;
- Meiners et al. (2018) synthesized chlorophyll-*a* data from historical sea-ice cores, however the scope was relatively limited compared to the current review;
- Hoppmann et al. (2020) reviewed the state of the literature on platelet ice, a form of ice crystals which forms in situ underneath ice shelves and accretes onto the base of fast ice (i.e., their review was focused on this aspect of fast ice); and
- Fraser et al. (2021) analyzed the first high spatio-temporal resolution, long time series (2000–2018) data set of Antarctic fast-ice extent, giving new circumpolar perspectives on its persistence, seasonality and trends, but its scope was limited to the (horizontal) extent of fast ice.

As such, there is a need for a publication that presents an up-to-date, complete (i.e., covering all known work) synthesis of the scientific knowledge of Antarctic fast ice. While aiming to present a broad review, we limit the scope to the following elements: Antarctic fast-ice formation, extent, and drivers and physical interactions (both atmospheric and oceanic); biogeochemistry; association with primary production; and its role as a habitat for grazers (excluding krill). Although there has been considerable work undertaken on the association between fast ice and higher trophic levels (e.g., Ainley et al., 2015; Emmerson & Southwell, 2022; Labrousse et al., 2021; Massom et al., 2009), we limit this review to consideration of no organisms higher than plankton grazers. Similarly, the influence of fast ice on Antarctic logistics (e.g., shipping, aviation) is not considered here; however we do cover fast-ice mechanical properties as they relate to ice strength. Anchor ice, which is a covering of ice crystals attached to the sea floor (Hoppmann et al., 2020), is somewhat related to both fast ice and platelet ice, but not covered here since a relatively recent dedicated review exists (Mager et al., 2013), and it is thought to be limited to one region of Antarctica: the southern Ross Sea (Mager et al., 2013).

Given the broad scope of this study, we have adopted elements of a systematic review in order to attempt to capture all known literature. Our review aims to be a qualitative synthesis of all knowledge within the scope set out above. More specifically:

- Within each major section, we perform a *Scopus* literature search using keywords (search strings given in Appendix A) designed to find most relevant publications;
- in addition, we relied on section-leader expert knowledge to identify missing publications;

19449208, 2023, 2, Downloaded from https://agupubs.onlinelibrary.wiley.com/doi/10.1029/2022RG000770 by University of Adelaide Alumni, Wiley Online Library on [16/08/2023]. See the Terms and Conditions (https://onlinelibrary.wiley.com/terms-and-conditions) on Wiley Online Library for rules of use; OA articles are governed by the applicable Creative Commons License

- many irrelevant publications are also returned in the search (e.g., the publication may have a passing reference to fast ice, resulting in a "false hit")—these were manually filtered out by section leaders;
- "gray literature" was excluded; as were publications which had not completed peer-review (e.g., voyage reports and "Discussions" papers—unless their inclusion was deemed essential by section leaders); and
- new material published after the original literature search was added during the review stage at the discretion of the leader of each section.

The paper is structured around seven major sections (Section 2 through Section 8), covering fast-ice physical properties and growth (Section 2); its large-scale distribution and seasonality via remote sensing (Section 3); its atmospheric (Section 4) and oceanic (Section 5) interactions, its biogeochemical interactions (Section 6), and its roles in primary (Section 7) and secondary production (Section 8). We then turn our attention to the potential future of these fast-ice aspects, based on Coupled Model Intercomparison Project (CMIP) Phase 6 projections to 2100 (Section 9). Section 10 then presents concluding remarks, with an emphasis on the gaps in the research and how these might best be filled.

2. Fast-Ice Growth, Properties and Seasonality

In this section, we provide an overview of the progression of physical properties of Antarctic fast ice, from initial growth under various atmospheric and oceanic conditions to the evolution of its thickness, and finally its breakup/decay. We also emphasize the important differences in physical properties between level (or "smooth") fast ice, which forms in sheltered locations such as in the lee side of promontories (Giles et al., 2008), and deformed ("rough") fast ice which forms when pack ice dynamically interacts in a way that renders it stationary, deforming in the process. We also consider snow on fast ice. For the physical, mechanical and optical properties of sea ice in general we refer the reader to reviews of Petrich and Eicken (2017), Timco and Weeks (2010), and Perovich (2017), respectively, and concentrate on properties that are particular to Antarctic fast ice. Finally, we consider the influence of physical properties on sea-ice algae, discuss progress in the simulation of fast-ice properties, and highlight the crucial gaps remaining in the field.

2.1. Growth, Evolution and Decay

2.1.1. Thermodynamic Formation: Level Fast Ice

Around the Antarctic coast, sea-ice growth is mainly the result of heat loss from the ocean to the atmosphere. As mentioned above, fast ice can be partitioned into level or rough fast ice (Figure 1), based on whether it forms thermodynamically/in situ (producing level fast ice) or dynamically (i.e., either from level fast ice that is broken and redistributed, or from pack ice which becomes fastened due to dynamic interactions, generally forming rough fast ice). Either form can be subsequently thickened by a number of processes.

Here we first consider the thermodynamic growth of level fast ice. In this case, initial ice formation is a relatively thin skin between the ocean and atmosphere over which there is considerable vertical heat transfer. If the surface of the ocean is disturbed by wind and waves, a soupy layer of millimeter-scale frazil ice crystals is first to form. If prevailing conditions are suitable (i.e., the layer of frazil crystals is not advected away from the coast), then fast ice grows as a thin (up to about 10 cm thick) layer of granular ice. Despite the initial turbulent conditions, this consolidation of granular ice can then form level fast ice. Isolated from wind-driven upper-ocean turbulence by this granular ice layer, columnar ice growth soon occurs at the base of the granular layer, resulting in a stratigraphy of "granular over columnar ice" which is frequently observed in level fast ice (Tang et al., 2007).

Columnar ice is also the usual mode of fast-ice thermodynamic thickening in relatively calm waters where oceanic heat flux is positive; defining heat flux as positive when it flows to the sea ice from the ocean. Near the fast-ice edge where stormy conditions prevail, frazil ice continues to be generated and the newly-formed fast-ice cover ice is subject to deformation, that is, ridging and rafting. Here, granular ice can occupy most of the 1–2 m thickness of the fast-ice cover (e.g., Veazey et al., 1994).

Once the ice has thickened sufficiently to obtain a positive freeboard (i.e., the upper ice surface lies above the water level), falling snow may accumulate (and remain relatively dry) on the upper surface. There, the snow may act as an insulating layer on top of the ice, or lead to snow-ice formation (Ushio, 2006). The latter takes place when the overlying snow cover reaches sufficient thickness to depress the ice surface to below the water level,

19449208, 2023, 2, Downloaded from https://agupubs.onlinelibrary.wiley.com/doi/10.1029/2022RG000770 by University of Adelaide Alumni, Wiley Online Library on [16/08/2023]. See the Terms and Conditions (https://onlinelibrary.wiley.com/terms-and-conditions) on Wiley Online Library for rules of use; OA articles are governed by the applicable Creative Commons License

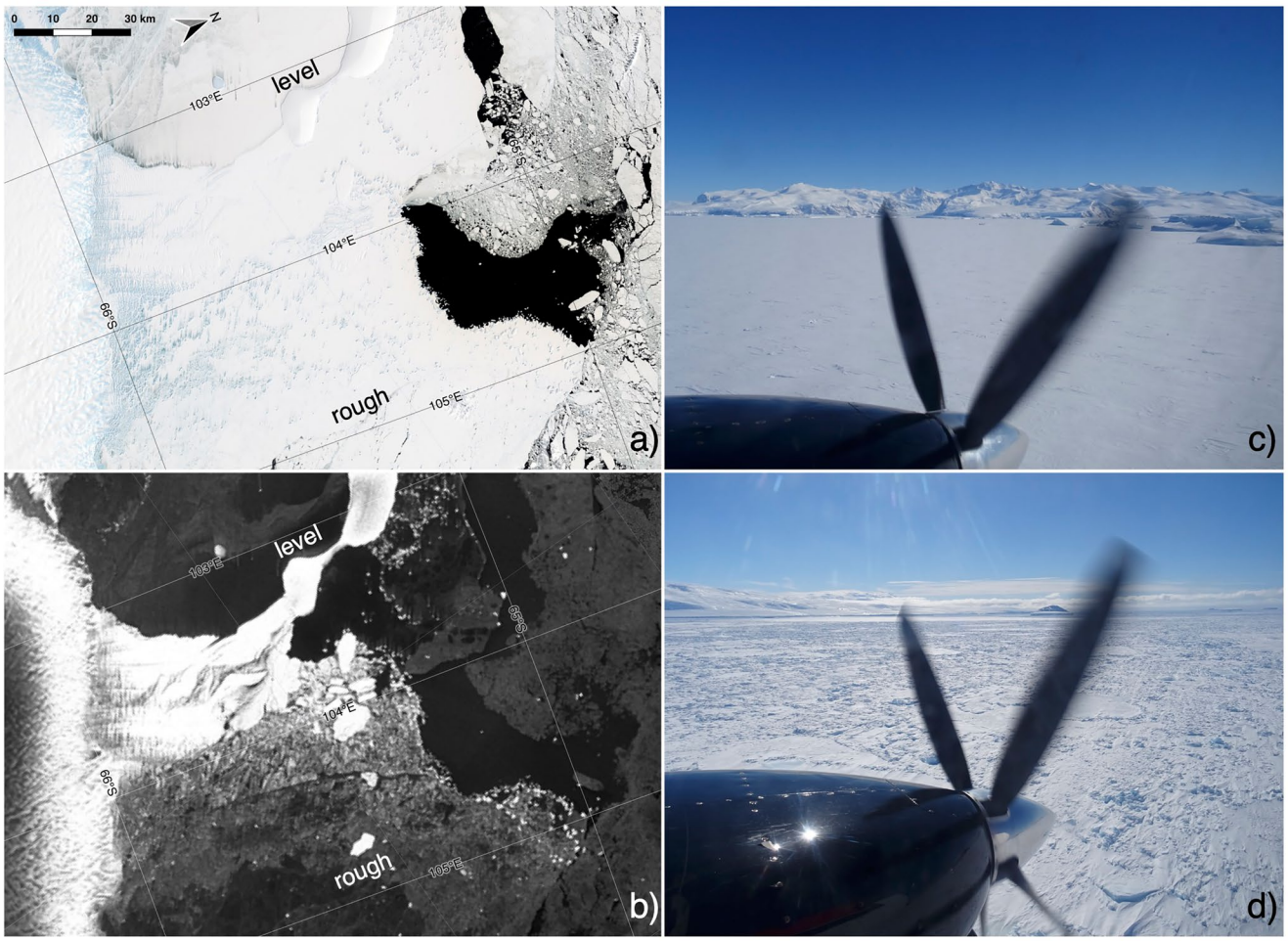

Figure 1. Satellite imagery and airborne photographs of level and rough fast ice. (a) Landsat 8 satellite image showing Bowman Island (103.1°E, 65.25°S) and the surrounding icescape on 28 November 2020. Note that the "rough" patch in the visible image only looks rough (at this scale) because of the presence of numerous grounded icebergs. (b) Similar to (a) but with synthetic aperture radar imagery (30 November 2020). Level and rough fast ice can be distinguished based on radar backscatter (higher for rough ice, creating a "brighter" radar signature). (c) Level fast ice in the vicinity of Parker Ice Tongue (166.4°E, 73.9°S), photographed from aircraft on 11 November 2017 (Credit: Christian Haas). (d) Rough fast ice in Moubray Bay (170.9°E, 72.0°S), photographed from an aircraft on 11 November 2017 (Credit: Christian Haas).

thus leading to flooding of the snow, forming slush, which subsequently freezes. Flooding can also occur if the ice temperature and salinity exceed critical thresholds that allow brine channels within the ice matrix to interconnect (generally above −5°C; Golden et al., 1998). Fast ice and its snow cover evolve together as a coupled sea ice-snow system (see Section 2.2) and their evolution can be monitored using ice mass balance buoys that measure the vertical temperature profile of the ice, its growth and melt, and snow accumulation and ablation (Richter-Menge et al., 2006; Richter et al., 2022).

Note that especially during austral autumn the thin fast-ice sheet may be easily broken out, for example, mostly due to encounters with passing cyclonic systems (Heil, 2006). After any early-season breakout and reformation events, the seasonal evolution of fast ice from autumn through winter is typically driven by high thermodynamic growth rates until the insulating properties of the ice and the overlying snow reduce the conductive heat flux through the ice column. Maximum annual fast-ice thickness for thermodynamically grown, first-year fast ice is typically reached toward the end of spring, when solar warming reduces the overlying protective layer of snow as well as weakening the gradient of the vertical conductive heat flux sufficiently to slow or cease thermodynamic growth at the base of the ice. The annual maximum fast-ice thickness displays large interannual variability (Heil, 2006) due to considerable variability in snow thickness and the amount of platelet ice accretion (Section 2.1.2).

19449208, 2023, 2, Downloaded from https://agupubs.onlinelibrary.wiley.com/doi/10.1029/2022RG000770 by University of Adelaide Alumni, Wiley Online Library on [16/08/2023]. See the Terms and Conditions (https://onlinelibrary.wiley.com/terms-and-conditions) on Wiley Online Library for rules of use; OA articles are governed by the applicable Creative Commons License

19449208, 2023, 2, Downloaded from https://agupubs.onlinelibrary.wiley.com/doi/10.1029/2022RG000770 by University of Adelaide Alumni, Wiley Online Library on [16/08/2023]. See the Terms and Conditions (https://onlinelibrary.wiley.com/terms-and-conditions) on Wiley Online Library for rules of use; OA articles are governed by the applicable Creative Commons License

2.1.2. Contribution of Platelet Ice to the Fast-Ice Cover

Recently it has been shown that ocean temperatures slightly below freezing are widespread in the surface waters of the Southern Ocean, with up to 6% of all recorded oceanographic profiles displaying in situ supercooling (Haumann et al., 2020). The formation of platelet ice, one result of this supercooling, is therefore a commonly-encountered feature of fast ice near marine-terminating continental ice around the coastline of Antarctica. Below we give a brief outline of its formation and properties, drawing on a recent extensive review of platelet ice and its role as a habitat by Hoppmann et al. (2020).

Melting/dissolution at the base of ice shelves cools and freshens the ice shelf-ocean boundary layer, producing a water mass with a potential temperature below the surface freezing point (Foldvik & Kvinge, 1974; Jacobs et al., 1985), called Ice Shelf Water (ISW; Figure 11). If the ISW ascends to shallower depths, the rise in its pressure-dependent freezing point may force it to become supercooled in situ, causing frazil ice crystals to persist in the water column. These ice crystals may be deposited under the ice shelf (e.g., Tison et al., 1998) and, where they can accrete to the ice-shelf base as "marine ice" (Galton-Fenzi et al., 2012). If ocean currents are favorable, they are also carried out from the ice shelf cavity and collect beneath adjacent fast ice (e.g., Gow et al., 1998; Günther & Dieckmann, 1999; N. J. Robinson et al., 2014; Tison et al., 1998). If they continue to be immersed in supercooled water, the crystals can grow (e.g., Wright & Priestley, 1922). This is most apparent close to the sea ice-water interface where pressure-induced in situ supercooling is greatest (Leonard et al., 2006, 2011). The frazil crystals may form a sub-ice platelet layer (SIPL): a porous and friable layer in an evolving state of consolidation (Crocker & Wadhams, 1989b; Moreçki, 1965). The presence of an SIPL increases basal roughness and hence drag at the underside of sea ice (McPhee et al., 2016; N. J. Robinson et al., 2017). Particle scavenging during the ascent of the buoyant frazil crystals, combined with their large surface area and the ease of nutrient exchange in the porous SIPL, means that this habitat harbors some of the highest concentrations of sea-ice algae on Earth (Arrigo et al., 2010).

Modeling has shown that supercooling alone is not sufficient for the formation of an SIPL (Dempsey et al., 2010; Wongpan et al., 2021). In addition, a critical flux of ice crystals from the ocean must be exceeded, and this flux depends on the growth rate of the solid, upper part of the sea ice (and hence the thickness of its snow cover); that is, an SIPL only forms when the conductive heat flux to the atmosphere is sufficiently low, otherwise the frazil crystals are subsumed into the regular columnar ice growth at the base. This concept has been confirmed by observation (Gough et al., 2012; Mahoney et al., 2011). The ice becomes consolidated (termed incorporated platelet ice) when the interstitial water between the crystals of the SIPL freezes (Gow et al., 1998; I. J. Smith et al., 2001) and this process allows consolidated ice to become thicker than it would be in the absence of platelet ice (Jeffries et al., 1993). An SIPL is less dense than water but denser than consolidated ice, so that its presence also alters the hydrostatic relationship between sea ice freeboard and thickness, influencing satellite altimeter determination of sea-ice thickness (S. Arndt et al., 2020; Price et al., 2014).

2.1.3. Dynamic Thickness Redistribution: The Formation of Rough Fast Ice

Other processes that can lead to ice thicknesses exceeding thermodynamic values include rafting and ridging, otherwise known as dynamic thickness redistribution. In contrast to "planar sheets" of level fast ice, ice rubble can pile up into linear pressure ridges or a rubble field to become rough fast ice, provided it remains attached to the coast or icebergs grounded offshore (Figure 2).

Giles et al. (2008) estimate using remote sensing that 33% of the area of East Antarctic fast ice in 1997–1999 was rough, indicating that deformation is a major determinant of overall fast-ice volume (assuming their estimated values of 1.7 and 5.0 m for smooth and rough fast ice, respectively), and providing strong rationale for studies of rough fast ice to be prioritized. Recently Langhorne et al. (2023) confirmed the pervasiveness of deformed fast ice in the western Ross Sea where rough ice occupied 50% of the volume of a 700 km airborne electromagnetic (AEM) thickness transect. The rough ice had a modal thickness of 3.3 m, while the level ice was 2.0 m. Near Inexpressible Island in the Ross Sea (163.7°E, 74.9°S), the dynamic formation of rough fast ice up to 3–4 m thick was observed after pack ice was blown into a small bay after almost 3 days of persistent onshore winds (Zhai et al., 2019). The roughness of the underside of rough fast ice is also greater than that of level ice, which can affect the under-ice drag coefficient and thus the degree of ocean mixing just below the fast ice (Inall et al., 2021).

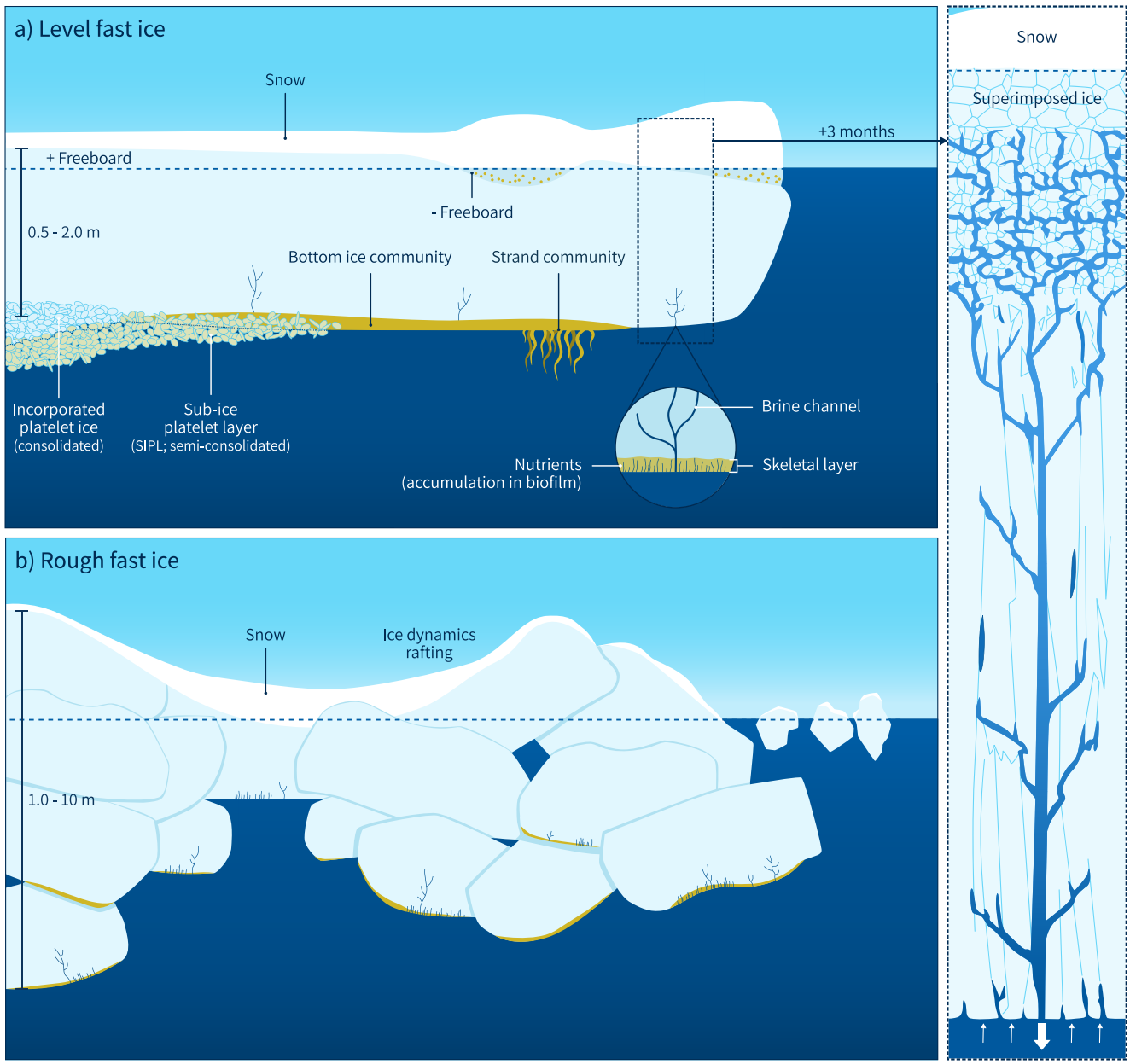

Figure 2. Schematic of vertical cross sections of Antarctic fast ice showing (a) level fast ice, and (b) rough fast ice. The ice shown represents an early austral spring case. In rough fast ice, biological material is assumed to exist despite a lack of sufficient in situ observations. The right-hand panel is an enlargement of the physical microstructure of a section of ice from panel (a), focusing on a brine drainage channel; here, ice is advanced in time by ~3 months and no biology is shown. Note that the freeboard can be positive (above) or negative (below sea level) depending on the thickness (hence weight) of the overlying snow cover.

2.1.4. Multi-Year Fast Ice

First-year sea ice is sea ice of not more than one winter's growth. If it does not melt completely in the summer, the remainder will gain more ice mass in the following winter, and becomes classed as second-year ice (and then multi-year sea ice in the following year). Due to the coarse resolutions of gridded products (e.g., Melsheimer et al., 2022) it is difficult to discriminate between second-year and multi-year ice. Hence only the latter term will be used herein. Multi-year fast ice occurs in sheltered embayments and anchored within and upstream of fields of icebergs grounded on banks/shoals up to ~400 m deep (Fraser et al., 2021; Giles et al., 2008). A transition from annual to multi-year fast ice has been observed to include additional thermodynamic growth and an increase in ice thickness from 2 to 3 m in the second year (Remy et al., 2007). Multi-year fast ice attached to the eastern edge

19449208, 2023, 2, Downloaded from https://agupubs.onlinelibrary.wiley.com/doi/10.1029/2022RG000770 by University of Adelaide Alumni, Wiley Online Library on [16/08/2023]. See the Terms and Conditions (https://onlinelibrary.wiley.com/terms-and-conditions) on Wiley Online Library for rules of use; OA articles are governed by the applicable Creative Commons License

of Mertz Glacier Tongue (MGT) prior to its 2010 calving (Leane & Maddison, 2018) had been estimated to be at least 25 years old and between 10 and 55 m thick (Massom et al., 2010). Such thickness is far in excess of that expected from heat loss to the atmosphere alone, indicating likely contributions from platelet accretion and/or snow-ice formation. The transition from meteoric ice to fast ice can be ill-defined. In a similar way to rifts within an ice shelf (Khazendar & Jenkins, 2003; Larour et al., 2021), gaps between icebergs may fill with platelet ice from below and snow from above, gluing the ice bodies together and causing phenomena such as flooding and snow ice formation. Such an ice mélange may persist for decades.

In multi-year fast ice without substantial snow-ice contribution, brine drainage during the warmer summer months causes the upper half of the ice to be fresher with a lower brine volume, which confers enhanced mechanical strength (Kharitonov & Borodkin, 2022; Remy et al., 2007). The contribution of snow-ice to the thickness of multi-year fast ice can be considerable (Kawamura et al., 1997; Kusahara et al., 2021), with estimates of up to 57% in ice at least three years old in Nella Fjord (76.35°E, 69.4°S; Tang et al., 2007) and 100% in parts of ∼2.5 m thick, 10-year-old ice in McMurdo Sound (165°E, 77.5°S; Gough et al., 2013).

2.1.5. Breakup and Decay

From late spring until summer, fast ice breaks up and decays due to warming air temperatures and higher radiation combined with ocean waves and winds. Unlike fast-ice melt in the Arctic (Petrich & Eicken, 2017), melt ponds are rarely observed in Antarctica. In the austral summer the penetration of solar radiation can cause internal melting to produce gap layers below the snow and ice surface, causing decay and loss of fast ice mechanical strength (e.g., Zhao et al., 2022). However, the annual loss of the fast ice is largely due to breakout (i.e., fast ice becomes detached from the coastline or grounded icebergs, thereby becoming pack ice) rather than complete in situ melt, especially once the receding pack ice no longer provides mechanical (Heil, 2006) or thermodynamic (S. Arndt et al., 2020) protection to fast ice (i.e., by preventing solar absorption and heating of the upper water column due to the presence of adjacent, high-albedo pack ice). Ephemeral mid-season breakouts can occur in conjunction with storms (Heil, 2006; Leonard et al., 2021), particularly in regions where fast ice relies on tensile strength for stability (i.e., in deeper-water regions with few grounded icebergs; Massom et al., 2009). In some regions it is predicted that wind-induced tensile failure is the most likely mode of fast-ice fracture over most of the year (Crocker & Wadhams, 1989a).

However the advent of summer, and the retreat of the pack ice, subjects the fast-ice cover to ocean swells (Crocker & Wadhams, 1989a; Langhorne et al., 1998; Ushio, 2006). These waves attenuate as they travel into the fast-ice cover (e.g., Voermans et al., 2021), so they have their largest amplitude close to the fast-ice edge, making it most likely that break-up will be initiated there. A comprehensive review of sea ice (including fast ice) and its interactions with ocean waves is provided by Squire (2020). In summary, there are many factors affecting fast-ice break-up, extent and frequency, for example, long-term atmospheric variations, effects of ocean swell and surface snow melting (Crocker & Wadhams, 1989a; Langhorne et al., 1998; Ushio, 2006), and these environmental aspects are expanded upon in Sections 4 and 5 of this review.

2.2. Snow on Fast Ice

Snow is a crucial element of the Antarctic fast-ice system. The thermal conductivity of snow is almost an order of magnitude less than sea ice (Maykut & Untersteiner, 1971), so its accumulation reduces the conductive heat flux from the ocean to the atmosphere, slowing ice growth rates. Snow accumulation can also lead to the thickening of the ice cover through snow–ice formation (Maksym & Markus, 2008). Critically, its presence on the ice surface significantly increases the albedo of the fast ice cover (Brandt et al., 2005; Hoppmann, Nicolaus, Paul, et al., 2015).

The transport and metamorphism of snow on fast ice are the result of atmospheric forcing from the marine and the continental systems. The latter is marked by katabatic winds, a persistent and highly unidirectional gravity wind funnelled downslope off the ice sheet by the local orography (Huot et al., 2021). Winds are a key determinant of the thickness distribution of snow on fast ice, on the scale of meters to tens of kilometers, with localized thickening in the form of both dunes and sastrugi (Filhol & Sturm, 2015). As opposed to pack ice, which may rotate in response to forcing from the surface ocean or atmospheric stress, fast ice is fixed in place, so the snow cover is especially prone to being shaped through exposure to the unidirectional katabatic winds encountered around the Antarctic coast. For example, the initial stage of snow redistribution exhibits snow ridges with two tails that

19449208, 2023, 2, Downloaded from https://agupubs.onlinelibrary.wiley.com/doi/10.1029/2022RG000770 by University of Adelaide Alumni, Wiley Online Library on [16/08/2023]. See the Terms and Conditions (https://onlinelibrary.wiley.com/terms-and-conditions) on Wiley Online Library for rules of use; OA articles are governed by the applicable Creative Commons License

face downwind separated by a steep slipface. Barchan dunes are the initial feature of dune formation, where they are associated with the transport of fresh snow by cyclones (Kuznetsov, 1960). These transient dunes tend to migrate under steady wind stress, that is, by katabatic winds, while on pack ice, barchans are more stable due to the wind-packing of snow and formation of internal layers (Massom, Eicken, et al., 2001).

While barchan dunes form due to a complex combination of both snow deposition and erosion, sastrugi describe snow features that result purely from erosion acting on wind-packed snow (Filhol & Sturm, 2015). Sastrugi are defined by their steep slopes facing the wind and gentle slopes on the opposing side that create sets of furrows. Importantly these transitional features of the snow cover evolution cause variations in the snow depth, with consequences for the thermal balance due to increased lateral heat fluxes through the snow and, importantly, an increase in the average thermal conductivity of snow (Kochanski et al., 2021).

The first few kilometers of fast ice from the shore tend to be relatively snow-free, especially in regions of persistent katabatic outflow (Allison, 1989; Fedotov et al., 1998; Kawamura et al., 1995). Beyond this, the fast ice may carry a substantial snow cover, due to both redistribution from katabatic winds and extensive precipitation from synoptic-scale systems (Heil, 2006; Petrov, 1967). It is not uncommon for the snow load to depress the ice freeboard below sea level, giving rise to flooding and, if temperatures permit, the formation of snow ice (Kawamura et al., 2006). Kawamura et al. (1997) further noted the presence of superimposed ice, which forms when meltwater percolating down through the snow column refreezes on contact with the fast-ice surface into an impermeable layer of ice with a polygonal structure. Superimposed ice may enhance the mechanical strength of fast ice in summer (Massom, Eicken, et al., 2001; Section 2.3.2 here), while also inhibiting ice-atmosphere gas exchange (Nomura et al., 2013). When unusually large snow accumulation occurred in the 1991–1992 season, fast-ice thickness growth was relatively limited in winter but more substantial in summer—the latter due to snow-ice formation. Later in the Antarctic fast-ice season, rotting near the upper surface (Heil et al., 1996) is associated with snow-free ice, while snow dunes and other remaining snow cover prevent or at least delay the near-surface melt of the fast ice. Ushio (2006), for example, draw a relationship between unusually early fast-ice breakup in 1997–1998 and relatively shallow snow coverage.

Systematic snow redistribution may occur in some regions, such as Lützow-Holm Bay where geostrophic northeasterly winds transport snow across the fast ice and preferentially redistribute it around 20–30 km from the eastern shore of the bay (Kawamura et al., 1995; Uto et al., 2006). As a consequence of this, snow depth and ice thickness both decrease toward the shore, which may be due to less snow preventing snow ice or superimposed ice formation in this region characterized by considerable snow-ice contribution to thickness (Kawamura et al., 1997). In addition, due to the higher absorption of solar radiation in regions of low snow cover, combined with the thinner ice in these regions, isolated pockets of complete fast-ice melt occur during summer (Uto et al., 2006).

Long-term fast-ice monitoring has been undertaken at several Antarctic coastal sites, either to support logistical operations or as part of scientific studies. In the lead-up to the 2007 International Polar Year, the science-driven Antarctic Fast Ice Network (AFIN) was established to monitor primary variables of ice- and snow thickness, and fast-ice freeboard and extent. A range of observing techniques including autonomous observatories are used. Recently the World Meteorological Organization's Global Cryosphere Watch called for sustained and consistent sea-ice and fast-ice observations, especially in the Southern Ocean. The challenge remains in sustainably obtaining standardized quality measurements of crucial fast-ice variables (Heil, Gerland, & Granskog, 2011). Observations of the distribution of snow thickness continue to be carried out, largely linked to AFIN, including in Atka Bay (8°W; S. Arndt et al., 2020), off Mawson (62.9°E, 67.6°S), Zhongshan (76.4°E, 69.4°S), Davis (78°E, 68.6°S) and Casey (110.5°E, 66.3°S) stations, and in McMurdo Sound (Brett et al., 2020; Price et al., 2014, 2019). The AFIN site off Davis Station has been adopted as a CryoNet observing site by the World Meteorological Organization's Global Cryosphere Watch.

2.3. Fast-Ice Physical Properties and Their Seasonality

2.3.1. Physical Properties

The physical properties of fast ice depend upon ocean salinity, temperature gradient during ice formation and formation rate, as well as ice composition and age. Consequently, the fundamental variables defining the fast-ice state are the ice temperature and salinity profiles, the fraction of brine and air (by volume) and with these its permeability, density, thermal conductivity, and crystal stratigraphy including c-axis alignment. In this section

19449208, 2023, 2, Downloaded from https://agupubs.onlinelibrary.wiley.com/doi/10.1029/2022RG000770 by University of Adelaide Alumni, Wiley Online Library on [16/08/2023]. See the Terms and Conditions (https://onlinelibrary.wiley.com/terms-and-conditions) on Wiley Online Library for rules of use; OA articles are governed by the applicable Creative Commons License

we refer the reader to the review of Petrich and Eicken (2017) for the physical properties of sea ice in general, and focus on the properties of ice types that cause Antarctic fast ice to be distinctive, such as snow ice or platelet ice.

Sea ice is a complex medium composed of pure ice lamellae, with all the salt in brine inclusions that are either connected or discrete, depending on temperature (generally connected for temperature greater than −5°C; see the review by Petrich & Eicken, 2017). Brine drainage channels are liquid conduits that extend through the ice, allowing gravity-driven brine drainage (Figure 2a). Such channels form naturally due to buoyancy-driven convection in the porous array of ice crystals bathed in dense salty brine. At the ice–ocean interface, heavy and salty brine is rejected from the sea ice structure and replaced by the fresher and lighter seawater from the underlying water column through brine convection (Figure 2).

The brine and air fraction, or porosity, of fast ice is governed by its temperature and bulk salinity, where the salinity of incorporated platelet ice is only very subtly different from the salinity of columnar ice (Gough et al., 2012). Sea-ice permeability (defined as the extent to which connected pores within a material permit liquid flow) can be calculated from the porosity (Freitag, 1999), and Wongpan, Hughes, et al. (2018) show, using temperature profiles of fast ice in McMurdo Sound, that the mean permeabilities of columnar and incorporated platelet ice are indistinguishable.

In general, air also exists in pockets within sea ice. The density of sea ice is a function of temperature and the enclosed volumes of air and brine, that is, its total porosity (e.g., Petrich & Eicken, 2017). In the first-year fast ice of McMurdo Sound, Price et al. (2014) measured density to be between 900 and 925 kg m^{-3}, while the observational record from the AFIN site at Davis Station estimates the fast-ice density to be just under 900 kg m^{-3} at the onset of austral spring (Heil, Massom, et al., 2011). In perennial, low salinity, fast ice in the Gulf of Transcription (East Antarctica) lower densities (down to 680 kg m^{-3}) have been found (Kharitonov & Borodkin, 2022).

Total porosity (air plus brine), which can be empirically calculated from measurements of sea-ice density, bulk salinity and temperature (Cox & Weeks, 1986), is also a controlling parameter for the thermal properties of fast ice. For example, using in situ temperature profiles of fast ice in McMurdo Sound as one of their sources, Pringle et al. (2007) derived a widely-used empirical equation for sea ice thermal conductivity, expressed in terms of ice temperature, bulk salinity and density.

2.3.2. Mechanical Properties

Sea-ice thickness determines most fundamental mechanical properties of a floating fast-ice cover. For example, thickness influences the load that can be supported (its bearing capacity), the ability of an icebreaker to make safe passage through the ice (Timco & Weeks, 2010; Weeks, 2010), and the ability of the ice to withstand incident ocean waves without fracturing (Crocker & Wadhams, 1989a; Langhorne et al., 2001). To predict the response of a fast-ice cover, knowledge of mechanical properties (tensile, flexural, shear, uni-axial compression, and multi-axial compression strength, borehole strength, failure envelope, creep, elastic and strain modulus, Poisson's ratio, fracture toughness, fatigue or friction) is also needed, with the requisite knowledge of parameters depending upon the stress configuration and mechanical problem under investigation. In addition to the thickness, the volume and geometry of the brine and air inclusions in sea ice are the primary controls on these mechanical properties (Weeks, 2010). The volume of inclusions is determined by the brine and air porosity, with porosity (or its square root) most frequently being used as the independent variable to characterize changes in mechanical parameters through the growth/decay cycle (Timco & Weeks, 2010). In turn, porosity is found from sea-ice density, bulk salinity and temperature (Cox & Weeks, 1986). The geometry of inclusions is determined by microstructure, but is believed to be of lesser influence (Timco & Weeks, 2010). The rate of loading or deformation rate also matters. In-depth reviews of the mechanical and engineering properties of sea ice are given in Weeks (2010) and Timco and Weeks (2010).

As discussed in Section 2.1.2, the presence of platelet ice and snow ice distinguish Antarctic fast ice from its Arctic counterpart. Very recent observations suggest that the mechanical strength of snow ice is much less than that of congelation ice (Q. Wang et al., 2022). These observations of flexural strength and uniaxial compressive strength were made on small samples of congelation ice and snow ice collected in Prydz Bay (East Antarctica) and tested in the laboratory at differing rates, to separate ductile and brittle behavior. As discussed in Section 2.1.2, incorporated platelet ice is only very subtly different in salinity and permeability from columnar ice (Gough et al., 2012; Wongpan, Hughes, et al., 2018). Thus the mechanical properties of incorporated platelet

19449208, 2023, 2, Downloaded from https://agupubs.onlinelibrary.wiley.com/doi/10.1029/2022RG000770 by University of Adelaide Alumni, Wiley Online Library on [16/08/2023]. See the Terms and Conditions (https://onlinelibrary.wiley.com/terms-and-conditions) on Wiley Online Library for rules of use; OA articles are governed by the applicable Creative Commons License

ice are expected to be very similar to those of columnar sea ice. No data on mechanical properties of the high porosity SIPL have been published (Hoppmann et al., 2020).

There are a handful of mechanical property measurements performed specifically on Antarctic fast ice, for example, the recent snow-ice study of Q. Wang et al. (2022) on East Antarctic fast ice. Urabe and Inoue (1988) sampled fast ice in Lützow-Holm Bay and found that crystallographically it was similar to that of the Arctic, comprising granular and columnar ice. The fracture toughness of this fast ice was shown to depend on grain size, while compressive strength varied as the square root of brine and air porosity (Urabe & Inoue, 1988). Flexural strength and fatigue measurements of the first-year fast ice in McMurdo Sound were made by subjecting cantilever beams to repeated bending with zero mean stress (e.g., Haskell et al., 1996; Langhorne et al., 1998, 1999). These beams were comprised mainly of columnar ice, but included between 10% and 35% incorporated platelet ice (Langhorne et al., 2015). Comparison with a compilation of flexural strengths from all regions, including a small number from Antarctica (Timco & O'Brien, 1994), confirmed that the crystallographic structure exerted less influence on the mechanical properties of the beams than porosity (Langhorne et al., 1999). The in situ mechanical properties of a fast-ice cover can also be deduced from its break-up by ocean surface waves. Voermans et al. (2021) use observations of wave dissipation and dispersion to provide a method that can estimate the elastic modulus of the ice based on wave attenuation and the theory of a thin elastic plate.

Partially frozen cracks in fast ice are likely to cause its mechanical strength to be lower than for a continuous cover (Langhorne et al., 2001). This motivated an examination of the crystal, porosity and salinity structure of linear cracks in fast ice, as well as the time evolution of the refrozen thickness (Petrich et al., 2007). Such cracks refreeze quasi two-dimensionally due to heat transfer to the atmosphere and to the adjacent host ice cover, producing an arch-shaped freezing interface. Again, the crystallographic structure of the refrozen material is believed to exert less influence on the mechanical properties than salinity, temperature or brine volume. An analytical equation was derived to estimate the time needed to obtain a certain refrozen thickness. Since the strength of refrozen cracks increases with their thickness (Langhorne & Haskell, 2004), this time estimate could be useful for operations on the ice.

2.3.3. Optical

The physical properties of sea ice and its snow cover directly affect its optical properties (Perovich, 2017). A large and growing body of in situ studies of sea ice optics has been carried out in the Arctic (e.g., Perovich & Polashenski, 2012). Sea-ice conditions around Antarctica differ from those in the Arctic, and limited studies of optical properties have been performed over Antarctic sea ice (e.g., Allison et al., 1993; Brandt et al., 2005; Hao et al., 2021; Pirazzini, 2004; Vihma et al., 2009; Weiss et al., 2012; Q. Yang, Liu, et al., 2016; Zatko & Warren, 2015).

To study the temporal evolution of Antarctic sea-ice optical properties, fast ice has been used preferentially over pack ice because of its immobility and logistical accessibility. Reporting on fast-ice conditions in 2010, Q. Yang et al. (2013) noted the key relationship between variability in local snow-cover thickness and properties and fast-ice albedo, with the albedo being highest for fresh snow and generally decreasing as the snow aged toward summer. Q. Yang, Liu, et al. (2016) measured a 2010–2011 time series of the broadband albedo on fast ice off Zhongshan Station (76.4°E) and included consideration of cloud cover and snowfall in parameterization of fast-ice albedo. Hao et al. (2021) extended the work of Q. Yang, Liu, et al. (2016) and investigated the impact of snowfall on the spectral albedo (350–920 nm) of fast ice from October to November of 2016 in the same area, to understand the physical processes and biological impacts at each wavelength and showed the fast-ice albedo to be influenced by blowing snow (a common occurrence over coastal fast ice; Massom, Eicken, et al., 2001), and also diurnal variability related to snow metamorphism and water content. These studies highlight the need to carry out more detailed observations in order to clarify and quantify the complex relationships between Antarctic fast-ice physical and optical properties.

2.4. Fast-Ice Simulation

By definition, fast ice is stationary sea ice which forms and remains attached to the coastline or among grounded icebergs. Given that prognostic simulation of fast ice in three dimensions has been achieved only very recently in the Antarctic (Huot et al., 2021; Van Achter, Fichefet, Goosse, Pelletier, et al., 2022; Van Achter, Fichefet,

19449208, 2023, 2, Downloaded from https://agupubs.onlinelibrary.wiley.com/doi/10.1029/2022RG000770 by University of Adelaide Alumni, Wiley Online Library on [16/08/2023]. See the Terms and Conditions (https://onlinelibrary.wiley.com/terms-and-conditions) on Wiley Online Library for rules of use; OA articles are governed by the applicable Creative Commons License

Goosse, & Moreno-Chamarro, 2022, expanded upon in Section 5 here), a one-dimensional (vertical) approach has more commonly been adopted to model fast-ice thickness.

Crocker and Wadhams (1989b) modeled the thickness of fast ice growing near an ice shelf, based on the work of Semtner (1976), and evaluated model results with observations from McMurdo Sound. The authors added the representation of an unconsolidated SIPL and the formation of snow-ice, which are two main features of fast ice in this area.

The second generation of one-dimensional fast-ice simulations was detailed by Hoppmann et al. (2020), and is summarized here. Since the work of Crocker and Wadhams (1989b), there have been many additional measurements of fast-ice thickness evolution. We discuss three models and their observation-based validation experiments conducted in McMurdo Sound. Buffo et al. (2018) modeled the incorporation of buoyant frazil crystals into the fast-ice base with a one-dimensional mushy-layer sea ice model. Focusing on the unconsolidated SIPL, Cheng et al. (2019) used a two-dimensional plume model and compared its thickness distribution with the measurements of K. G. Hughes et al. (2014) and found that the vertical distribution of frazil concentration primarily controlled the thickness of the layer. Recently, Wongpan et al. (2021) modified the LIM1D model (Vancoppenolle et al., 2010) by increasing the initial brine fraction in newly forming ice, and using advective desalination for the brine rejection, and found that their simulated thickness of both consolidated and unconsolidated ice agree well with observations collected by Gough et al. (2012).

For the case of fast-ice growth in regions of minimal influence from ice shelves, the oceanic heat flux values used are positive (see Section 5 for the negative oceanic heat flux discussion). Y. Yang, Zhijun, et al. (2016) simulated the growth of fast ice in Prydz Bay (East Antarctica) from March 2006 to March 2007 and found that after tuning the model the oceanic heat flux decreased from 25 to 5 W m^{-2} in the growth season, and in summer it increased back to 25 W m^{-2}. Zhao et al. (2017) and Zhao, Cheng, et al. (2019) simulated fast-ice thickness evolution with simultaneous second-year ice ablation, along with the influence of snow cover off Zhongshan Station in Prydz Bay and obtained a maximum ice thickness range consistent with observations using oceanic heat flux equal to 30 W m^{-2}. Zhao et al. (2020) developed a fast-ice thickness prediction system for Prydz Bay fast ice. This system can forecast the fast ice and snow thickness for the next 10 days using a weather forecast as input data using seasonal oceanic heat flux estimated from previous studies in the range of >0–30 W m^{-2}. Li et al. (2022) used a high-resolution snow/ice thermodynamic model to simulate fast-ice thickness along Mawson Coast (62°E) from 2006 to 2018 and found from their sensitivity experiments that an oceanic heat flux of 20 W m^{-2} matches well with the observed thickness.

Arrigo et al. (1993) were the first to incorporate a biogeochemical component into one-dimensional fast-ice simulation. Based on field observations, Lim et al. (2019) performed one-dimensional fast-ice simulations and found that using a sea ice-specific value for silicic acid uptake can improve upon the previously-used value taken from phytoplankton experiments, suggesting that to include sea-ice processes in large-scale models, sea-ice algal-specific optimized values are needed (see Section 6 for more details).

2.5. Gaps

Although considerable work has been undertaken on observing and understanding the growth and structure of Antarctic fast ice, we consider the following areas to be research priorities:

- Existing observation sites should be maintained and coordinated to facilitate the detection of trends in fast-ice properties (especially ice thickness);
- Observations of ice properties should be obtained in new regions and extended toward summer (a time when site safety becomes an issue), with a focus on multi-year fast ice (which is currently only well-observed in Lützow-Holm Bay) and rough fast ice (currently only observed on an ad-hoc basis); and
- Observation systems should leverage technical innovations, including in power systems (to facilitate automated wintertime observation), satellite uplinks (to encourage the long-term deployment of measurement/monitoring systems in remote locations) and remote sensing technology (e.g., to expand the network of AEM thickness measurements, as expanded on in Section 3 of this review).
- Long-term observing sites should be approved CryoNet sites (https://globalcryospherewatch.org/cryonet/) following standards in sea-ice best practices and sharing of data following the Findability, Accessibility, Interoperability, and Reuse principles.

19449208, 2023, 2, Downloaded from https://agupubs.onlinelibrary.wiley.com/doi/10.1029/2022RG000770 by University of Adelaide Alumni, Wiley Online Library on [16/08/2023]. See the Terms and Conditions (https://onlinelibrary.wiley.com/terms-and-conditions) on Wiley Online Library for rules of use; OA articles are governed by the applicable Creative Commons License

3. Large-Scale Distribution, Seasonality and Thickness Estimates From Remote Sensing

Not only is Antarctic fast-ice extent a key climate variable in its own right, given its sensitivity to oceanic and atmospheric forcing (covered here in detail in Sections 4 and 5), but its volume and properties also provide important measures of its storage of freshwater, its modes of formation, and its key ecological/biological and biogeochemical roles (Giles et al., 2008). Moreover, fast-ice distribution strongly influences the size of important coastal polynyas (Fraser et al., 2019; Massom, Hill, et al., 2001), to affect the formation rates of sea ice and associated Antarctic Bottom Water (AABW) (Ohshima et al., 2013)—with implications for global ocean thermohaline (overturning) circulation and climate. Satellite remote sensing is crucial to the measurement and monitoring of Antarctic fast-ice distribution, properties and thickness (Lubin & Massom, 2006), given its extensive coverage (Fraser et al., 2012, 2021; Li et al., 2020), differing modes of formation (Fraser et al., 2012; Giles et al., 2008) and wide range of thicknesses (Li et al., 2022; Massom et al., 2010). Here we provide a broad overview of remote sensing techniques used and associated findings, with a focus on both covering papers which have mapped fast ice in some way, as well as detailing the contribution of other papers to the body of knowledge regarding large-scale fast-ice distribution, seasonality and thickness, noting that comprehensive coverage of technical aspects of fast-ice remote sensing techniques is provided in Section 5.9.3 of Lubin and Massom (2006).

3.1. Regional-Scale Studies of Antarctic Fast-Ice Distribution

Until recently, our knowledge of the distribution of Antarctic fast ice and its variability emanated primarily from East Antarctic aerial photography (e.g., Fedotov et al., 1998) and from regional-scale satellite-based assessments using various visible, thermal infrared (TIR; Massom et al., 2009) and synthetic aperture radar (SAR) data sets (Giles et al., 2008). While relatively limited in both space and time, these studies highlighted strong regional differences and variability in the fast-ice system. For example, Massom, Hill et al. (2001) used NOAA Advanced Very High Resolution Radiometer (AVHRR) imagery from 1999 to show a close coupling between fast-ice extent off Adélie Land and sea-ice production in the adjacent Mertz Glacier Polynya (145°E, 66.7°S). Ushio (2006) also used cloud-free AVHRR imagery to create a time series of fast-ice extent within Lützow-Holm Bay (40°E) for 1980–2004. This was then used to investigate the factors controlling the breakout of this fast ice (see the following section). Working in the same region, Aoki (2017) used a combined time series of AVHRR and Moderate Resolution Imaging Spectroradiometer (MODIS) imagery to study the relationship between fast-ice breakout in Lützow-Holm Bay and tropical sea-surface temperature. Massom et al. (2009) used AVHRR imagery from 1992 to 1999 to highlight substantial interannual variability in the timing and extent of seasonal fast ice, and in the prevalence of intra-seasonal breakout events, along the Adélie Land coast, and its impact on emperor penguin breeding success. Michael and Hill (2003) used AVHRR visible and TIR imagery to manually digitize the extent of Antarctic fast ice from 1992 to 1999 on a monthly basis in the vicinity of five Antarctic coastal locations (near Mawson Station (62.87°E, 67.60°S), Davis Station (78°E, 68.58°S), Casey Station (110.5°E, 66.28°S), Dumont d'Urville Station (140°E, 66.66°S), and Terra Nova Bay (164.5°E, 74.83°S)). The longest limited-region study of fast ice also occurred in this region, in a study by Labrousse et al. (2021), which also aimed to explain emperor penguin breeding success from 1979 to 2017.

The largest-scale fast-ice study without automation is that of Fraser et al. (2012). In this study, cloud-free composite images of the surface were assembled from MODIS imagery over a 20-day period (Fraser et al., 2009). From these, the extent of East Antarctic fast ice was manually digitized at a resolution of 2 km/pixel, for the period March 2000 to December 2008 (Fraser et al., 2010). This study thus presented the first dedicated large-scale, regular and continuous data set of Antarctic fast ice, from which conclusions about its extent, seasonality and variability could be reliably drawn, although the objectivity of the resulting maps is somewhat reduced by the need for manual classification. This was the first study to show the large-scale climatological cycle of fast-ice extent, with minimum extent occurring in the day-of-year (DOY) range of 61–80 in most years. Timing of the maximum extent was found to be more variable, but occurred at DOY 261–280 on average. Fast ice was found to comprise between ~4.5% and ~30% of overall East Antarctic sea-ice area in September and February, respectively. The study also reiterated the close relationship between fast-ice maximum extent and the location of grounded icebergs. An apparent trend toward increasing fast-ice extent in the Indian Ocean sector (20°E–90°E) was later shown to be an artifact of the relatively short time series used in the study (Fraser et al., 2021).

19449208, 2023, 2, Downloaded from https://agupubs.onlinelibrary.wiley.com/doi/10.1029/2022RG000770 by University of Adelaide Alumni, Wiley Online Library on [16/08/2023]. See the Terms and Conditions (https://onlinelibrary.wiley.com/terms-and-conditions) on Wiley Online Library for rules of use; OA articles are governed by the applicable Creative Commons License

Box 1. The influence of icebreaker passage on fast-ice breakout

Icebreakers are purpose-built vessels designed to push their way through sea ice. They are employed in both polar regions to resupply stations, open ice channels for other vessels, or to conduct marine science. Icebreaker passage has the potential to destabilize fast ice (Mahoney, 2011) by the creation of an artificial lead (Hotzel & Noble, 1979), which takes around 2 weeks in conditions suitable for refreezing to regain its original mechanical properties (Cornett, 1982; Dome Petroleum, 1979). If the channel is made when the surface is not freezing, then it can persist much longer. The destabilization of Antarctic fast ice was first discussed by S. Kim, Saenz, et al. (2018), working in McMurdo Sound (165°E, 77.5°S). Fast ice forms seasonally throughout much of the Sound (Fraser et al., 2021), and an icebreaker cuts a channel through this fast ice as part of the summertime station resupply. S. Kim, Saenz, et al. (2018) statistically analyzed the relationship between icebreaker arrival date at McMurdo Station (166.7°E, 77.85°S) and the subsequent date of fast ice minimum extent. They found a significant correlation between these quantities ($R^2 = 0.197$, $p < 0.01$) indicating that mechanical, icebreaker-induced destabilization may play a role in fast-ice breakout in some regions of Antarctica, however the reason for the long lag of 24 ± 9 days between icebreaker passage and subsequent fast-ice breakout is unclear.

In Figure 3 we present a new example showing the track of an icebreaker into fast ice in Prydz Bay (73.5°E, 68.8°S), and its subsequent breakout, to illustrate that this phenomenon is not limited to deep embayments such as McMurdo Sound. Approximately 670 km^2 broke out in the hours following the start of fast ice-breaking, indicated in yellow. A subsequent, much larger (~10,800 km^2) breakout occurred on 29 November 2021, indicated in red, with the broken-out ice sharing a border with the icebreaker channel, indicating destabilization of the fast ice along the ship track. This example (a) shows that icebreaker-induced fast-ice breakout is not limited to McMurdo Sound, (b) is far greater in areal extent than the McMurdo Sound examples studied by S. Kim, Saenz, et al. (2018), and (c) suggests that a systematic study into the importance of this mechanism around Antarctica, and its impacts on related atmospheric, oceanic and biological systems, would be highly valuable.

In another study, S. Kim, Saenz, et al. (2018) used hand-digitised MODIS images to produce a climatology of fast-ice extent in McMurdo Sound (165°E, 77.5°S), during sunlight months (October to April) from 2002 to 2014. Based on the high correlation between fast-ice extent in MODIS data and passive microwave-derived sea-ice extent over the period of 1978–2014, they describe a trend toward more complete summertime breakout, later timing of the minimum extent, and earlier refreezing (although this is somewhat at odds with ship log-based records of McMurdo Sound fast-ice extent over the same time period (Ainley et al., 2015) which indicate an insignificant increasing trend in fast-ice extent). S. Kim, Saenz, et al. (2018) were also the first to draw attention to the correlation between icebreaker passage and localized fast-ice breakout, a topic which is expanded upon in Box 1 of this review.

SAR imagery is extensively used for monitoring the Earth's polar regions, owing to its very high spatial resolution (as low as sub-meter), its ability to penetrate clouds, and its lack of reliance on solar illumination, allowing it to be used year-round (Lubin & Massom, 2006). Lythe et al. (1999) used a combination of SAR radar backscatter and TIR imagery to distinguish level multi-year fast ice from other sea-ice types, although this approach is likely to be less effective in areas where the fast ice spans a range of different roughness characteristics and ages.

The use of SAR imagery as a navigational aid in fast ice-covered regions has been reported near Zhongshan Station (76.4°E, 69.37°S; X. Wang, Cheng, et al., 2014). Although limited in spatial (~50 × 50 km) and temporal extent (a single snapshot in November 2012), this study affirmed the utility of C-band, horizontally-polarized transmit/receive (HH) SAR imagery in distinguishing regions of level and deformed fast ice. By this technique, tide crack locations could also be retrieved. C-band SAR imagery was used for similar manual fast-ice retrieval and roughness classification in the Ross Sea by Zhai et al. (2019).

19449208, 2023, 2, Downloaded from https://agupubs.onlinelibrary.wiley.com/doi/10.1029/2022RG000770 by University of Adelaide Alumni, Wiley Online Library on [16/08/2023]. See the Terms and Conditions (https://onlinelibrary.wiley.com/terms-and-conditions) on Wiley Online Library for rules of use; OA articles are governed by the applicable Creative Commons License

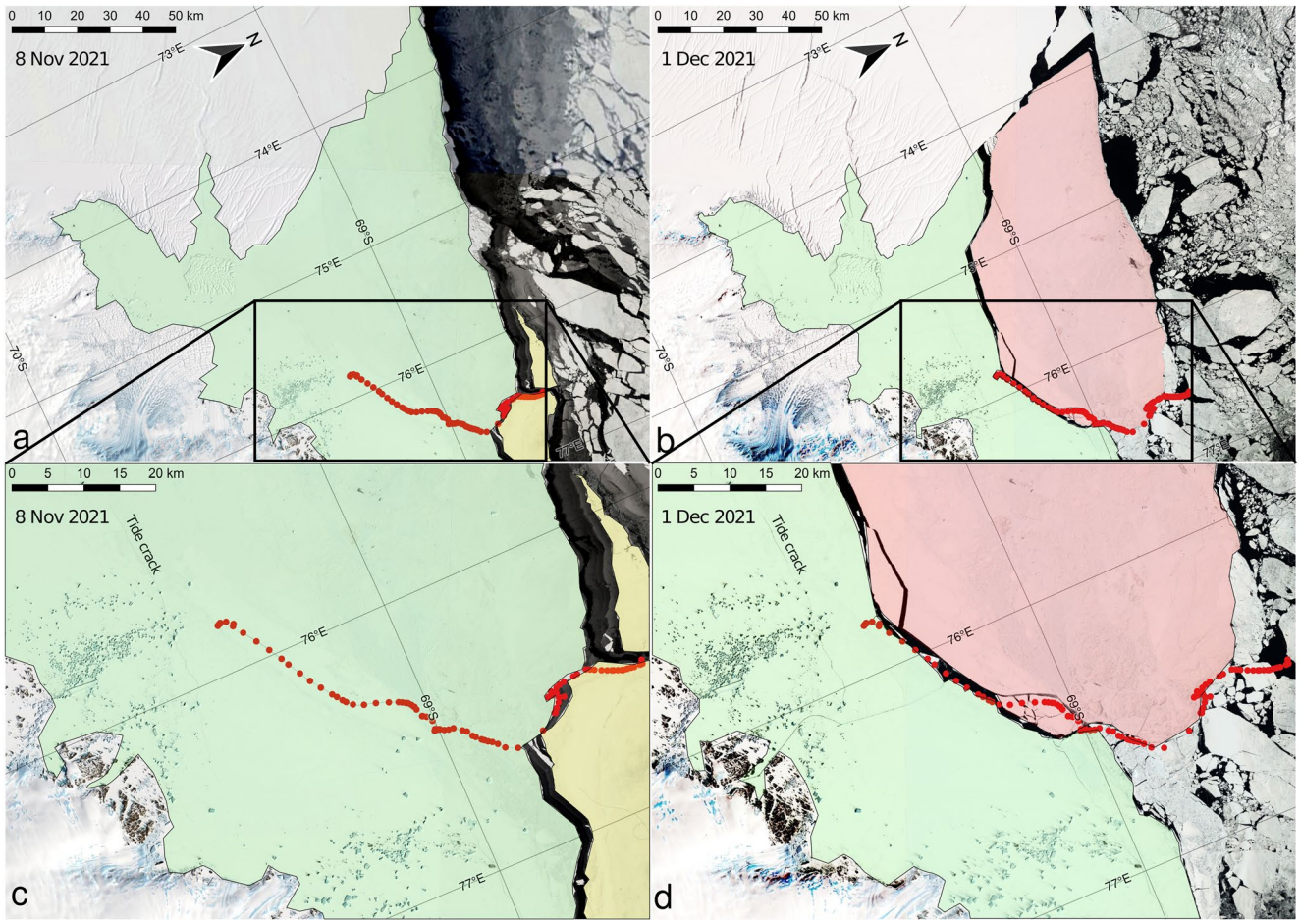

Figure 3. (a) Composite satellite image showing fast ice (green shading) in eastern Prydz Bay, East Antarctica, on 8 November 2021. (b) As for panel (a) but for 1 December 2021. Panels (c) and (d) are enlargements of (a) and (b), respectively. The track of an icebreaker through the fast ice is indicated with red circles. Recently broken-out fast ice is indicated in yellow shading for 8 November (~670 km^2), and red shading for 1 December (~10,800 km^2), illustrating that both breakouts occurred along the icebreaker track. High-resolution Landsat-8 "pansharpened" images in (a–d) were created by merging the high-resolution panchromatic band with lower resolution (30 m) red-green-blue (RGB imagery), obtained from https://earthexplorer.usgs.gov/. The Geospatial Data Abstraction Library (https://doi.org/10.5281/zenodo.5884351) was used for the pansharpening operation. Note that in the top half of panel a where Landsat imagery is not available, NASA MODIS imagery is used. Figure created using Quantarctica 3 (Matsuoka et al., 2021).

SAR imagery has also been used in limited area studies of the relationship between fast-ice extent and the behavior of adjacent glacier tongues and ice shelves. These include the studies of: (a) Massom et al. (2015), who inferred mechanical coupling between fast-ice and the MGT (144.7°E, 67.50°S) using RADARSAT C-band SAR imagery (covered here in more detail in Section 5); (b) Miles et al. (2017), who used Envisat ASAR imagery to determine the extent of both the terminus of outlet glaciers and fast ice in Porpoise Bay (115.5°E, 32.0°S); and (c) Gomez-Fell et al. (2022), who used a semi-automated fast-ice retrieval algorithm (developed by Mahoney et al., 2004) with Sentinel-1 C-band imagery to quantify the close mechanical coupling between fast ice and the Parker Ice Tongue (166.0°E, 73.9°S).

3.2. Unlocking Circum-Antarctic Fast-Ice Studies With Automated Extent Retrieval

Manual extraction of the distribution of fast ice from satellite imagery is time-consuming on large spatial scales, and suffers from relatively high levels of subjectivity compared to automated techniques. Here we describe recent advances in the semi- and near-fully-automated extraction of fast-ice extent, and discuss the benefits of these techniques in terms of their ability to provide long-term, large-scale and consistent data sets of fast-ice extent.

19449208, 2023, 2, Downloaded from https://agupubs.onlinelibrary.wiley.com/doi/10.1029/2022RG000770 by University of Adelaide Alumni, Wiley Online Library on [16/08/2023]. See the Terms and Conditions (https://onlinelibrary.wiley.com/terms-and-conditions) on Wiley Online Library for rules of use; OA articles are governed by the applicable Creative Commons License

SAR imagery is particularly suitable for automation due to its insensitivity to cloud cover and ability to penetrate polar darkness. Giles et al. (2008) used SAR image cross-correlation to provide two "snapshots" of East Antarctic fast-ice extent (85°E–170°E) in the Novembers of 1997 and 1999. By this technique, areas of sea ice with a near-zero velocity between the image pairs (separated by between <1 and ~20 days) are labeled as fast ice. As discussed in the introduction to this review, November was assumed to be the month of maximum extent (following Fedotov et al., 1998), but this was subsequently shown to occur in late September to early October in most years (Fraser et al., 2012, 2021). In a demonstration of an automation technique, M. Kim et al. (2020) used pairs of SAR images separated by 5 days in conjunction with a sophisticated hybrid object classification/machine learning algorithm to successfully classify fast ice in West Antarctica. Although only demonstrated on seven image pairs in 2007 and 2010, this technique shows great potential for mapping fast ice with a high degree of automation, even in regions where grounded icebergs are present (which may lead to false classification of fast ice when using the image cross-correlation technique of Giles et al., 2008).

In a development of earlier MODIS-based fast ice retrieval work, Fraser et al. (2020) released a circum-Antarctic fortnightly fast-ice data set at a resolution of 1 km per pixel. Semi-automated retrieval of the fast-ice edge was achieved, resulting in a long-term fast-ice record (March 2000–February 2018) and reducing subjectivity compared to earlier large-scale MODIS composite-based fast-ice classification (Fraser et al., 2012).

The 18-year mean fast ice persistence is presented in Figure 4, based on the data set of Fraser et al. (2020). This data set was subsequently analyzed to provide baseline knowledge of fast-ice extent, variability, seasonality and trends (Fraser et al., 2021), revealing that Antarctic fast-ice:

- undergoes a seasonal ~threefold increase in extent, from ~221,000 km^2 (mid-March) to ~601,000 km^2 (late September/early October);
- can naturally be partitioned into eight regions based on extent co-variability;
- exhibits regional variability in trend magnitude (and sign) across the 18-year study period, ranging from +2.81 ± 0.50%/year (Bellingshausen Sea) to −2.59 ± 0.69%/year (Weddell Sea), and an overall (marginally-significant) trend of −0.19 ± 0.18%/year;
- can form either seasonally (first-year or seasonal fast ice), or persist throughout the summer in some years (multi-year fast ice), with the latter forming within protected embayments, upstream of protrusions into the (westward) coastal current, or in association with dense fields of grounded icebergs; and
- forms over a bathymetric depth of, on average, ~400 m, although this varies regionally from ~200 (Bellingshausen Sea) to ~450 m (Australia and Amundsen Sea sectors), depending on coastal configuration and iceberg grounding depth/configuration.

Continent-wide data sets featuring automated retrieval of Antarctic fast ice have been provided in three other publications, including:

- M. Kim et al. (2015), which detailed the use of multiple satellite sensors in a machine learning framework, suggesting the utility of such techniques for fast-ice retrieval, although resulting maps of fast-ice distribution are somewhat unrealistic (e.g., fast ice throughout much of the central Weddell Sea);
- Nihashi and Ohshima (2015), which produced a fully-automated estimate of Antarctic fast-ice extent from 2003 to 2012 based on relatively low-resolution Advanced Microwave Sounding Radiometer for EOS (AMSR-E) passive microwave data, using techniques first detailed by Tamura et al. (2006), although it was first suggested by the authors and later demonstrated (Fraser et al., 2019) that this data set is insensitive to young fast ice (<3 months old); and
- Li et al. (2020), which derived semi-automated maps of Antarctic fast-ice extent for the Novembers of 2006–2011 and 2016–2017 from SAR imagery (i.e., a time of rapid fast-ice retreat, limiting its use as a climatically-representative time series).

Although circumpolar in scale, the contributions of these three publications to knowledge on fast-ice distribution and seasonality has been relatively limited due to the noted shortcomings. They do, however, indicate the potential for a higher degree of automation in fast-ice extent retrieval.

19449208, 2023, 2, Downloaded from https://agupubs.onlinelibrary.wiley.com/doi/10.1029/2022RG000770 by University of Adelaide Alumni, Wiley Online Library on [16/08/2023]. See the Terms and Conditions (https://onlinelibrary.wiley.com/terms-and-conditions) on Wiley Online Library for rules of use; OA articles are governed by the applicable Creative Commons License

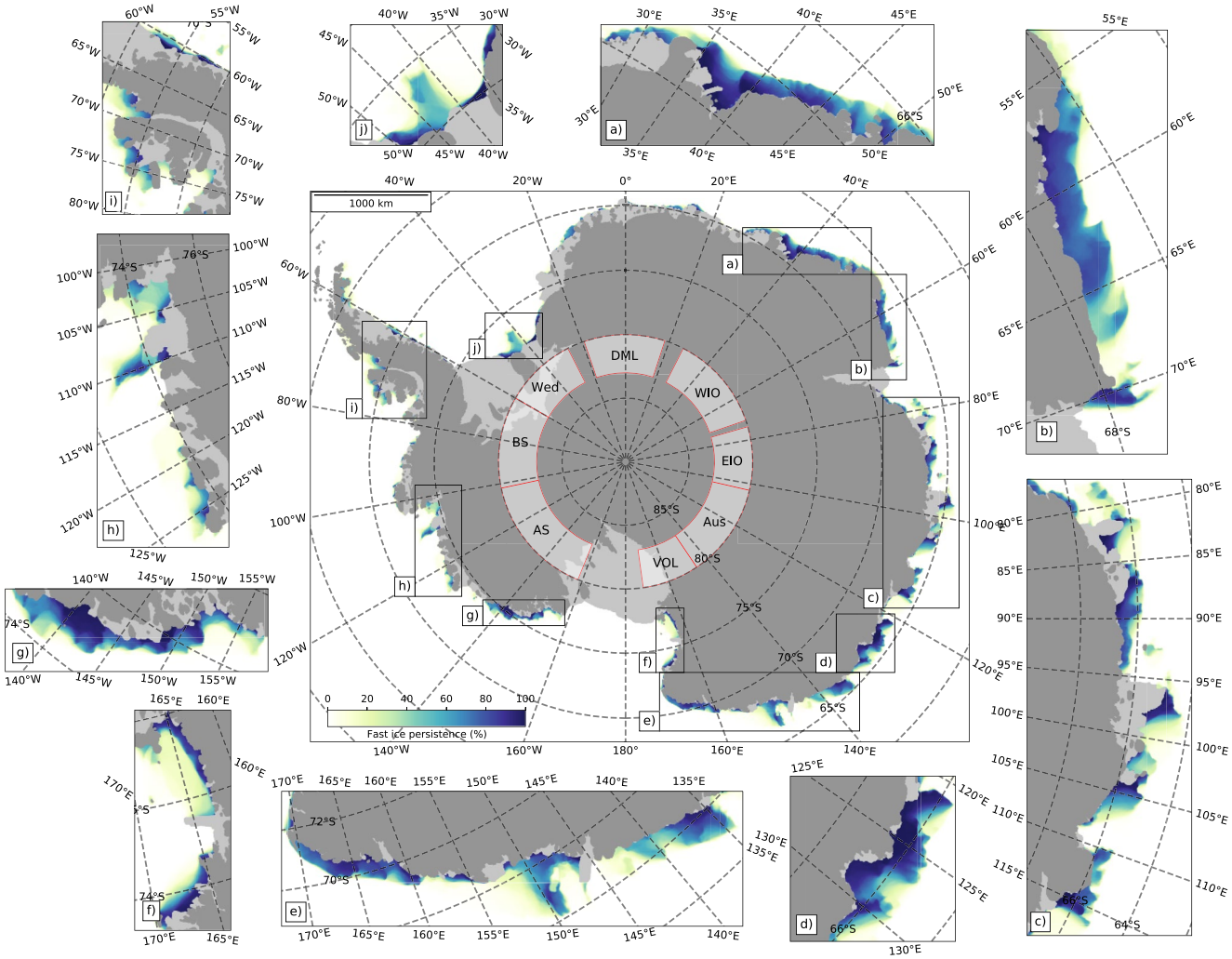

Figure 4. Mean fast-ice persistence distribution, over the period from March 2000 to March 2018 and based on the data set of Fraser et al. (2020). Inset maps (a–j) are enlarged maps of selected regions. Fast-ice regions, as defined in Fraser et al. (2021), are indicated in the center. DML is Dronning Maud Land, WIO is Western Indian Ocean, EIO is Eastern Indian Ocean, Aus is the Australian sector, VOL is Victoria and Oates Lands, AS is Amundsen Sea, BS is Bellingshausen Sea, and Wed is Weddell Sea.

3.3. Antarctic Fast-Ice Thickness Remote Sensing

The principal challenge with remote sensing of the thickness of sea ice, landfast or otherwise, is the detection of the underside of the ice from above. Although ice-penetrating radar is a widely used tool for measuring the thickness of glaciers and ice sheets (e.g., Gogineni et al., 1998), the brine within sea ice greatly limits the penetration depth of microwave energy compared with freshwater ice. As a result, measurement of sea ice thickness with ice-penetrating radar has so far been limited to surface-based observations (Bradford et al., 2016) and wide-bandwidth sensors (Holt et al., 2009), which have yet to be implemented in an airborne or satellite platform. As a result, space-based methods for determining sea-ice thickness rely on observations of the upper surface, which prove problematic for fast-ice applications.

3.3.1. Microwave Backscatter-Based Classification and Estimates of Fast-Ice Thickness

The study of East Antarctic fast-ice distribution by Giles et al. (2008) was also the first to use backscatter-derived observations of surface roughness as a means of inferring Antarctic fast-ice thickness. In this region, level fast ice was estimated to comprise ∼67% of fast ice, with the remainder being rough fast ice. By assuming mean thicknesses of 1.7 m for level fast ice (broadly in line with an observed mean value of 1.24 m for level first-year fast ice in Lützow-Holm Bay by Nakamura et al., 2009) and 5.0 m for deformed fast ice, Giles et al. (2008)

19449208, 2023, 2, Downloaded from https://agupubs.onlinelibrary.wiley.com/doi/10.1029/2022RG000770 by University of Adelaide Alumni, Wiley Online Library on [16/08/2023]. See the Terms and Conditions (https://onlinelibrary.wiley.com/terms-and-conditions) on Wiley Online Library for rules of use; OA articles are governed by the applicable Creative Commons License

derived the first large-scale estimate of East Antarctic fast-ice volume. While fast ice was found to comprise only 8.3% of ice extent, it made up an estimated 28% of volume. Nakamura et al. (2009) looked at the thickness and C-band backscatter of level first-year ice in Lützow-Holm Bay in December 2004. Comparing ice thickness observations acquired along an icebreaker track with near-coincident Envisat ASAR data, they identified a negative relationship between fast-ice thickness and the ratio of vertically and horizontally co-polarized backscatter coefficients. This relationship is explained by the cooling of the ice surface that occurs as ice thickens in winter and the associated reduction in brine volume, which enhances microwave penetration and volume scattering. Nakamura et al. (2009) derive a linear relationship ($R^2 = 0.72$) over fast-ice thicknesses ranging from approximately 0.5–2.2 m, but the technique has not been applied more widely.

3.3.2. Altimetric Estimates of Fast-Ice Thickness

Altimetry-based methods rely on the principle of isostatic balance for floating bodies to determine the thickness of the ice from the measurement of freeboard, or the height of the ice or snow surface relative to the waterline (e.g., Kwok, 2004; Laxon et al., 2013). As a result, altimetric sea-ice thickness measurements are highly sensitive to uncertainties in snow depth, which must be determined independently, and the densities of ice, water and snow (Kwok & Cunningham, 2008), all of which affect the freeboard for ice of a given thickness. Additionally, to account for the dynamic topography of the sea surface, it is necessary to obtain altimetric measurements of sea surface height (SSH) in leads and polynyas within the ice pack. Such areas of open water are rarely encountered within fast ice cover. Sea ice freeboard measurements from the Ice, Cloud and Land Elevation Satellite (ICESat)-2 laser altimetry are excluded if they are more than 10 km from a lead in which SSH could be determined (Kwok et al., 2019). Recent work by Landy et al. (2021) suggests that this length scale can be extended in some cases, but this still represents a limitation for measuring the thickness of extensive regions of fast ice.

Nonetheless, Massom et al. (2010) used the Geoscience Laser Altimeter System (GLAS) onboard the original ICESat altimeter to retrieve the freeboard of the thick multi-year fast ice attached to the eastern flank of the MGT prior to its calving in early 2010. This fast-ice feature, ranging in age from 20 to 35 years old, was estimated to be between 10 and 55 m thick, depending on the densities of snow and ice assumed in the hydrostatic calculation. Such growth in thickness is suggested to be possible due to the contribution from platelet ice deposition onto the base of the fast ice (Hoppmann et al., 2020, see also Section 2.1.2).

Price et al. (2015) retrieved McMurdo Sound fast-ice freeboard using the Ku-band Synthetic Interferometric Radar Altimeter-2 (SIRAL-2) onboard the European Space Agency's CryoSat-2 radar altimeter. Depending on the waveform retracker used, the retrieved freeboard was determined to correspond to somewhere between the snow-ice and snow-air interfaces. This work provides the basis for systematic monitoring of Antarctic fast-ice freeboard, regardless of cloud cover, but may be limited to regions of fast ice uncontaminated by the presence of icebergs, due to the relatively large footprint of ~380 × 1,650 m.

3.3.3. Radiometric Estimates of Fast-Ice Thickness

Radiometric techniques measure the passive emission of thermal radiation from the sea ice and rely on the fact that the surface temperature of the ice decreases as the ice thickens (e.g., Nihashi et al., 2009; Tamura et al., 2007; Tian-Kunze et al., 2014). However, this relationship becomes less sensitive as the ice thickness increases (and particularly as it accumulates a snow cover), and measurements are therefore typically limited to ice thinner than approximately 0.5 m (Jezek et al., 2019; Tamura et al., 2007) with little or no snow cover. Hence, although TIR radiometry may potentially be used to infer/model the thickness of fast ice during the early stages of formation, we are not aware of any such measurements in the literature.

3.3.4. Electromagnetic Sounding Estimates of Fast-Ice Thickness

As an alternative to satellite-based measurement, AEM sounding can be used to determine sea-ice thickness over the full range of thicknesses found in the polar regions (e.g., Haas et al., 2009; Mahoney et al., 2015), but over smaller areas and shorter time spans. By remotely sensing the positions of the upper and lower surfaces of the ice and snow cover relative to the instrument, AEM measurements supplemented with a laser altimeter typically achieve accuracies of better than 10% of the total snow-plus-ice thickness, without sensitivity to uncertainties in sea surface topography or the densities of snow, ice and seawater. Snow depth must still be determined independently to obtain an observation of sea-ice thickness, but AEM measurements are significantly less sensitive to uncertainty in snow depth than radiometric or altimetric techniques. Thus, although AEM cannot provide the

19449208, 2023, 2, Downloaded from https://agupubs.onlinelibrary.wiley.com/doi/10.1029/2022RG000770 by University of Adelaide Alumni, Wiley Online Library on [16/08/2023]. See the Terms and Conditions (https://onlinelibrary.wiley.com/terms-and-conditions) on Wiley Online Library for rules of use; OA articles are governed by the applicable Creative Commons License

same spatial coverage as satellite-based observations, it is a well-suited technique for remotely sensing the thickness of fast ice over limited areas and time periods. Moreover, Haas et al. (2021) recently demonstrated the ability of AEM to measure both the thicknesses of fast ice and the unconsolidated SIPL beneath. The technique has been used in McMurdo Sound (Haas et al., 2021), and on a transect covering ∼700 km of springtime fast ice along the Victoria Land coast (∼165°E, 75°S) in the western Ross Sea (Langhorne et al., 2023).

3.4. Gaps in Our Knowledge, Future Focus Regions

Currently, the contribution of remote sensing to the overall knowledge of fast-ice physical properties is limited due to the regional nature or short time series of most studies. Future studies should focus on providing large-scale, consistent and continuous measurements of fast-ice extent and thickness, in order to provide baseline knowledge on the seasonality, variability and trends in these parameters. Although detailed knowledge about the distribution, variability and trends in fast-ice extent has been gained in the last decade, considerable gaps remain. Regular maps of fast ice need to be reliably produced with a high degree of automation, in order to produce an objective fast-ice extent data set. Although automation presents significant challenges (e.g., performance under all sky conditions and during times of melt), the potential of SAR-based techniques has been shown in recent publications (e.g., Selyuzhenok & Demchev, 2021). An ideal data set would have the following attributes: automated, objective, with a long instrumental record, using freely-available source imagery, high resolution, accurate, able to retrieve fast-ice extent at all times of the year, circumpolar, and ability to be used in the presence of icebergs and different types of fast-ice (i.e., level and rough). As shown in several publications (e.g., M. Kim et al., 2015, 2020), there is also the potential to use machine learning-based techniques to enhance the automation of fast-ice retrieval. Multi-sensor fusion also has the potential to contribute to automated enhanced classification (as demonstrated by Lythe et al., 1999).

Similarly, our knowledge of the distribution of fast-ice roughness is also lacking. Combining maps of fast-ice distribution with images of SAR backscatter (Segal et al., 2020) or roughness maps determined from multi-angle visible imagery (e.g., Johnson et al., 2022) hold the key to increasing our knowledge in this area. Laser altimetry, with its fine spatial resolution (e.g., 17 m footprint in the case of the ICESat-2), can also be used to determine the roughness of ice (van Tiggelen et al., 2021), though such techniques have yet to be implemented over Antarctic fast ice.

While automation has the potential to enable objective fast-ice mapping into the future, information on historical fast-ice extent is still lacking. Although weekly ice charts are produced for Antarctica (e.g., the collaboratively-produced Russian Arctic and Antarctic Research Institute (AARI)-US National Ice Center (NIC)-Norwegian Meteorological Institute (NMI) charts), these have not been used extensively for fast-ice studies, likely owing to inconsistent format before standardization, and an absence of studies validating the fast-ice component of these charts. A study on the accuracy and reliability of the fast-ice component of Antarctic ice charts would be valuable, and potentially enable studies of historical fast ice similar to that of Y. Yu et al. (2014) in the Arctic.

Processes acting at small spatial scales and timescales shorter than typical repeat intervals of polar-orbiting satellites represent another gap in our understanding of fast ice. Interferometric SAR (InSAR) provides a means of observing the mm-scale relative surface motion and is a well-established tool in the field of geodesy (e.g., Simons & Rosen, 2007). InSAR cannot typically be applied to drifting sea ice, since the surface motion between satellite acquisitions is too great to maintain coherence. However, InSAR has successfully been applied to map Arctic fast-ice extent (Dammert et al., 1998; Meyer et al., 2011), assess its relative stability (Dammann et al., 2019), and quantify micro-scale strain (Dammann et al., 2018). Additionally, using short-temporal baseline InSAR data from the TanDEM-X mission, Mahoney et al. (2016) demonstrated the ability to map infragravity waves propagating through pack ice and fast ice. To our knowledge, InSAR analysis of fast ice in Antarctica has only been reported once (Han & Lee, 2018), but with the possible role of fast ice in sheltering ice shelves from the influence of ocean waves, we anticipate this could become an important field of research.

In the Arctic, coastal radars have been used to observe short-lived events associated with the formation, deformation and detachment of fast ice since the 1970s (Jones et al., 2016; Mahoney et al., 2007; Shapiro & Metzner, 1989). In concert with co-located atmospheric and oceanic measurements and, in some cases, Indigenous knowledge (Druckenmiller et al., 2009), these studies have provided insight into the role of grounded ridges in anchoring

19449208, 2023, 2, Downloaded from https://agupubs.onlinelibrary.wiley.com/doi/10.1029/2022RG000770 by University of Adelaide Alumni, Wiley Online Library on [16/08/2023]. See the Terms and Conditions (https://onlinelibrary.wiley.com/terms-and-conditions) on Wiley Online Library for rules of use; OA articles are governed by the applicable Creative Commons License

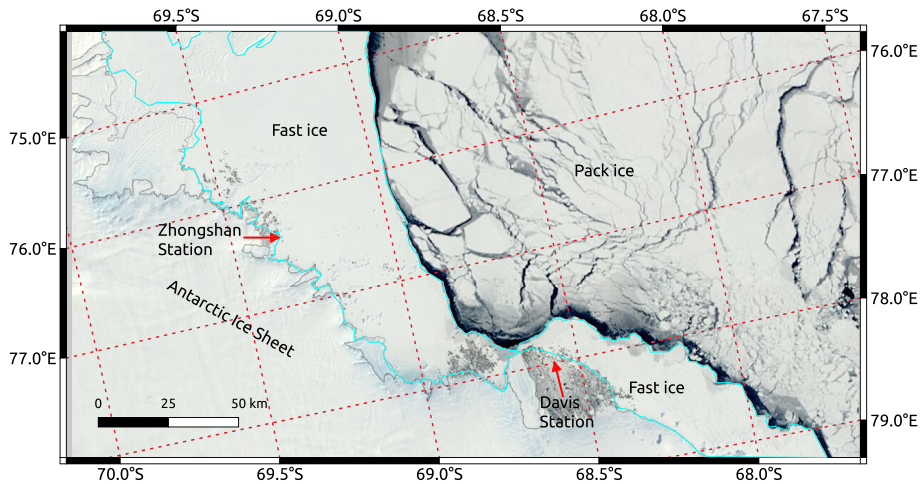

Figure 5. A true-color composite NASA MODIS image of the eastern Prydz Bay region during a time of extensive fast ice cover (10 April 2022). Fast ice is outlined in cyan. Satellite imagery from NASA Earth Observing System Data and Information System Worldview (https://worldview.earthdata.nasa.gov/).

fast ice and the influences of winds, tides, ocean currents, and waves during detachment events. More recently, Dammann et al. (2020, 2022) have applied ground-based radar interferometry for observing micro-scale strain in Arctic sea ice at timescales of minutes. This work has demonstrated the ability to observe pre-fracture ice deformation, the propagation of surface wave fronts through ice, and coupling between floating and grounded ice. Once again, we are not aware of the deployment of any coastal radar system—either interferometric or non-interferometric—in Antarctica, but we anticipate this could provide new insights into episodic processes controlling timing, extent, and stability of Antarctic fast ice for scientific and operational purposes.

4. Atmospheric Interactions With Fast Ice

The atmosphere plays a key role in shaping the Antarctic fast-ice environment, across a wide range of spatio-temporal scales—from micro- through synoptic to regional and seasonal to annual. Major atmospheric factors affecting Antarctic fast-ice formation, breakup/melt and resultant duration and extent of coverage, thickness, age, mechanical strength and properties include: air temperature (e.g., Heil, 2006); synoptic wind speed and direction (e.g., Heil, 2006; Heil, Massom, et al., 2011; Massom et al., 2009); the degree of storminess and the incidence of wind-generated ocean waves (e.g., Crocker & Wadhams, 1989a); and snow accumulation, wind redistribution (aeolian) and melt (e.g., Kawamura et al., 1997; Ushio, 2006). These factors will be examined in more detail in regional case studies provided below.

Fast ice also influences the atmosphere by modifying the energy balance near the surface. This influence occurs directly via ice-albedo feedback (see Section 2.3.3), and also indirectly by the role played by fast ice in the production of gas-phase biogenic chemical species that play a role in aerosol production (Charlson et al., 1987; see also Section 6.5.2).

In the remainder of this section, we primarily overview the reported influence of various atmospheric processes on differing fast-ice environments from different parts of both East and West Antarctica, including regional maps where appropriate. We then highlight the relationships between Antarctic fast ice and large-scale climate patterns and teleconnections. The research cited highlights the complex nature of atmosphere-fast ice interactions, and the vulnerability of Antarctic fast ice to changing atmospheric conditions.

4.1. Davis and Zhongshan Stations, Princess Elizabeth Land

Much of our understanding of fast ice-atmosphere relationships comes from long-term observational programs or dedicated studies at and near to Antarctic research stations, extended spatially by atmospheric reanalyses and satellite studies. At Australia's Davis Station (78°E; see Figure 5), in a study of the local annual fast ice from the 1950s to 2003, Heil (2006) found the maximum thickness of first-year fast ice to be significantly correlated with

19449208, 2023, 2, Downloaded from https://agupubs.onlinelibrary.wiley.com/doi/10.1029/2022RG000770 by University of Adelaide Alumni, Wiley Online Library on [16/08/2023]. See the Terms and Conditions (https://onlinelibrary.wiley.com/terms-and-conditions) on Wiley Online Library for rules of use; OA articles are governed by the applicable Creative Commons License

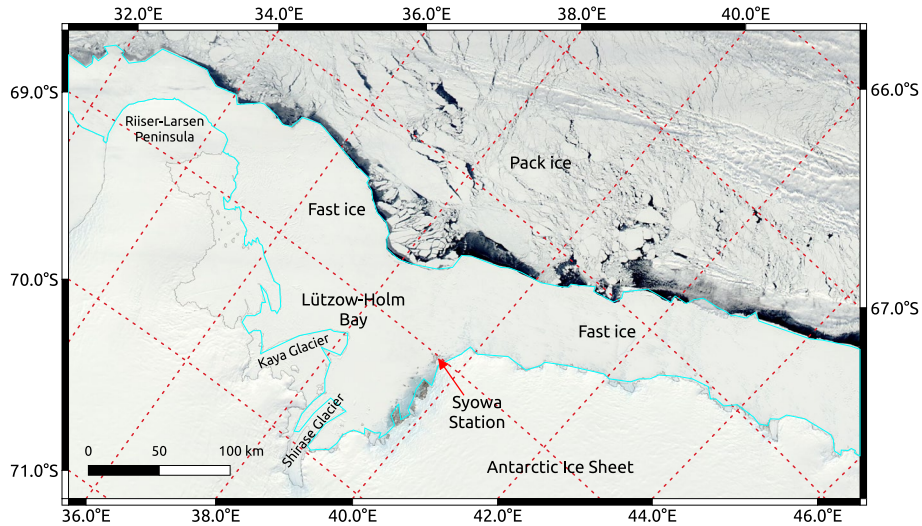

Figure 6. A true-color composite NASA MODIS image of the Lützow-Holm Bay region during a time of extensive fast ice cover (16 October 2022). Fast ice is outlined in cyan. Satellite imagery from NASA Earth Observing System Data and Information System Worldview (https://worldview.earthdata.nasa.gov/).

winter surface air temperature (69% of variance explained), with the annual fast-ice persistence/duration also depending strongly on winter and spring temperatures. Heil (2006) also attributed large observed inter-annual variability in the fast-ice characteristics off Davis to wind and storminess, which have dominant influences on maximum ice thickness and annual breakout timing and extent, respectively.

Approximately 100 km to the south-west and in the region of China's Zhongshan Station (76.3°E; also indicated in Figure 5), the fast ice is more perennial, but with periodic breakouts (Zhao, Yang, et al., 2019). Y. Yang, Zhijun, et al. (2016) combined meteorological and fast-ice thickness measurements from 2006 to 2007 to develop a one-dimensional thermodynamic fast-ice model tuned with albedo and oceanic heat flux (see also Section 2.4). Considerable work has been undertaken here on the snow cover overlying fast ice (Q. Yang et al., 2013; Q. Yang, Liu, et al., 2016; Hao et al., 2021), including both optical and thermodynamic influences; these are covered in Section 2 of this review.

In an analysis of the fast-ice radiation environment for 2010–2015, L. Yu et al. (2017) found surface temperature to be the main determinant of the seasonal ice melting. Building on earlier work, Zhao, Cheng et al. (2019) showed from measurements in 2012–2016 that local fast-ice thickness decreases with increasing snow-cover thickness. This is not surprising given the strong insulative properties of snow and its influence in decreasing the rate of thermodynamic ice growth (Sturm & Massom, 2016). Working in Quilty Bay close to Zhongshan, Shah et al. (2017) showed the fast ice to be characterized by distinctive layering (upper low density with an underlying high density) that is influenced by the coastal easterly wind field, which also plays a dominant role in controlling snow distribution on the fast ice in the area. Knowledge gained at and around Zhongshan Station has been applied to the development of an operational fast-ice forecast model, the Fast Ice Prediction System, which was first demonstrated in the 2017/2018 season (Zhao et al., 2020).

4.2. Lützow-Holm Bay, Dronning Maud Land

The extensive region of fast ice off Syowa Station (39.6°E; see Figure 6) has also been subject to long-term scrutiny and monitoring by the Japanese Antarctic Research Expedition, from the perspective of atmospheric influences on observed variability (spatial and temporal) in its thickness, properties, distribution and duration. Lützow-Holm Bay normally contains predominantly multi-year fast ice, but this breaks out every few years (Ushio, 2006), and a number of case studies have cast light on this phenomenon (Kawamura et al., 1995). As with work conducted at Zhongshan Station, much of the work on atmospheric fast ice drivers in this region has focused on the roles of the overlying snow cover. This work is explained in detail in Section 2, but can be summarized

19449208, 2023, 2, Downloaded from https://agupubs.onlinelibrary.wiley.com/doi/10.1029/2022RG000770 by University of Adelaide Alumni, Wiley Online Library on [16/08/2023]. See the Terms and Conditions (https://onlinelibrary.wiley.com/terms-and-conditions) on Wiley Online Library for rules of use; OA articles are governed by the applicable Creative Commons License

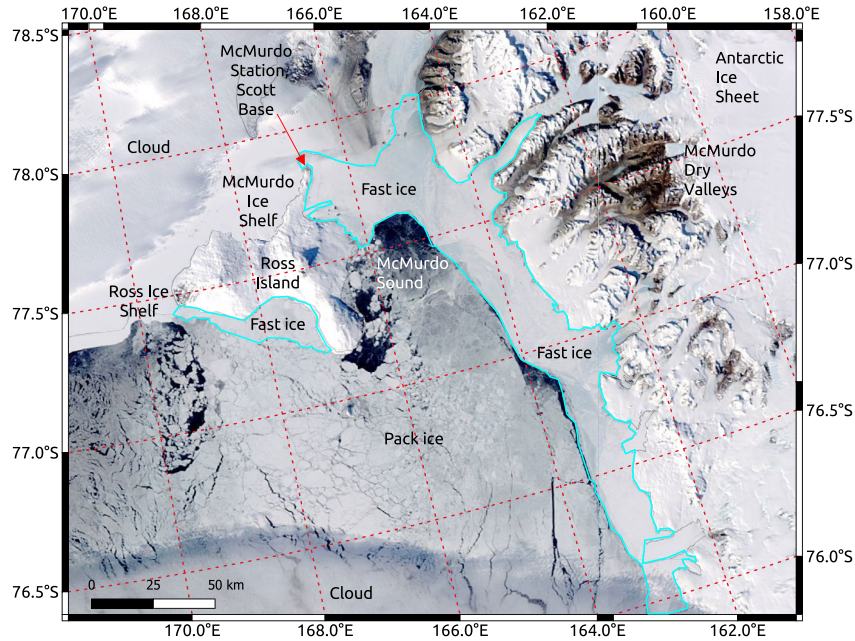

Figure 7. A true-color composite NASA MODIS image of the McMurdo Sound region during a time of extensive fast ice cover (26 October 2019). Fast ice is outlined in cyan. Satellite imagery from NASA Earth Observing System Data and Information System Worldview (https://worldview.earthdata.nasa.gov/).

by noting that heavy snow appears to stabilize fast ice due to formation of snow-ice (Kawamura et al., 1997; Ushio, 2006). Surface melt has been noted to precede breakout here (Enomoto et al., 2002).

4.3. McMurdo Sound, Victoria Land

Fast ice-atmosphere interactions have long been studied in the southern Ross Sea (165°E, 77.5°S) in the vicinity of McMurdo Station (United States) and Scott Base (New Zealand; indicated in Figure 7), where fast ice typically forms in March–April and breaks out in the following January–February. There, fast-ice coverage extent and duration are impacted by seasonal variability in the strength of storms (Heine, 1963), particularly during winter (Leonard et al., 2021). Moreover, the strength of winter storms affects fast-ice conditions in the following summer (Leonard et al., 2021). Regarding fast-ice formation, Zhai et al. (2019) show the importance of local- and large-scale weather events and how low temperatures combined with low wind speed to promote fast-ice formation in the northern part of Terra Nova Bay (164.5°E, 74.8°S) in September 2017. In the following month, this ice was supplemented by strong wind-driven onshore compaction of pack ice, which developed into fast ice with the aid of low temperatures. Such is the importance of the atmosphere in driving fast-ice variability in this region that extensive fast ice was only observed in satellite imagery in 4 out of 15 years between 2003 and 2017.

In an early study, Prebble (1968) showed that the timing and extent of fast-ice breakout are linked to the dispersion of protective pack ice in the Ross Sea (see also the study of Massom et al., 2018). Crocker and Wadhams (1989a) found that thermal decay plays only a minor role in fast-ice breakup/retreat in the region, with wind-induced tensile failure being the only likely mode of fracture for most of the year and ocean swell being a dominant influence during summer. Katabatic winds peaking in July-August are a key cause of winter breakouts, which also dictates interannual variability in growth periods and seasonal variability of thickness (Cozzi, 2014).

4.4. Other Locations

Strong fast ice-atmosphere linkages are also apparent in other Antarctic sectors. For example, Massom et al. (2009) showed in a study covering 1992–1999 how wind direction is a major determinant of strong interannual variability in the large area of annual fast ice on the Adélie Land coast off the French station Dumont d'Urville (shown in Figure 8). This study further implicated strong and persistent southeasterly winds in very low fast-ice coverage

19449208, 2023, 2, Downloaded from https://agupubs.onlinelibrary.wiley.com/doi/10.1029/2022RG000770 by University of Adelaide Alumni, Wiley Online Library on [16/08/2023]. See the Terms and Conditions (https://onlinelibrary.wiley.com/terms-and-conditions) on Wiley Online Library for rules of use; OA articles are governed by the applicable Creative Commons License

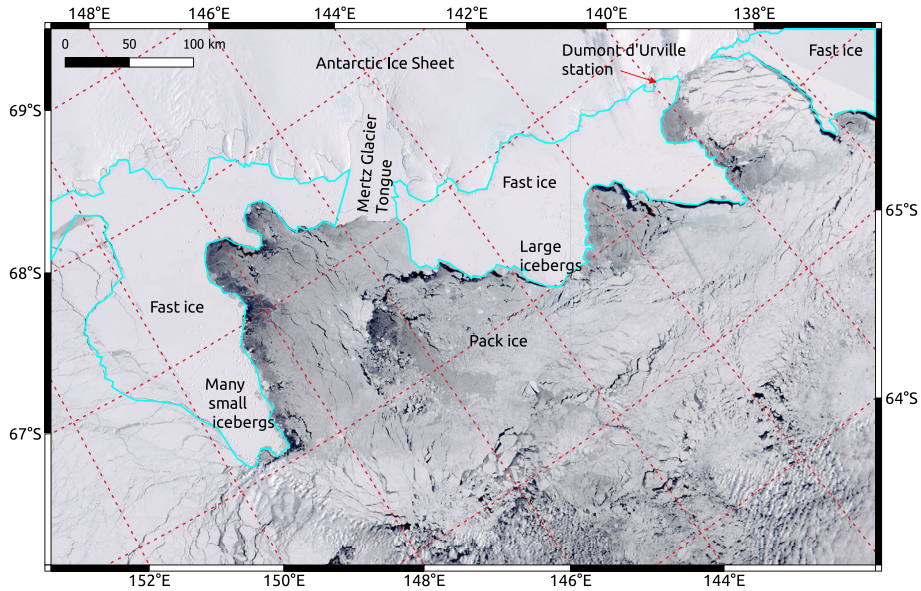

Figure 8. A true-color composite NASA MODIS image of the Mertz Glacier region during a time of extensive fast ice cover (29 September 2019). Fast ice is outlined in cyan. Satellite imagery from NASA Earth Observing System Data and Information System Worldview (https://worldview.earthdata.nasa.gov/).

observed in US Argon spy satellite images from August and October 1963. The importance of wind direction in this region is further highlighted by Z. Wang, Turner, et al. (2014), who found that cyclone-induced winds caused ice compaction and rapid development of fast ice near the coast at 144°E (aided by the large grounded iceberg B9B; Leane & Maddison, 2018). Moving to the west, a major breakup of multi-year fast ice in Porpoise Bay (near 128°E) in 2007 was attributed to both atmospheric circulation anomalies in December 2005 which weakened the ice through a combination of surface melt, and a change in the wind direction prior to breakup (Miles et al., 2017). On the Antarctic Peninsula, Massom et al. (2018) and Wille et al. (2022) have further shown the importance of persistent warm northerly winds ("atmospheric rivers") in the anomalous breakup of fast ice adjacent to the Wilkins and Larsen A and B ice shelves, aided by wind-driven pack ice removal and exposure to ocean waves. The importance of wave action in fast ice breakup was also highlighted by Herman et al. (2021) in a case study of the flow-size distribution in the vicinity of the Shackleton Ice Shelf. In a long-term study conducted over 2010–2019 in Atka Bay (7.5°W) in the Weddell Sea (see Figure 9), S. Arndt et al. (2020) found snow accumulation to be a major factor in fast-ice formation in the bay, with a significant role being played by flooding of the snow-ice interface (related to heavy snowfall and air temperature). In this location, strong easterly winds govern the snow accumulation on fast ice, and also trigger its breakup in summer.

4.5. Large-Scale Effects

While the multiple studies above highlight the key role of atmospheric processes in forging the Antarctic coastal fast-ice environment, relatively few studies have investigated the relationships between fast ice and large-scale atmospheric variability, for example, the Southern Annular Mode (SAM) and El Niño-Southern Oscillation (ENSO). A general limitation for this aspect of fast-ice research, as for pack ice studies, has been the length of records available for large-scale comparisons, with most direct observations of Antarctic fast ice commencing in the late 1950s, and high-quality satellite data and global reanalyses only becoming available since the late 1970s.

A unique and particularly important record for long-term studies of large-scale atmospheric influences on fast ice in the Antarctic region has been accumulated since 1903 at the South Orkney Islands in the northwestern Weddell Sea (Murphy et al., 1995, 2014). This record, which records the start and end dates when the local fast ice is estimated as supporting the weight of a typical "scientist," shows time-varying multi-year periodicity which has non-stationary relationships with either ENSO or SAM. The timing of annual fast-ice breakout is influenced by westerly/north-westerly winds associated with the SAM, while the formation date is influenced by regional oceanic and sea-ice conditions in the preceding 18 months. The latter aspects suggest that preconditioning of

19449208, 2023, 2, Downloaded from https://agupubs.onlinelibrary.wiley.com/doi/10.1029/2022RG000770 by University of Adelaide Alumni, Wiley Online Library on [16/08/2023]. See the Terms and Conditions (https://onlinelibrary.wiley.com/terms-and-conditions) on Wiley Online Library for rules of use; OA articles are governed by the applicable Creative Commons License

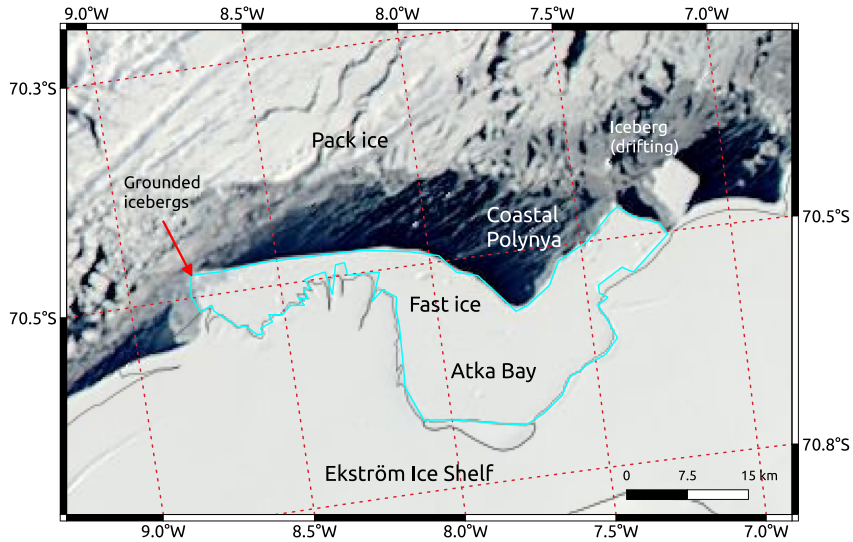

Figure 9. A true-color composite NASA MODIS image of Atka Bay during a time of extensive fast ice cover (10 October 2020). Fast ice is outlined in cyan. Satellite imagery from NASA Earth Observing System Data and Information System Worldview (https://worldview.earthdata.nasa.gov/).

local conditions due to the influence of ENSO can occur over the preceding summer and winter seasons. However and due to the non-stationarity of correlations with climate patterns, Murphy et al. (2014) note that caution is needed in interpreting the influence of teleconnections in the region using records of only a few decades in length.

Further afield, three studies have examined large-scale atmospheric influences on fast ice in East Antarctica. In their analysis of Adélie Land fast ice in 1963 and 1992–1999, Massom et al. (2009) showed how the greater prevalence of strong winds from the south-southeast and associated with a positive SAM led to a relatively low fast-ice extent in certain years (1998 and 1999), by breaking up the fast ice and dispersing it seawards. In contrast, prevailing winds with more of an easterly component tended to create more extensive fast ice by pushing pack ice into the region to dynamically supplement the fast-ice coverage there. Massom et al. (2009) also found no conclusive relationship between ENSO and Adélie Land fast ice, with below-average fast-ice extents coinciding with both La Niña (1998 and 1999) and El Niño (1963 and 1993), while well above average fast-ice extent and persistence in 1994 also coincided with an El Niño event.

In Lützow-Holm Bay, Aoki (2017) described a significant positive correlation between the latitude of the fast-ice edge over 1997–2016 and sea surface temperatures in the eastern equatorial Pacific region, indicating a linkage with ENSO. The proposed mechanism of the linkage follows other previous studies of teleconnections from ENSO in the region that is, atmospheric circulation off Dronning Maud Land is influenced by a Rossby wave train that propagates eastward and poleward from the eastern Pacific. This favors clearer skies near the Antarctic coast in summer, heating the surface ocean and reducing sea-ice coverage through autumn—to expose the coastal region to ocean swells and coastal currents that reduce local fast-ice coverage in winter (shown in Figure 10). As noted by Aoki (2017), the mechanism by which large-scale atmospheric processes affect the extent and rapidity of fast-ice breakup in Lützow-Holm Bay suggest a complex interplay between atmosphere and ocean interactions which may have wider relevance to attributing observed fast-ice variability in other Antarctic coastal sectors. In another study from the Indian Ocean sector, Fraser (2011) found an overall correlation of 0.45 between coastal fast-ice extent and the Southern Oscillation Index for 9 years (2000–2008).

4.6. Gaps in Our Knowledge of Fast Ice-Atmosphere Interactions

As discussed in this section, the atmosphere is a key domain in forcing and responding to environmental influences of fast ice. There has been much progress in understanding interactions between fast ice and the atmosphere, but the following areas stand out as requiring particular future focus.

19449208, 2023, 2, Downloaded from https://agupubs.onlinelibrary.wiley.com/doi/10.1029/2022RG000770 by University of Adelaide Alumni, Wiley Online Library on [16/08/2023]. See the Terms and Conditions (https://onlinelibrary.wiley.com/terms-and-conditions) on Wiley Online Library for rules of use; OA articles are governed by the applicable Creative Commons License

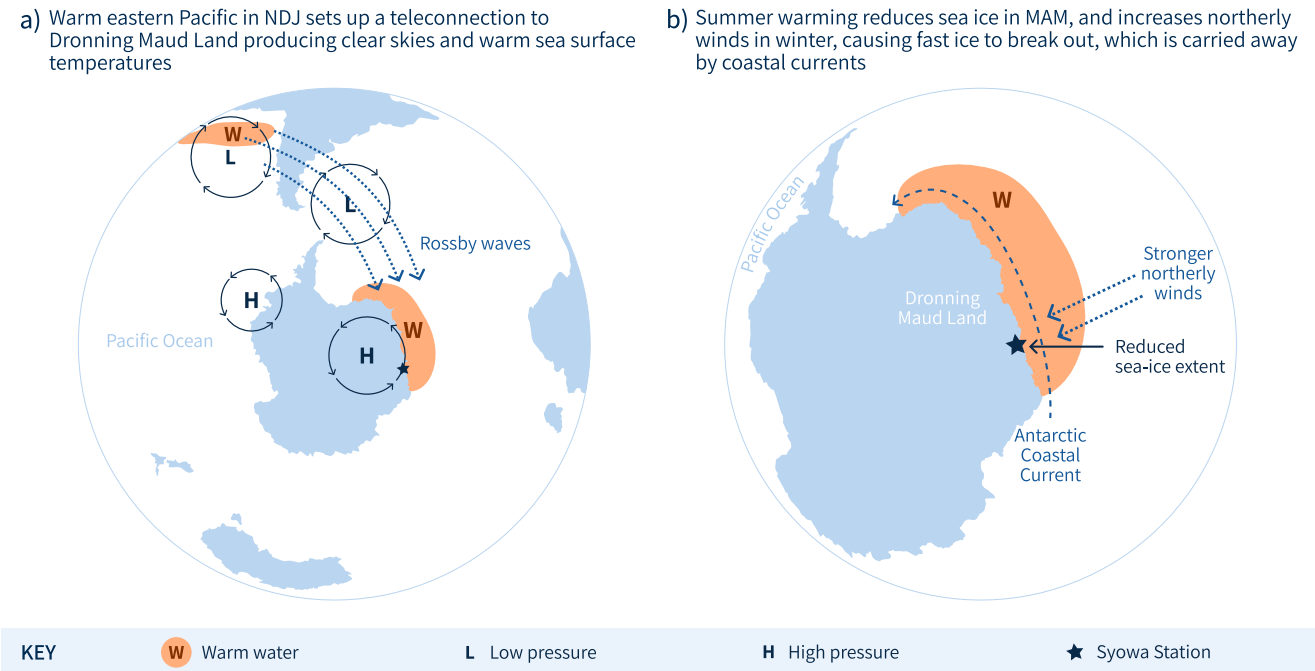

Figure 10. Summary of the large-scale atmospheric teleconnection process that favors reduced winter fast-ice near Syowa station in East Antarctica, according to findings by Aoki (2017). (a) Anomalous warm ocean temperatures in the tropical eastern Pacific Ocean in austral summer (NDJ) provide a teleconnection to Dronning Maud Land in Eastern Antarctica via a train of Rossby waves. (b) The resulting clear skies in the sea-ice zone near Syowa Station produce anomalous northerly winds, which reduce sea-ice extent in autumn (MAM) and favor enhanced winter fast-ice breakout.

There remains a strong need to continue and expand local studies of fast ice processes and their atmospheric interactions. New insights are likely to be gained by comprehensive automated measurements of basic variables such as in-situ temperature, brine concentration and heat flux, as well as regular synoptic measurements of the near-surface atmosphere and sub-ice water column. In this regard, automated stand-alone imaging systems (such as visible-light and near-infrared cameras) to obtain contextual data, and the use of drones and other deployable systems for remotely operated measurements, are likely to be particularly useful.

The large-scale climate modes evidently play a role in regionally influencing fast-ice properties such as extent and duration. This aspect has flow-on effects back the atmosphere. For example, as fast ice changes the size and locations of coastal polynyas, fast-ice distribution can locally influence heat fluxes from the ocean to the atmosphere in coastal regions. However, the apparent non-stationarity of the large-scale and local processes involved in the interactions between fast ice and the atmosphere, as well as the relative lack of long-term data sets, continue to pose challenges in developing an Antarctic-wide understanding. Further studies are needed to tease out the processes and climate system interactions responsible, particularly using circum-Antarctic data sets and atmosphere-ocean-sea ice model simulations. The latter component is considered in Section 5.

5. Ocean and Meteoric Ice Interactions With Fast Ice

Antarctic fast ice has complex, bi-directional links with physical aspects of the Southern Ocean. On the one hand, fast-ice formation and breakout (when fast ice breaks away to become pack ice; see also Sections 3 and 4 of this Review), as well as changes in thickness, are directly influenced by near-surface ocean properties such as temperature and salinity (e.g., Brett et al., 2020), as well as remote glaciological interactions such as platelet ice formation and accretion due to the creation of supercooled water underneath upstream ice shelves (as detailed in Hoppmann et al., 2020). On the other hand, the distribution of fast ice (shown in Figure 4 in Section 3) can drive changes in physical ocean properties, including the concentrated production of sea ice and subsequent formation of Dense Shelf Water (DSW) in persistent regions of open water adjacent to the coast known as coastal polynyas (Fraser et al., 2019), and modulate the on-shelf properties of Winter Water (WW) and modified Circumpolar Deep Water (mCDW; Herraiz-Borreguero et al., 2015; Kusahara et al., 2021). A summary of our understanding

19449208, 2023, 2, Downloaded from https://agupubs.onlinelibrary.wiley.com/doi/10.1029/2022RG000770 by University of Adelaide Alumni, Wiley Online Library on [16/08/2023]. See the Terms and Conditions (https://onlinelibrary.wiley.com/terms-and-conditions) on Wiley Online Library for rules of use; OA articles are governed by the applicable Creative Commons License

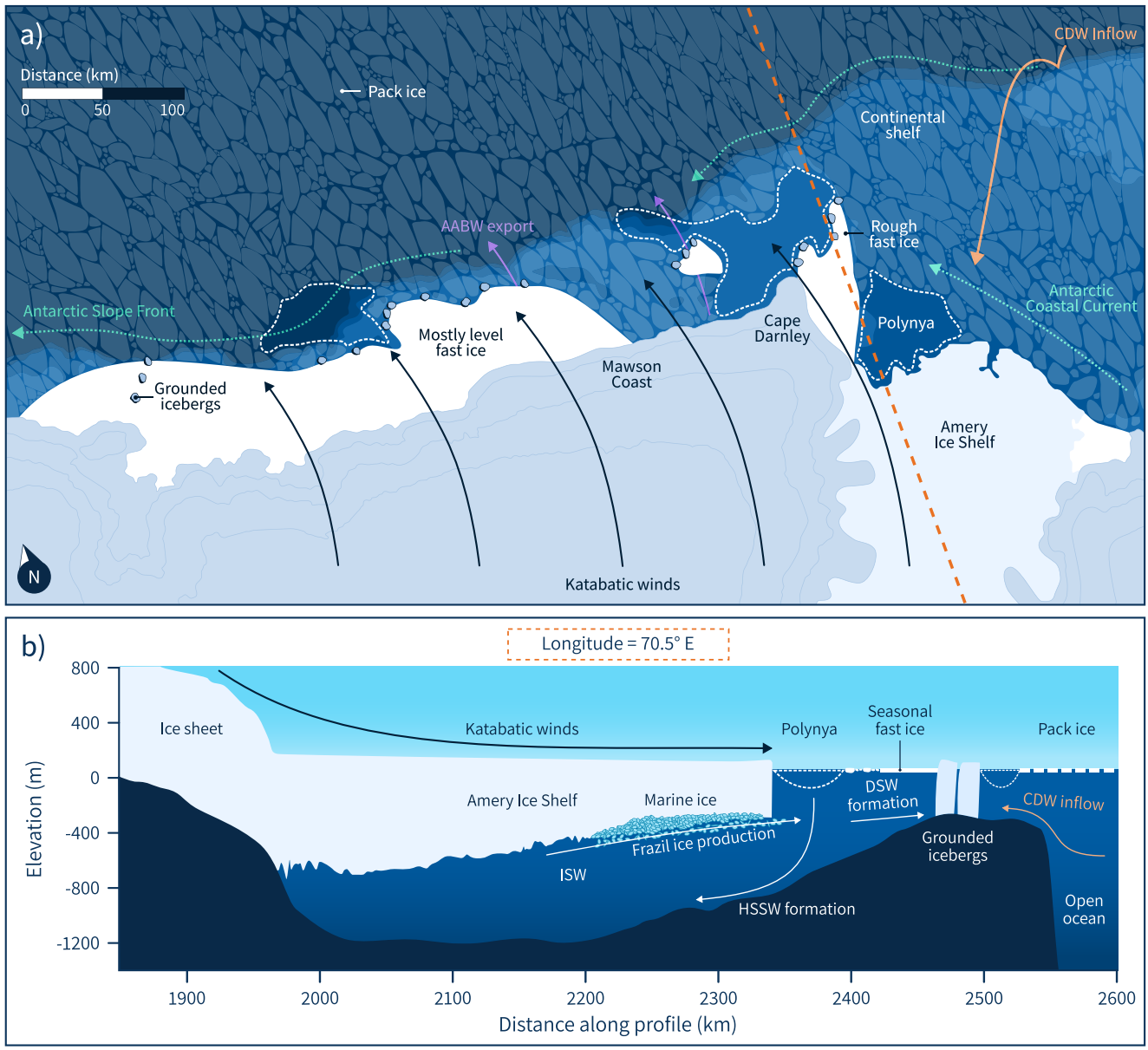

Figure 11. Schematic representation of wintertime fast ice-ocean-atmosphere interaction, based on the Mawson Coast/Prydz Bay region, East Antarctica. (a): Plan view indicating the location of fast ice (white) and the Amery Ice Shelf (light blue). Fast-ice distribution is controlled by the location of grounded icebergs (indicated as small blue polygons here). Coastal polynyas are outlined in dashed white lines, and form in the oceanic and atmospheric lee of both fast ice and the Amery Ice Shelf. (b): Transect along 70.5°E, chosen to highlight a range of coastal elements, including seasonal fast ice to the east of Cape Darnley, bounded by coastal polynyas to the northwest and southeast. This panel also highlights many interactions between fast ice and physical ocean properties detailed in the text. AABW is Antarctic Bottom Water. CDW is Circumpolar Deep Water. DSW is Dense Shelf Water. HSSW is High Salinity Shelf Water. ISW is Ice Shelf Water. Coastline and topographic data are from BedMachine version 3 (Morlighem et al., 2017).

of these links is provided in this section (and graphically depicted in Figure 11), along with coverage of the importance of the mechanical coupling between fast ice and floating glacial ice including ice shelves and glacier tongues.

5.1. Fast Ice-Ocean Interaction Observations

Strong offshore (primarily katabatic, as detailed by Huot et al., 2021) winds flowing out from the continent push pack ice away from the coast, forming regions of open water called coastal or latent-heat polynyas (Barber &

19449208, 2023, 2, Downloaded from https://agupubs.onlinelibrary.wiley.com/doi/10.1029/2022RG000770 by University of Adelaide Alumni, Wiley Online Library on [16/08/2023]. See the Terms and Conditions (https://onlinelibrary.wiley.com/terms-and-conditions) on Wiley Online Library for rules of use; OA articles are governed by the applicable Creative Commons License

Massom, 2007; Morales Maqueda et al., 2004). These polynyas are "hot spots" of heat transfer between the ocean and the atmosphere (e.g., Tamura et al., 2016), and are associated with fast ice in several ways:

- The presence of fast ice (and glacier tongues) is an important element for the formation of most Antarctic coastal polynyas by preventing the general westward (or northward along Victoria Land, ∼165°E, 75°S) advection of sea ice in the Antarctic Coastal Current (ACoC, depicted in Figure 11), thus enlarging coastal polynyas and encouraging higher sea-ice production; (Fraser et al., 2019; Massom, Hill, et al., 2001; Nihashi & Ohshima, 2015). High rates of sea-ice production can lead to the formation of DSW, which is a precursor to the formation of AABW in some regions (if it is able to overflow from the continental shelf into the deep ocean; Ohshima et al., 2013; Williams et al., 2010);
- Coastal polynyas are areas of intense frazil ice formation (e.g., Nakata et al., 2021; L. Thompson et al., 2020), some of which is incorporated into downstream fast ice (Massom, Hill, et al., 2001);
- High Salinity Shelf Water (HSSW) formation and buoyancy loss from intense sea-ice production within coastal polynyas during winter (Herraiz-Borreguero et al., 2015) primes the water column for thermohaline circulation and transports heat energy from the ocean surface. If the resulting HSSW is able to access a sub-ice shelf cavity, it can drive basal melting of ice shelves (Jacobs et al., 1992, see Figure 11c); and
- As described in Section 2.1.1, supercooled ISW can be formed as a result of the HSSW melting the base of the ice shelf. The ISW is relatively fresh and rises along the basal slope of the ice shelf, becoming in situ supercooled as the pressure decreases. Frazil ice can form within the ISW plume and grow into larger platelet ice crystals. Platelet ice can freeze onto the base of nearby fast ice and increase its thickness by accumulating into a porous mass of unconsolidated crystals called an SIPL (Langhorne et al., 2015; Hoppmann et al., 2020). This mechanism is enhanced during times of strong offshore winds and high polynya activity, and the thickness of the consolidated platelet ice and the SIPL can provide a metric for the volume of supercooled ISW outflowing for a given year (Brett et al., 2020).

In the case of thermodynamically-grown fast ice, the maximum thickness of fast ice in the Southern Ocean is influenced by heat exchange with the ocean, and thus upper ocean stratification (Maksym, 2019). In regions away from the influence of platelet ice, a typical average winter oceanic heat flux of 0–2 W m^{-2} (i.e., a positive oceanic heat flux) is observed, for example, in the Prydz Bay region (75°E, 68°S; Heil et al., 1996; Lei et al., 2010). This positive ocean heat flux increases in spring (to about 20 W m^{-2}), often due to solar heating of the upper ocean in nearby regions of low sea-ice concentration. Heil et al. (1996) show that average annual oceanic heat flux correlates with maximum fast-ice thicknesses, with a decrease from 11 to 6 W m^{-2} leading to an increase in thickness from 1.3 to 1.8 m. In regions where platelet ice is not observed, summer ocean heat fluxes under fast-ice in the Amundsen Sea (centered on ∼115°W) are of similar magnitude, averaging 17–19 W m^{-2}, and variable because of episodes of deep water upwelling (Ackley et al., 2015).

As discussed in Section 2, platelet ice is widely considered to be a component of fast ice in most regions around Antarctica, although observations are sparse and focused upon centers of human activity (see distribution in Figure 4 of Hoppmann et al., 2020). Platelet ice is associated with a negative ocean heat flux (Langhorne et al., 2015), that is, there is an apparent flow of heat from ice to ocean. Consequently, fast ice that includes a component of platelet ice is thicker than it would otherwise be (Hoppmann, Nicolaus, Hunkeler, et al., 2015; Hoppmann, Nicolaus, Paul, et al., 2015; I. J. Smith et al., 2012). For example, for first-year ice close to the McMurdo Ice Shelf, at least 0.25 m of the 2 m thick fast ice cover formed due to heat loss to the ocean (Gough et al., 2012; Purdie et al., 2006; Trodahl et al., 2000). Similarly, multiyear fast ice attached to the MGT (145°E, 67°S), was estimated to be between 10 and 55 m thick, and frazil accumulation must have contributed to its thickness (Massom et al., 2010).

Sea-ice thickness (including fast ice) is also influenced by the stabilization (stratification) of the upper water column in front of an ice shelf by the production of meltwater in deep ice shelf cavities. Using an ocean model with ice shelf cavity thermodynamics, Hellmer (2004) predicted that sea ice is up to 0.2 m thicker because deep convection is reduced, causing less heat transfer to the ocean surface and increasing sea-ice thickness. Since ice shelves occupy approximately half of the coastline (Fretwell et al., 2013), meltwater from the continent has the potential to affect large areas of the Southern Ocean.

As detailed in Hoppmann et al. (2020), platelet ice is a common feature in the western Ross Sea, particularly McMurdo Sound (165°E, 77°S) and Terra Nova Bay (e.g., 165°E, 75°S; Langhorne et al., 2015; Vacchi et al., 2012, and references therein), in Atka Bay in the southeastern Weddell Sea (7.5°W, 70.5°S; e.g., S. Arndt

19449208, 2023, 2, Downloaded from https://agupubs.onlinelibrary.wiley.com/doi/10.1029/2022RG000770 by University of Adelaide Alumni, Wiley Online Library on [16/08/2023]. See the Terms and Conditions (https://onlinelibrary.wiley.com/terms-and-conditions) on Wiley Online Library for rules of use; OA articles are governed by the applicable Creative Commons License

et al., 2020; Günther & Dieckmann, 1999, and references therein), and in East Antarctica (e.g., Moreçki, 1965; Penrose et al., 1994). In 1992, in the earliest fast-ice observation in the Amundsen Sea, Veazey et al. (1994) reported platelet ice only in a small portion of a single core. With this exception, there are no observations of platelet ice in the Amundsen and Bellingshausen seas (centered on ∼80°W) and along the Sabrina Coast (115°E–122°E; Hoppmann et al., 2020), probably because the continental shelf in these areas experience incursions of relatively warm Circumpolar Deep Water (CDW; Jacobs et al., 2011).

For a number of reasons, as detailed in Hoppmann et al. (2020), platelet ice may even be absent in close proximity to ice shelf cavities that are cold enough to produce ISW. The absence of platelet ice observations in front of parts of the Filchner–Ronne (centered on ∼55°W, 79°S) and the Ross (centered on ∼178°W, 81°S) ice shelves (Jacobs et al., 1985; Jeffries & Adolphs, 1997) are examples.

5.2. Numerical Modeling of Fast Ice and the Impact on Antarctic Coastal Environments

The horizontal spatial scale of Antarctic fast ice ranges from a few to ∼200 km (Fraser et al., 2012; see Figure 6 of this review for scale). Since the horizontal resolution of ocean components in current-generation climate models, which are used for centuries-long simulations and projections, is approximately one degree, fast ice and its effects have not been represented in such numerical models. However, recent satellite observations suggest that fast ice plays a vital role in shaping the icescape in polar coastal environments (Fraser et al., 2012; Nihashi & Ohshima, 2015), being particularly critical in locations of coastal polynyas, dense water formation, and the associated surface fluxes between atmosphere and ocean. Several modeling studies have demonstrated that different treatments of Antarctic coastal ocean grid points which should be covered with fast ice can have pronounced impacts on the accurate simulation of deep water formation and ocean thermohaline circulation (Hellmer, 2004; Kusahara & Hasumi, 2014; Stössel et al., 2007).

Numerical modeling of fast ice as a component of sea ice models is comparatively advanced in the Arctic, compared to the Antarctic. Recent Arctic sea-ice modeling studies (Lemieux et al., 2015; Lemieux et al., 2016) introduced a basal stress parameterization and modification of sea-ice tensile strength (König Beatty & Holland, 2010) to incorporate the sea-ice anchoring effect in shallow regions. This combination of the two modifications successfully reproduced the distribution of fast ice in several Arctic coastal regions. The addition of tidal currents further enhanced the realism of fast-ice simulation, by more realistically representing the ocean-ice stress field (Lemieux et al., 2018). On the Antarctic continental shelf, the presence of grounded icebergs plays a dominant role in the formation of fast ice (Fraser et al., 2012; Massom, Hill, et al., 2001), thus introducing another element of complexity when aiming for accurate prognostic modeling of Antarctic fast ice. As a first effort to include the dynamic effects of fast ice without dealing with the complexities of its prognostic modeling, several regional studies that include the blocking effect of sea ice by prescription of grounded icebergs have simulated the effects of fast-ice distribution to some extent (Kusahara et al., 2010), and others have prescribed a realistic (although static) fast-ice cover based on observations (Cougnon et al., 2017; Kusahara et al., 2017, 2021), in order to enhance the realism of their simulations.

Recent work (Huot et al., 2021; Van Achter, Fichefet, Goosse, & Moreno-Chamarro, 2022; Van Achter, Fichefet, Goosse, Pelletier, et al., 2022) has demonstrated the significant achievement of realistic prognostic Antarctic fast-ice simulation in regional high-resolution sea ice-ocean models with a spatial resolution of approximately 2 km for the first time, by combining the modified tensile strength parameterization of König Beatty and Holland (2010) and Lemieux et al. (2016) together with a relatively simple "fastening" mechanism whereby grounded icebergs are prescribed as single grid cell "islands" (but without dynamic or thermodynamic interactions with the ocean in the case of Huot et al., 2021). The latter study used their realistic fast-ice simulation to study in detail the effects of increasing the resolution of the atmospheric forcing component of the model, finding that their model was able to accurately reproduce the location and strength of sea-ice production. Van Achter, Fichefet, Goosse, Pelletier, et al. (2022) and Van Achter, Fichefet, Goosse, and Moreno-Chamarro (2022) studied the effects of realistic fast ice on the basal melt of the adjacent Totten and Moscow University ice shelves (∼112°E–122°E, 67°S) in present-day and future warming conditions. Both analyses greatly benefited from more realistic on-shelf ice-ocean interaction made possible with prognostic fast ice. These studies have paved the way for prognostic Antarctic fast-ice simulation, and point to the future of high-resolution coastal sea ice-ocean model studies where the inclusion of fast ice becomes the rule, rather than the notable exception. At present, there are no circum-Antarctic studies with simulated fast-ice, but with the recent release of a data set of high resolution,

19449208, 2023, 2, Downloaded from https://agupubs.onlinelibrary.wiley.com/doi/10.1029/2022RG000770 by University of Adelaide Alumni, Wiley Online Library on [16/08/2023]. See the Terms and Conditions (https://onlinelibrary.wiley.com/terms-and-conditions) on Wiley Online Library for rules of use; OA articles are governed by the applicable Creative Commons License

satellite-based circum-Antarctic fast ice distribution (Fraser et al., 2020) which has the potential to be used as a validation data set, it is expected that such circumpolar fast ice modeling studies will be conducted in the near future.

From a physical oceanographic perspective, the presence of fast ice largely modifies surface fluxes of momentum, heat, and freshwater. Figure 11 depicts the major oceanographic features that influence fast ice. In the rest of this subsection, we review studies that have focused on the physical roles of fast ice and its impact on Antarctic coastal environments.

5.3. Regional Effects of Fast Ice on Ocean Conditions

The Southern Ocean is characterized by a predominant westerly wind regime at latitudes of about 55°S, and experiences the frequent passage of eastward-traveling extra-tropical cyclonic systems. Further south, along the Antarctic coast, south-easterly katabatic-driven winds predominate over the coastal margin throughout the year, with a maximum wind speed occurring in winter and a minimum in summer (Budd, 2004). The momentum input to the ocean associated with these south-easterly near-coastal (and, further to the north, easterly) winds is the driving force for the ACoC and Antarctic Slope Front (ASF) current (see Figure 11), located on the shelf and just offshore of the shelf break regions, respectively (A. F. Thompson et al., 2018).

Since fast ice is horizontally immobile, its presence prohibits wind stress input to the ocean, and this has impacts on the ocean structure and currents. The presence of fast ice leads to logistical difficulties for in situ observation of the ocean below fast ice. Under such circumstances, Lützow-Holm Bay in East Antarctica (centered on ~37°E, 69°S), Ryder Bay on the West Antarctic Peninsula (68.5°W, 67.5°S), and Atka Bay serve as examples of well-studied areas where fast-ice cover is well established, and is relatively easy to access from coastal stations. At these locations, there are oceanographic data near or under fast ice that cover a relatively extensive area (Lützow-Holm Bay) or for multi-year (Ryder Bay and Atka Bay). As a result, the relationship between fast-ice cover and oceanic variability has been relatively well studied. In this subsection, we focus on these regions and describe the related literature below.

Along the Antarctic coastal margins, stronger alongshore wind stresses in autumn and winter increase Ekman convergence (downwelling), thickening the WW layer, and weaker wind stresses in the summer season relax the Ekman convergence, leading to a relatively thin WW layer. In a regional study of Lützow-Holm Bay (depicted in Figure 6), Hirano et al. (2020) pointed out that this mechanism can be used to explain seasonal changes in the thickness of the CDW below the WW layer, which intrudes from the shelf break to the bay. Kokubun et al. (2021) also confirmed, from biologging data (Weddell seals), the seasonal cycle of the WW over the relatively extensive region from 35°E to 50°E. Observational and theoretical studies (Ohshima, 2000; Ohshima et al., 1996) revealed that the distribution of fast ice plays a critical role in the direction and magnitude of sub-seasonal coastal current under the fast ice, using in situ current observations and wind-driven shelf wave theory including the insulation effect of wind stresses by the fast-ice cover.

Kusahara et al. (2021) performed numerical experiments of an ocean-sea ice-ice shelf model with and without fast-ice cover in Lützow-Holm Bay. By this combination of experiments, the authors were able to examine the roles of fast-ice interactions with the ocean and cryosphere. In their model, fast-ice covered regions were treated as thin ice shelf grid cells, and there were no dynamical or thermodynamical atmosphere-ocean interactions, except for realistic representation of freshwater flux to the ocean based on the basal melt rate of fast ice. In the experiment without fast-ice cover, the newly-formed cold and saline water mass associated with winter sea-ice production in the bay destratified the local water column. On the other hand, multi-year fast ice (in the experiment with fast-ice cover) contributed to strengthening the stratification in the bay by a combination of a very effective thermal insulating effect and stratification from the surface input of meltwater, from the basal melt of the fast ice. The difference in the ocean stratification between the two experiments plays a major role in regulating regional coastal water mass transport and formation, impacting ice-ocean interaction at the Shirase Glacier located in the southern part of the bay.

Brearley et al. (2017) showed from multi-year mooring observation that in Ryder Bay, the presence or absence of fast ice causes significant differences in the ocean mixing between surface and subsurface waters, affecting the ocean stratification and heat content. In the absence of fast ice, wind stress on the ocean surface enhances the mixing of Antarctic Surface Water (AASW) and CDW, whereas in the presence of fast ice, mixing is not excited,

19449208, 2023, 2, Downloaded from https://agupubs.onlinelibrary.wiley.com/doi/10.1029/2022RG000770 by University of Adelaide Alumni, Wiley Online Library on [16/08/2023]. See the Terms and Conditions (https://onlinelibrary.wiley.com/terms-and-conditions) on Wiley Online Library for rules of use; OA articles are governed by the applicable Creative Commons License

and thus the mixing of surface and subsurface waters is suppressed. Inall et al. (2021) also showed that while fast ice suppresses the total turbulence in the ocean beneath it, tides can excite turbulence in a thin boundary layer just below the fast ice, which is comparable in magnitude to wind-driven turbulence in a fast ice-free surface. This indicates that fast ice plays a dual role in insulating wind-driven turbulence input to the ocean while providing a solid boundary for generating tidal turbulence.

S. Arndt et al. (2020) found that summertime warm AASW formed in sea ice-free areas in front of the fast ice is responsible for regulating the summer evolution of fast ice in Atka Bay (depicted in Figure 9). The easterly wind pushes the warm surface water in summer under the fast ice. This mechanism is similar to mode 3 melting that Jacobs et al. (1992) introduced to account for ice-shelf basal melting. Since it is much thinner than the Antarctic ice shelf, fast ice is more vulnerable to ocean surface conditions interacting with the atmosphere, compared to an ice shelf.

5.4. Couplings Between Fast Ice and Ice Shelves

In this section, we provide a brief overview of current knowledge of potentially-important and region- and season-dependent roles of fast ice in modulating the dynamics, extent and stability of floating ice-sheet margins around Antarctica, based largely on satellite observations. Evidence for strong mechanical coupling comes from the MGT in East Antarctica (Massom et al., 2010), where a large slab of perennial fast ice estimated to be up to at least 25 years old and tens of meters thick remained attached to the eastern glacier-tongue flank until the MGT calved in 2010. Time series analysis of satellite SAR images from 1997 to 2007 showed that the fast ice advanced with the floating glacier tongue and deformed with it, with major rift systems that originated in the MGT propagating for large distances into the multi-year fast ice and persisting and co-evolving there. These factors led Massom et al. (2010, 2015) to surmise that fast ice is an additional factor influencing the stability (i.e., increasing the structural integrity) of floating Antarctic ice-sheet margins (including ice shelves) while also decreasing iceberg calving (see also Wuite, 2006). At the same time, satellite SAR interferometry work around Campbell Glacier Tongue (Terra Nova Bay) by Han and Lee (2018) has shown that glaciers can exert substantial shear strain on fast ice.

Close temporal coincidence observed between iceberg calving events and breakouts of adjacent fast ice observed in certain locations around Antarctica implies causality between fast ice and calving processes (calving is defined here as the physical detachment of ice chunks from the termini of glaciers or ice shelves). W. Robinson and Haskell (1990) identified a fast-ice breakout event as being the primary driver of a March 1990 calving of the Erebus Glacier Tongue in McMurdo Sound (Ross Sea), via its effect in directly exposing the tongue to incoming ocean swell waves that would otherwise be damped by the presence of a protective fast-ice buffer (e.g., Voermans et al., 2021)—with fast-ice breakout also being an apparent factor in a subsequent (2013) calving event (Stevens et al., 2013). Unimpeded by fast ice (and surrounding pack ice), ocean swells can exert flexural strains on ice-shelf outer margins, to potentially enlarge existing structural weaknesses there such as rifts and crevasses (Holdsworth & Glynn, 1978), thereby increasing the likelihood of and/or triggering outer-margin fracture and iceberg calving (Massom et al., 2018). This also depends on other ice shelf-specific factors, such as the structural integrity and physical setting (Cook & Vaughan, 2010).

At the same time, the breakout of fast ice also enables free-floating (ungrounded) icebergs to drift away from their calving locale. When present and due to its consolidated stationary nature, fast ice can hold such icebergs in place, to delay/prevent their dispersal from area of origin. For example, the large iceberg created by the calving of the Ninnis Glacier Tongue (George V Coast) in 2001 remained stationary adjacent to its calving point for at least 18 months, and only drifted away following a breakup of adjacent perennial fast ice (Massom, 2003).

The apparent key role of fast ice presence/absence in modulating iceberg calving and dispersal is further illustrated in other satellite-based observations from both East and West Antarctica. Miles et al. (2017) revealed a large near-simultaneous calving of 2,900 km^2 of ice across six marine-terminating outlet glaciers in Porpoise Bay (Wilkes Land, East Antarctica) in January 2007, following the breakup of adjacent multi-year fast ice. Also in East Antarctica, a major calving of the Shirase Glacier Tongue (SGT) immediately followed a large fast-ice breakup in Lützow-Holm Bay (Aoki, 2017). Miles et al. (2023) confirmed the relationship between fluctuations in the seaward extent of the SGT and fast-ice presence/absence, with periods of ice-tongue advance and lengthening being correlated with persistent fast ice and shortening/loss events following sporadic fast-ice breakouts

19449208, 2023, 2, Downloaded from https://agupubs.onlinelibrary.wiley.com/doi/10.1029/2022RG000770 by University of Adelaide Alumni, Wiley Online Library on [16/08/2023]. See the Terms and Conditions (https://onlinelibrary.wiley.com/terms-and-conditions) on Wiley Online Library for rules of use; OA articles are governed by the applicable Creative Commons License

(largely in summer; see also Aoki, 2017). The effect of fast ice in limiting iceberg calving (and dispersal), thereby enabling ice-front advance, is also shown for the Cook Ice Shelf (George V Land) by Miles et al. (2018). Further work by Arthur et al. (2021) highlights the role of a breakout of multi-year fast ice in triggering a rapid breakup of part of the structurally-weak Voyeykov Ice Shelf in Wilkes Land in 2007. In a similar fashion, a major calving of the full 18 km length of the Parker Ice Tongue in Victoria Land in March 2020 coincided with anomalous breakouts of the enclosing fast ice (Gomez-Fell et al., 2022).

Other satellite-based work (Massom et al., 2018) showed that major rapid disintegration events of the Wilkins Ice Shelf (western Antarctic Peninsula) in 2008 and 2009 coincided with the breakup and removal of fast ice attached to its fractured and weakened northern and northwestern fronts. These fast-ice breakout events in turn coincided with the lack of a protective pack-ice buffer offshore; fast ice is itself vulnerable to breakup by ocean swells (Langhorne et al., 2001), which can be damped by adjacent pack ice (e.g., Stopa et al., 2018). These observations again imply that when present, fast ice can play an important role in maintaining the structural integrity of weakened outer margins of ice shelves whilst also protecting them from ocean swells—to decreasing the likelihood of ice-shelf breakup/disintegration (Massom et al., 2010, 2018). In a subsequent study in the Amundsen Sea Embayment (2000–2018), Miles et al. (2020) showed that an increasingly fractured and weakened Thwaites Glacier Tongue has dependency on fast ice for its structural integrity, and is therefore vulnerable to changes in fast-ice persistence. Fast ice has also been shown to be a key factor in modulating the outer-margin stability of the Larsen C and D ice shelves on the eastern Antarctic Peninsula by Christie et al. (2022).

Work on the Totten Ice Shelf (Greene et al., 2018) further shows that fast ice can act as a physical buttress to modulate the seasonal dynamics of advancing ice shelves, with an annual acceleration in ice discharge following spring fast-ice breakup. Moreover, Gomez-Fell et al. (2022) showed that in summer with its lower fast-ice coverage, the Parker Ice Tongue experienced higher velocities (by 11%) compared to winter. Elsewhere, there is little/no evidence that fast ice plays any substantial role in buttressing the Shirase Glacier (Miles et al., 2023), with Nakamura et al. (2010) recording only a minimal (0.8% ± 1.3%) change in ice speed at the grounding line following a partial fast-ice breakout event in 1998, and Nakamura et al. (2022) reporting no distinguishable ice-speed change after a subsequent fast-ice breakout in 2017.

Taken together, the findings presented above suggest that fast-ice change has implications for the fate of Antarctic ice-sheet margins, future ice-sheet discharge and sea-level rise (Massom et al., 2018)—but that this relationship also has strong ice shelf-specific and seasonal dependence. Much is still to be learned, however, about the exact nature of the fast ice-ice shelf couplings, and substantial gaps remain in our quantitative understanding of the linkages and their model parameterization and investigation.

5.5. Infrequent Major Changes in Grounded Iceberg Distribution

Although fast-ice extent varies seasonally and inter-annually to some degree, it generally forms and breaks out following a regular climatological pattern (Fraser et al., 2021). Off the Adélie and George V Land region, East Antarctica (135°E–155°E), there was extensive fast ice to the east of the MGT and nearby grounded icebergs. As detailed by Massom et al. (2010), the MGT, grounded icebergs and fast ice were closely linked, and formed the local complex "icescape," causing profound impacts on the ocean conditions, particularly through dense water mass formation (Cougnon et al., 2017). In early 2010, a large portion of the MGT calved (Tamura et al., 2012) following the ungrounding of giant iceberg B9B, which had been grounded east of the MGT for several decades (Leane & Maddison, 2018). The MGT calving resulted in a significant breakout of the local fast ice, significantly changing the icescape off the Adélie and George V Land region (Fogwill et al., 2016). This complete reconfiguration in icescape has changed the locations and size of coastal polynyas, the associated sea-ice formation, and the subsequent DSW formation (Kusahara et al., 2011, 2017; Tamura et al., 2012). Observational studies (Lacarra et al., 2014; Shadwick et al., 2013) reported regional freshening over the Adélie Depression just after the calving event and implicated the root causes were the local melting of a large amount of very thick fast ice (Massom et al., 2010). Several other examples of equally dramatic icescape change exist, for example, the calving of iceberg B15A from the Ross Ice Shelf in 2001, which grounded in the southwestern Ross Sea for several years, thus blocking the seasonal export of sea ice from McMurdo Sound and leading to anomalously extensive fast-ice cover in the Sound (Brunt et al., 2006). This kind of infrequent event can have a significant impact on the Antarctic coastal ocean environment. Such changes, which could potentially occur anywhere along the Antarctic coastal margin (especially as ice shelf retreat progresses into the 21st century; Greene et al., 2022), make

19449208, 2023, 2, Downloaded from https://agupubs.onlinelibrary.wiley.com/doi/10.1029/2022RG000770 by University of Adelaide Alumni, Wiley Online Library on [16/08/2023]. See the Terms and Conditions (https://onlinelibrary.wiley.com/terms-and-conditions) on Wiley Online Library for rules of use; OA articles are governed by the applicable Creative Commons License

medium- and long-term prediction of fast-ice extent difficult, even if prognostic fast ice is incorporated into sea ice-ocean models.

5.6. Gaps in Our Knowledge of Fast Ice-Ocean-Ice Margin Interaction

As discussed in this section, the incorporation of prognostic fast ice into regional and circum-Antarctic coupled sea ice-ocean models is a high priority. The formation of Antarctic fast ice results from complicated interactions between sea ice, ocean, atmosphere, coastal configuration, bathymetry and grounded icebergs (of which no large-scale data set currently exists), and its accurate model representation is perhaps a more challenging problem than its Arctic counterpart. Nevertheless, as shown by Huot et al. (2021) and Van Achter, Fichefet, Goosse, Pelletier, et al. (2022), this problem is tractable, and the benefits of solving it are numerous. Waves are another missing component from most regional ice-ocean coupled models, and likely control the nature and timing of fast-ice breakout in many regions (Crocker & Wadhams, 1989a). A further benefit in simulating wave-ice interaction is that the resulting wave field incident upon ice shelves may also be used for studies of ice shelf-wave interaction (including wave-induced flexure, calving and disintegration; Teder et al., 2022).

6. Biogeochemical Sources, Pathways and Sinks in Antarctic Fast Ice

In this section we aim to show that in terms of biogeochemistry, fast ice is differentiated from pack ice due to its proximity to coastal sources of nutrients. This proximity to the coast and several Antarctic bases has also allowed more time series experiments to be carried out on fast ice compared to pack ice, although these temporal studies do remain short-lived (<1 month) relative to the duration of fast ice (often >9 months). Data emanating from fast ice time series experiments therefore allow an easier parameterization of biogeochemical models than pack ice data, as well as comparison between field data and model outputs. Fast ice, being more likely to be multi-year, allows higher accumulation of nutrients, ice-associated (sympagic) algae and carbon including exopolysaccharides (EPS), leading to a "high nutrient high chlorophyll paradox." The higher biomass relative to first-year pack ice may also lead to greater fluxes of climate relevant gasses per unit area of fast ice. Conversely, and highlighting the complexity of this dynamic environment, greater mean thickness of multi-year fast ice compared to pack ice with lower internal permeability due to insulation may impact the exchange between the overlying atmosphere and sympagic algae or the underlying water column.

6.1. Nutrients

6.1.1. Macronutrients

The major source of nutrients to Antarctic fast ice is seawater, with a small contribution from the atmosphere (Duprat et al., 2019; Nowak et al., 2018). Surface water macronutrient concentrations in autumn are influenced by vertical mixing with circumpolar deep water (CDW) as well as the degree of biological nutrient uptake by phytoplankton blooms in the preceding summer season and subsequent remineralization of the organic matter produced in seawater (Henley et al., 2017, 2020). Turbulent mixing via wind and stronger tidal currents on the coast can also contribute to this flux (Brearley et al., 2017; Inall et al., 2021), even when fast ice sits atop. Incorporation of nutrients via platelet layers can contribute to the higher stocks in fast ice than pack ice (Arrigo et al., 1995) in regions close to or downstream of ice shelves (Günther & Dieckmann, 1999). Nutrient concentrations in basal fast ice are generally much larger than in upper or internal layers where concentrations occasionally fall below the detection limits of the analytical instruments (Lim et al., 2019).

6.1.2. Iron

The vertical profiles of the micronutrient dissolved iron (DFe) in fast ice generally show strong basal enrichment and may also display surface enrichment (Duprat et al., 2019; Grotti et al., 2005; van der Merwe et al., 2011). Particulate iron (PFe) often has an L-shaped vertical profile, displaying a pronounced basal ice enrichment that generally correlates positively with chlorophyll-*a* (Chl*a*) and particulate organic carbon (POC) (Duprat et al., 2019; Grotti et al., 2005; van der Merwe et al., 2009, 2011). While both pack and fast ice rely on active uptake and incorporation into internal or external pools within sympagic algae communities to recreate the observed distribution of DFe and PFe, the ambient seawater concentration near coastal fast ice results in higher Fe enrichment in basal fast ice compared to pack ice (Lannuzel et al., 2016). This particularly high PFe content

19449208, 2023, 2, Downloaded from https://agupubs.onlinelibrary.wiley.com/doi/10.1029/2022RG000770 by University of Adelaide Alumni, Wiley Online Library on [16/08/2023]. See the Terms and Conditions (https://onlinelibrary.wiley.com/terms-and-conditions) on Wiley Online Library for rules of use; OA articles are governed by the applicable Creative Commons License

stems from the proximity of fast ice to coastal sources like subglacial discharge of meltwater (Duprat et al., 2019) and resuspension of marine sediments (Grotti et al., 2005), which are generally enriched in coastal waters in comparison to dust sources in the overlying atmosphere. The main source of Fe to fast ice is from below (as for other nutrients), although dust supply from ice-free areas such as the McMurdo Dry Valleys (De Jong et al., 2013) and the Vestfold Hills (Duprat et al., 2019) can be deposited atop fast ice. This atmospheric Fe may eventually percolate through the fast-ice cover when brine volume fraction increases, and become available for biological uptake by sympagic algae communities.

Ligands include a wide range of molecules which bind to DFe due to attraction between their negative charge and the positive charge of DFe. This binding prevents particle scavenging and conversion to the particulate fraction, and therefore increases the availability of DFe in sea ice for sympagic algae. Ligands may be of organic and/or inorganic origins, and include EPS (see below), humic substances (Hassler et al., 2020; Laglera et al., 2020; Powell & Wilson-Finelli, 2003), and siderophores (Velasquez et al., 2011). Aeolian (i.e., wind-carried) deposition and glacial meltwaters may also supply Fe-binding ligands along the Antarctic coast and therefore, to fast ice (Genovese et al., 2023; Gerringa et al., 2012; Hassler et al., 2020). Regardless of their origin and nature, Antarctic fast ice exhibits high concentrations of Fe-binding ligands (Genovese et al., 2023; Lannuzel et al., 2015) relative to Antarctic seawater (Southern Ocean Ligand Collection; A. J. Smith et al., 2022). When fast ice melts in spring and summer, it has the potential to enrich seawater with DFe and ligands, thereby increasing Fe availability and boosting local phytoplankton productivity (De Jong et al., 2013; Duprat et al., 2019; van der Merwe et al., 2011). Such Fe fertilization events from fast ice are not restricted to summer, with large-scale blooms also confirmed in autumn from satellite images and in situ measurement off Cape Darnley (Lieser et al., 2015).

6.1.3. Nutrient Limitation

It is assumed that nutrients are not limiting for fast-ice algae and that instead, light availability generally controls the spatial distribution of ice algae (Cota et al., 1991). However, nutrient levels can become limiting toward the end of the bloom season as algae biomass peaks, typically in summer. Vertical sampling of fast ice from McMurdo Sound also revealed evidence of progressive nutrient limitation with distance above the ice/water interface (McMinn, Skerratt, et al., 1999). This is especially the case for silicate which tends to become depleted much faster than nitrate and phosphate based on time series observations carried out in fast ice at Casey (van der Merwe et al., 2009), Dumont d'Urville (Roukaerts et al., 2021) and Davis (Lim et al., 2019) research stations. Empirical silicate uptake studies as well as biogeochemical modeling suggest that silicate demand by fast-ice diatoms is much higher than for open ocean diatoms, with half saturation constants of 50–60 μM measured (Arrigo & Sullivan, 1994; Arrigo et al., 1993; Lim et al., 2019; Saenz & Arrigo, 2012, 2014) relative to 3.9 μM in the ocean. Iron is generally not considered limiting for ice algae in fast ice (Duprat et al., 2019; van der Merwe et al., 2009) although sea-ice algae Fe uptake rate experiments have yet to be carried out.

6.2. Organic Matter

Organic matter concentrations in fast ice can be several orders of magnitude higher than in seawater or pack ice (Herborg et al., 2001; Thomas & Dieckmann, 2002; Thomas et al., 2001). This organic matter can either be produced in sea ice in situ via biological activity or originate from seawater and become trapped during sea-ice formation (Giannelli et al., 2001).

6.2.1. Dissolved and Particulate Organic Carbon (DOC and POC)

DOC has been observed with generally consistent concentrations along vertical sea-ice horizons due to incorporation during formation (e.g., 30.5 ± 21 μM; van der Merwe et al., 2009), but also enhanced within basal and platelet ice (e.g., 1,277 μM; Cozzi, 2008) coincident with sympagic algae growth. The particulate fraction generally displays a similar L-shaped vertical profile to Chl*a* (Meiners et al., 2018). POC maximum concentrations were observed in the lower 5–10 cm of fast ice collected in East Antarctica (e.g., 2,100 μM in van der Merwe et al. (2011); 3,270 μM in Lim et al. (2019); 2,600 μM in Roukaerts et al. (2021)) and Terra Nova Bay in the Ross Sea (2,767 μM in Cozzi & Cantoni, 2011). The lowest 3 cm of ice, that is, the ice-ocean interface layer, may display POC concentrations up to 25,000 μM (Roukaerts et al., 2021) coincident with pronounced green-brown discoloration.

19449208, 2023, 2, Downloaded from https://agupubs.onlinelibrary.wiley.com/doi/10.1029/2022RG000770 by University of Adelaide Alumni, Wiley Online Library on [16/08/2023]. See the Terms and Conditions (https://onlinelibrary.wiley.com/terms-and-conditions) on Wiley Online Library for rules of use; OA articles are governed by the applicable Creative Commons License

6.2.2. Exopolysaccharides (EPS)

EPS are organic molecules produced by sea-ice algae and bacteria, occurring externally to the cells. EPS span across multiple size ranges from dissolved (<0.4 μm) to particulate (>0.4 μm) size fractions (Verdugo et al., 2004). EPS are hypothesized to facilitate cryoprotection in this salinity and temperature-extreme environment (Krembs et al., 2011). However, the production of EPS in fast ice, and sea ice generally, may go beyond cryoprotection. EPS are negatively charged (Kaplan et al., 1987), potentially favoring the retention of positively charged ions such as dissolved Fe^{2+} and Fe^{3+} in sea ice (Meiners & Michel, 2017) and helping explain the high Chl*a*—high nutrients paradox observed in fast ice for some elements (see below).

Particulate EPS can constitute, on average, 50% of POC, and was found to correlate significantly with both POC and Chl*a* (van der Merwe et al., 2009) therefore suggesting an algal origin of sea-ice EPS (Aslam et al., 2016). Therefore, particulate EPS tends to accumulate through the growth season due to and coincident with the sympagic algal community (van der Merwe et al., 2009). As a result, multi-year fast ice, with high POC and Chl*a* and multiple seasons of autochthonous EPS production should lead to higher concentrations of EPS than in first year pack ice. However, targeted studies are required in multi-year Antarctic fast ice to quantify the particulate but also the potentially large dissolved EPS fraction.

6.3. High Nutrients—High Chl*a* Paradox: The Role of Microbial Biofilms

In the surface ocean, proxies of algal biomass (e.g., Chl*a* and POC) are generally negatively correlated with dissolved nutrient concentrations due to phytoplankton uptake of nutrients for growth. This inverse correlation has also been observed in Antarctic pack and fast ice between proxies of algal biomass and dissolved Fe (normalized to brine volume, van der Merwe et al., 2009). However, in a paradox somewhat unique to sea ice with high biomass accumulation, a co-occurrence of high concentrations of Chl*a* (and POC) and macronutrients has been observed in basal Antarctic fast ice (Fripiat et al., 2015; Lim et al., 2019; Riaux-Gobin et al., 2013; Roukaerts et al., 2021; Thomas & Dieckmann, 2002; van der Merwe et al., 2011). This paradox has made realistic sea-ice biogeochemistry model simulations of both Chl*a* and nutrients difficult in fast ice. As more nutrients are supplied than utilized, an alternative internal source of nutrients may be unaccounted for. Roukaerts et al. (2021) used a combination of time series field data and Nutrient, Phytoplankton, Zooplankton and Detritus (NPZD) modeling to put forward the potential role of biofilms in reconciling the high Chl*a*, high nutrients paradox observed in Antarctic fast ice. The biofilm concept allows both nutrient uptake by sea-ice autotrophs and simultaneous and coincident recycling by sea-ice heterotrophs within sub-centimeter scales. The biofilm therefore leads to a mutualistic interaction between autotrophs and heterotrophs in fast ice. The high nutrient, high Chl*a* feature may also occur in pack ice, but a lack of time series studies makes comparison with model outputs more difficult in pack ice than fast ice.

6.4. Organic Carbon Flux Below Fast Ice

Since DOC and POC (including EPS and iron-binding ligands) are enriched in fast ice relative to seawater (Cozzi, 2014; Genovese et al., 2023; Lannuzel et al., 2015; van der Merwe et al., 2009), their release into seawater when fast ice melts has important ramifications on coastal productivity, export and carbon burial in sediments. Sediment trap deployments under pack ice are logistically challenging due to increased water depth and exposure to storms making moorings prone to failure. As a result, seasonal carbon export data are lacking in pack ice. However, sediment traps deployed under fast ice off the King Sejong Station show that the lithogenic and biogenic particle fluxes change through the season, with lithogenic particles (from snow melt and sediment resuspension) dominating the pool of particles exported year-round toward the seafloor in the area. The biogenic winter flux is an order of magnitude lower than the summer contribution, which peaks in January and February as a result of fast-ice melt (Khim et al., 2007). A significant fraction of diatoms under fast ice may however be consumed by heterotrophic dinoflagellates, as seen off Syowa Station in summer (Ichinomiya et al., 2008) and as a consequence the export rate can be highly variable. The export of organic carbon and biogenic silica (diatom frustules) from fast ice to the sediments is clearly preserved in sediment cores, as seen in McMurdo Sound where local production within and below sea ice and by advection from open water areas of the southwestern Ross Sea were suggested to enrich sediments in carbon and silica (Dunbar et al., 1989). Organic matter derived from fast

19449208, 2023, 2, Downloaded from https://agupubs.onlinelibrary.wiley.com/doi/10.1029/2022RG000770 by University of Adelaide Alumni, Wiley Online Library on [16/08/2023]. See the Terms and Conditions (https://onlinelibrary.wiley.com/terms-and-conditions) on Wiley Online Library for rules of use; OA articles are governed by the applicable Creative Commons License

ice has been shown to support a large fraction of total benthic biomass (e.g., 39%–71%; Wing et al., 2018), and affects the habitat and diet of coastal Antarctic benthic species (Caputi et al., 2020; Cozzi, 2014).

6.5. Gases

The seasonal formation and melt of fast ice directly controls how much carbon dioxide (CO_2) is exchanged between the ocean and the atmosphere. Fast ice can act as a source or sink of CO_2, depending on seasonal changes in sea-ice physics, chemistry, and trophic (autotrophic vs. heterotrophic) structure (van der Linden et al., 2020). Fast ice also regulates the emission of other climate-relevant gases such as dimethyl sulfide (DMS) (B. Delille et al., 2007) which possibly initiates a negative climate feedback.

6.5.1. Carbon Dioxide

Studies on CO_2 dynamics in Antarctic fast ice are rare and have exclusively focused on temporal rather than regional trends. Initial work carried out in East Antarctica near Dumont D'Urville Station during a time series in November–December showed that fast ice is a sink of CO_2 in spring (B. Delille et al., 2007), a result supported by later assessments in Antarctic pack ice (B. Delille et al., 2014). This CO_2 drawdown in spring fast ice is driven by autotrophic activity, which also promotes the decrease of partial pressure of CO_2 (pCO_2). The process may be aided by calcium carbonate ($CaCO_3$) precipitation, leading to a shift from CO_2 oversaturation to a marked CO_2 undersaturation (pCO_2, 30 dPa) within the brine system over the course of a month-long study (B. Delille et al., 2007, 2014). Building on this initial work in spring, a year-round survey was carried out in fast ice at Cape Evans (van der Linden et al., 2020). Results show that the drivers of CO_2 dynamics are depth-dependent, given that CO_2 uptake or emission via biotic and abiotic processes vary between surface, interior and basal fast ice. In surface ice, and similar to the spring time series mentioned above, CO_2 outgassing from sea ice to the atmosphere was observed in the winter time, while CO_2 uptake was observed later in the season in spring (van der Linden et al., 2020). In addition to this seasonal pattern, a diurnal signal was also observed, possibly as a consequence of freeze-melt cycles or biological activity on the surface of the fast ice. Physical processes dominated the pCO_2 decrease in the ice interior, regardless of the season. Dense biological activity and the presence of a biofilm in basal fast ice may promote calcium carbonate precipitation. The seasonal shifts between CO_2 over and under-saturation in brines translate into fluctuations in pH relative to seawater, with potential flow-on effects for algal growth. Incubation experiments carried out on dinoflagellate-dominated assemblages sampled near Scott Base suggest that late-summer fast-ice brine communities were however not significantly affected by the high and low pH values over the tested 7.12–8.87 range (McMinn et al., 2017), although growth rates were reduced at both pH extremes.

6.5.2. Dimethylsulfoniopropionate (DMSP) and Dimethyl Sulfide (DMS)

Sea-ice algae produces large amounts of DMSP, a precursor of the cloud condensation nuclei-forming gas DMS. Marine bacteria produce DMSP (Curson et al., 2017) but their potential contribution to DMSP and DMS production has yet to be observed in sea ice. Given its high algal biomass and associated DMS content, the seasonal melt of Antarctic sea ice leads to elevated DMS concentrations in seawater (Trevena & Jones, 2006). Sea ice can also emit DMS to the atmosphere via venting through surface sea ice as well as leads within the ice (Zemmelink et al., 2005; Zemmelink et al., 2008). As a consequence, significant DMS fluxes (up to 11 μmol m^{-2} d^{-1}) from sea ice have been detected in the Antarctic sea-ice zone (Nomura et al., 2012; Zemmelink et al., 2006). The effect of DMS-rich, melting fast ice has also been observed along the Antarctic coast near Davis Station in summer, where the DMS concentrations in surface seawater were highest immediately following the breakout of the fast ice (Trevena & Jones, 2006). In a study from the icebreaker Shirase in the 2009/10 summer, Koga et al. (2014) however found evidence that the presence of multi-year fast ice represents a continuous and persistent barrier that locally inhibits ocean-to-atmosphere emissions of DMS.

Fast ice has disproportionately high primary productivity relative to its surface area (Arrigo et al., 1998, 2003), and may well be a significant source of DMS along the Antarctic coast and contribute to atmospheric aerosols formation events. Only a handful of field studies have explored the concentrations of DMS and DMSP in Antarctic fast ice and as a consequence, evaluating the global significance of fast-ice DMS using sea-ice coupled models is still in its infancy. Sea-ice biogeochemical models with DMS parameterization are only just emerging in the Arctic (Hayashida et al., 2020) and have yet to be initiated in the Antarctic realm. Field studies do show that DMS and DMSP concentrations in Antarctic fast ice are high and vary greatly both spatially and seasonally (Trevena

19449208, 2023, 2, Downloaded from https://agupubs.onlinelibrary.wiley.com/doi/10.1029/2022RG000770 by University of Adelaide Alumni, Wiley Online Library on [16/08/2023]. See the Terms and Conditions (https://onlinelibrary.wiley.com/terms-and-conditions) on Wiley Online Library for rules of use; OA articles are governed by the applicable Creative Commons License

et al., 2000; Trevena & Jones, 2006). DMSP concentrations may differ between fast ice of different thicknesses (Trevena et al., 2003), with the greatest concentration of DMSP commonly occurring in newly formed sea ice (Trevena & Jones, 2006). Sea-ice texture could play a role, with isolated DMS and DMSP maxima recorded in interior ice corresponding to platelet crystals found in Cape Evans (Carnat et al., 2014). The production of DMSP and DMS in fast ice is also closely associated with biological activity, with bulk ice DMSP + DMS and Chl*a* concentrations highly correlated, suggesting that the high bulk ice DMSP + DMS concentrations are caused mainly by the presence of autotrophic sympagic algae within the sea ice collected near Syowa Station and Dumont d'Urville Station (B. Delille et al., 2007; Nomura, Kasamatsu, et al., 2011, respectively). Similar findings were recorded in Prydz Bay, with DMSP and Chl*a* concentrations in fast ice significantly correlated in surface and deep interior sea-ice sections (Trevena & Jones, 2012) and at Cape Evans during winter-spring transition (Carnat et al., 2014).

6.5.3. Bromoform

Bromoform ($CHBr_3$) is a volatile organic compound produced by phytoplankton and seaweed and emitted from the ocean to the atmosphere. In the atmosphere, phytochemical degradation of bromoform creates reactive forms of bromine which can deplete ozone. The production of bromoform by sea-ice algae is suggested as an important contributor to atmospheric bromoform levels in ice-covered regions (e.g., Sturges et al., 1992). The production of bromoform is not limited to summer however, with one study revealing significantly greater production in winter sea ice than in spring and overall, 10 times more bromoform production than Antarctic seawater (Abrahamsson et al., 2018). Measurements along the Antarctic coast (C. Hughes et al., 2009) and associated fast ice are rare. One field study evaluated bromoform in fast ice slush collected during a summer time-series in Lützow-Holm Bay, with slush water consistently characterized by lower bromoform concentrations and lower salinity compared to the under-ice seawater (Nomura, Ooki, et al., 2011). Bromoform concentrations in slush water were positively correlated with salinity with higher coefficients observed above a salinity of 5 than below. In this study, no obvious contribution of sea-ice algae to bromoform production was found. This result contrasts with coastal seawater observations at Rothera Oceanographic and Biological Time Series in Marguerite Bay where the highest bromocarbon concentrations were found to coincide with the maximum phytoplankton biomass (C. Hughes et al., 2009). These contrasting results may come from the lack of biomass measured in fast-ice slush compared to coastal seawater and sea ice. Given these uncertainties, year-round measurements of bromoform from fast ice are required to quantify the contribution to the overall seasonal ice zone bromoform emission and to properly evaluate the impact of Antarctic fast ice on ozone depletion events over the Southern Ocean.

6.6. Fast-Ice Biogeochemical Knowledge Gaps

Multi-seasonal and decadal time series data on key variables relevant to biogeochemistry in fast ice are currently non-existent. This will require a dedicated monitoring effort and potentially the development of novel hardware to collect year round observations. These efforts should start near Antarctic bases initially and expand to understudied regions. Multi-season fast-ice sampling has been conducted in very few regions under the AFIN with a focus on sea-ice physics. There is currently no data set with a comprehensive set of concomitant measurements of physical, chemical and biological variables (Carnat et al., 2014; Günther & Dieckmann, 1999). Existing multi-disciplinary data sets are generally short (approx. one month) and may lack key observations such as snow thickness (Meiners et al., 2018). The existing data sets may also be operationally biased toward thinner ice floes over rafted and thicker, multi-year fast ice floes due to the ease of sampling. High-resolution, multi-season data sets containing a suite of parameters are needed to improve sea-ice biogeochemical model performance (Miller et al., 2015; Steiner et al., 2015). This monitoring is necessary to establish baseline understanding to make reliable and quantitative estimates of future changes.

7. Fast Ice as a Habitat for Primary Producers

7.1. The Role of Fast Ice in Antarctic Ecosystems

Fast ice constitutes an integral, highly seasonally varying component of Antarctic coastal and nearshore ecosystems. It serves as a temporal reservoir for nutrients and, in particular when snow covered, strongly controls light availability for pelagic (in the water column) and benthic (on the seafloor) primary producers. Fast ice provides a habitat for ice-associated (sympagic) communities consisting of various organism groups including viruses,

19449208, 2023, 2, Downloaded from https://agupubs.onlinelibrary.wiley.com/doi/10.1029/2022RG000770 by University of Adelaide Alumni, Wiley Online Library on [16/08/2023]. See the Terms and Conditions (https://onlinelibrary.wiley.com/terms-and-conditions) on Wiley Online Library for rules of use; OA articles are governed by the applicable Creative Commons License

bacteria and heterotrophic and autotrophic protists (the latter are more commonly referred to as sea-ice algae). In terms of biomass, these communities are generally dominated by sea-ice algae. Sympagic algae are particularly important for Antarctic marine ecosystems as they provide a spatially-concentrated source of fixed carbon to both microbial food webs and higher trophic levels. Importantly, fast-ice algae are available as food when primary production in the water column is low (Meiners et al., 2018).

7.2. Fast-Ice Algal Communities

Sympagic algal communities flourish in distinct micro-habitats of Antarctic fast ice. The development of these micro-habitats is coupled to the physicochemical properties of sea ice which are shaped by sea-ice formation and growth processes (Ackley & Sullivan, 1994, also Section 2 of this review). Based on their occurrence in the sea-ice column, the communities can be classified into three main types: surface, interior, and bottom communities (Ackley et al., 1979; Arrigo, 2017; Carnat et al., 2014; Horner et al., 1992; Meiners et al., 2018; Van Leeuwe et al., 2018). Bottom-ice communities can be further divided into interstitial ice algal communities associated with thermodynamically grown columnar ice, consolidated platelet ice layer communities, SIPL communities, and strand communities consisting of filaments that are only loosely attached to the bottom of the fast ice and are suspended into the water column (e.g., Arrigo, 2017; Arrigo et al., 1995; Grossi & Sullivan, 1985; McConville & Wetherbee, 1983). Ice accretion at the ice-water interface can incorporate and trap bottom communities into the interior of the sea ice. Key environmental factors shaping the distribution and seasonal development of fast-ice microalgal communities include light, ice temperature and related brine salinity, nutrients as well as habitable pore space (e.g., brine volume), and colonizable crystal surface area. Fast-ice algal communities generally thrive in those microhabitats that provide stable environmental conditions, have sufficient light and are most closely coupled to the under-ice water column for access to nutrient supply, for example, bottom-ice layers (Arrigo, 2017).

Microalgal (unicellular) communities inhabiting Antarctic fast ice can be diverse. Fast-ice algal communities are comprised of a subset of Antarctic coastal phytoplankton and benthic microalgae species, and in terms of biomass are generally dominated by diatoms (Bacillariophyceae). Bottom-ice interstitial communities are dominated in particular by a specific group called pennate diatoms, that is, diatoms with one elongated cell axis such as species of the genera *Navicula*, *Nitzschia*, *Entomoneis*, *Pleurosigma*, *Synedra*, and *Pinnularia*. Strand communities, associated with fast ice at coastal locations, are often formed by the tube-dwelling diatom species *Berkeleya adeliensis* (Belt et al., 2016; Riaux-Gobin et al., 2003; Shetye et al., 2019). Sub-ice platelet layers, characterized by very high porosities (~75%) and nutrient availability, harbor communities consisting of both pennate and centric diatom species such as *Fragilariopsis* spp. and *Chaetoceros* spp., respectively (Riaux-Gobin et al., 2003; Saggiomo et al., 2017). Diatom-dominated interior communities have been reported from autumn sea ice as well as spring sea ice, but during summer, interior fast-ice layers are often dominated by mixed communities of smaller algae (<20 μm), in particular flagellates including dinoflagellates such as *Gymnodinium* spp. (Archer et al., 1996). Ephemeral surface communities can occur in summer when harsh environmental conditions in the upper parts of the fast-ice cover ameliorate. They generally consist of cryo- and halotolerant chrysophytes and dinoflagellates, which have been reported from the surface of fast ice in McMurdo Sound (165°E, 77.5°S; Stoecker et al., 1998), but may also be dominated by diatoms such as *Navicula* spp. (D. H. Robinson et al., 1997). Within the fast ice, ice algae respond to seasonal changes in light, temperature and nutrients by undergoing a species succession. In early spring, species adapted to very low light but sufficient nutrients dominate (McMinn et al., 2010). These are gradually replaced by taxa with greater photosynthetic capacity but lower demand for nutrients (Stoecker et al., 1998, 2000). There is now increasing evidence that many of these successional changes are mediated by virus infection (McMinn et al., 2020).

7.3. Biomass and Primary Production

Volumetric fast-ice algal cell concentrations and standing stocks vary by several orders of magnitude, both vertically within the ice cover but also horizontally on the sub-meter scale (Arrigo, 2017; Van Leeuwe et al., 2018). A standard, although invasive and spatially restricted, method to quantify bulk ice algal biomass is to measure ice algal photosynthetic pigment (i.e., chlorophyll-*a* (Chl*a*)) concentrations from melted ice-core samples (Meiners et al., 2012; Miller et al., 2015). Volumetric Chl*a* concentrations from Antarctic fast ice cores range over 5 orders of magnitude from <1 to 10,100 mg m^{-3} in melted sea ice (summarized by Arrigo, 2017). Extremely high ice algal

19449208, 2023, 2, Downloaded from https://agupubs.onlinelibrary.wiley.com/doi/10.1029/2022RG000770 by University of Adelaide Alumni, Wiley Online Library on [16/08/2023]. See the Terms and Conditions (https://onlinelibrary.wiley.com/terms-and-conditions) on Wiley Online Library for rules of use; OA articles are governed by the applicable Creative Commons License

biomass concentrations (with values regularly >1,000 mg Chl*a* m^{-3} of melted ice) have been reported for highly porous SIPLs (Arrigo, 2017; Arrigo et al., 1995; 2014; Günther & Dieckmann, 1999; Smetacek et al., 1992; Wongpan, Meiners, et al., 2018). Analyzing a compilation of existing circum-Antarctic fast-ice core data (i.e., not including SIPLs), Meiners et al. (2018) report a range of <0.1–219.9 mg Chl*a* m^{-2} for depth-integrated biomass per unit area. They found that seasonal changes in integrated Antarctic fast ice algal Chl*a* are primarily driven by changes in the bottom layers of the fast ice, with peaks in integrated biomass occurring in autumn and spring (Meiners et al., 2018). Integrated values of >30 mg Chl*a* m^{-2} were generally associated with the spring bottom fast-ice algal bloom occurring in September to October, depending on environmental factors such as insolation, snow thickness and ice thickness (Meiners et al., 2018). Overall, fast-ice algal growth and biomass distribution are controlled by small-scale processes occurring on the brine channel scale which in turn are a function of larger-scale icescape features and seasonal changes in environmental drivers (Meiners et al., 2018; Remy et al., 2007).

Owing to the difficulties of measuring primary production in a semi-solid sea-ice matrix, the high spatial variability in ice algal biomass and the temporal (diurnal, seasonal) variability in ice algal photosynthesis, comparable data on fast-ice algal primary productivity remain scarce (Arrigo, 2017). A variety of methods including radioactive and stable-isotope tracer uptake, determination of temporal changes in biomass, as well as oxygen microelectrode (McMinn et al., 2000; Trenerry et al., 2002) and optode (Campbell et al., 2016, 2017) measurements have been employed to determine photosynthetic rates of ice algal communities. The multitude of methods employed for distinct communities at spatially and temporally variable scales complicates the comparability of data from isolated studies. The relative contribution of fast-ice algal production to overall primary production (sympagic, pelagic and benthic) for the ice-covered period in Antarctic nearshore ecosystems has been estimated to range between 50% and 65% (McMinn et al., 2010). The overall contribution of fast-ice algal production to total primary production appears to be positively linked with ice-season duration (Archer et al., 1996; Meiners et al., 2018). Ice algal communities in the lowermost third of the ice cores dominate seasonal changes in biomass and thus productivity during most of the year. Regional variability of bottom ice algal production and biomass is largely controlled by the presence/absence of biomass-rich and highly productive platelet ice layers. In addition, snow is considered a key driver of ice-algal biomass productivity and spatial variability. Early during the spring season ice algal production is generally light limited, while spring melt of snow and ice decreases light attenuation leading to potential photo-inhibition as well as ablation of the bottom ice habitats resulting in the loss of algae to the water column (McMinn, 1996; McMinn & Ashworth, 1998). Deeper snow during this spring-summer transitional period likely protects the bottom ice habitat from higher light and ablation, resulting in an extended ice algal bloom in snow-covered fast-ice areas. Van Leeuwe et al. (2018) provide a detailed overview of sea-ice algal photosynthetic parameters, including for Antarctic fast-ice communities. They summarize data on fast-ice algal maximum photosynthetic capacity, the slope of photosynthesis versus light curves which serves as a proxy for ice-algal light affinity, and the index for photoadaptation. Overall their analyses suggest that sea-ice communities show a high capacity for photoacclimation but low maximum productivity compared to Southern Ocean phytoplankton. Low carbon assimilation rates are likely a result of adaptation to extreme conditions of reduced light and ice temperature, in particular in sea-ice interior layers during winter and early spring (Van Leeuwe et al., 2018).

7.4. Ice Algal Adaptations to Extreme Environmental Conditions

In this section we describe how (fast-) ice algae are adapted to the harsh environmental conditions of their habitat. We have tried to focus on using Antarctic fast ice literature as much as possible, but also describe some more general concepts derived from the wider (sea ice) literature, as it was sometimes necessary to cite non-fast-ice literature to convey key concepts.

Antarctic fast ice is characterized by steep and seasonally-changing gradients in light, temperature, brine salinity as well as ice porosity affecting nutrient availability for ice algae. Ice algal species are adapted to the physically-distinct characteristics of their micro-habitats and have adopted a variety of mechanisms to cope with the extreme environmental conditions in sea ice. These include extracellular and intracellular approaches, the formation of resting spores and cysts, and likely also behavioral approaches. Extracellular approaches for diatoms comprise the production of extracellular polymeric substances (EPS; also Section 6.2.2. of this review) which create a protective mucous envelope around cells and may anchor them to the ice surface within brine inclusions

19449208, 2023, 2, Downloaded from https://agupubs.onlinelibrary.wiley.com/doi/10.1029/2022RG000770 by University of Adelaide Alumni, Wiley Online Library on [16/08/2023]. See the Terms and Conditions (https://onlinelibrary.wiley.com/terms-and-conditions) on Wiley Online Library for rules of use; OA articles are governed by the applicable Creative Commons License

(Krembs & Deming, 2008; Krembs et al., 2011), as well as production of ice-binding proteins that prevent ice growth in the immediate vicinity of cells. Ice-binding proteins are characterized by their ability to separate the melting and growth temperatures of ice (thermal hysteresis) and to inhibit ice recrystallization (Bayer-Giraldi et al., 2011). They also likely promote the attachment of cells by shaping the microstructure of ice (Bayer-Giraldi et al., 2011; Raymond et al., 1994). Intracellular mechanisms include changes in fatty acid composition to regulate the fluidity of cell membranes at low temperatures, such as the incorporation of polyunsaturated, short-chain, branched, or cyclic fatty acids. In particular, the extent of unsaturation of the fatty acids in membrane lipids plays a major role in avoiding membrane rigidification caused by low temperatures (Morgan-Kiss et al., 2006). Temperature and salinity changes have also been shown to induce the production of compatible compounds such as proline and dimethylsulfoniopropionate (DMSP) in Antarctic sea-ice diatoms (Dawson et al., 2020; Kameyama et al., 2020; Trevena et al., 2003). In response to deteriorating environmental conditions, fast ice flagellate taxa, in particular dinoflagellates and chrysophytes, can form resting spores that appear to help survival and dispersal of cells after release from the ice and/or winter survival in the ice (Archer et al., 1996; Stoecker et al., 1992). Aumack et al. (2014) showed the ability of an Arctic bottom-ice pennate diatom to vertically migrate in response to changing snow conditions affecting light levels at the bottom of the ice, and similar strategies are very likely employed by closely-related diatoms species colonizing Antarctic fast ice.

Ice algae employ various mechanisms to remain photosynthetically active under both changing and often very low light conditions which are characteristic of autumn and early spring conditions, and particularly experienced in sea ice bottom layers. Sympagic algae acclimate to low irradiance levels by adjusting pigment compositions and expansion of light-harvesting complexes (Petrou et al., 2016; van Leeuwe & Stefels, 2007). Changes in the structure of photosynthetic units may be accompanied by a decrease in their numbers and pigment packaging within the cells (Barlow et al., 1988) and can be species specific (Arrigo et al., 1998). In addition, ice algae also show chromatic acclimation in response to changes in sea ice transmitted light-spectra influenced by spectral light absorption by snow, ice and surface and interior ice algal layers (self-shading; D. H. Robinson et al., 1995; McMinn et al., 2005; Wongpan, Meiners, et al., 2018).

Fast-ice algae are also exposed to a number of other highly stressful environmental conditions. Every year, like other polar microorganisms, they must survive many months of darkness (McMinn & Martin, 2013). However, they have been shown to be able to survive for up to 4 months of darkness and then recover. The ability of sea-ice diatoms to modify their metabolic activity in dynamic and extreme light regimes enhances their ability to survive and thrive. Maintaining essential metabolic processes in the dark is critical for photosynthesis to occur rapidly upon re-illumination. Maintenance metabolism (or the ability to live in the dark), may be one of the fundamental reasons why diatoms dominate Antarctic sea-ice ecosystems (Kennedy et al., 2019). In contrast, during late spring and summer, high levels of irradiance can result in photoinhibition. However, ice algal communities have been shown to have high levels of plasticity in their light-acclimation abilities (Petrou et al., 2011). Ice algae are not only sensitive to the amount of irradiance but also to the spectral distribution. Because the annual peak in ozone depletion, ice transparency and algal biomass coincide in late October, it was thought that they might be particularly susceptible to elevated ultraviolet B radiation (McMinn, Ashworth, & Ryan, 1999; McMinn et al., 1994). However, using field manipulations and laboratory experiments, Ryan et al. (2012) demonstrated no net effects of additional UV on the growth or photosynthesis of fast-ice bottom communities. Somewhat surprisingly, there was no evidence for the production of UV-absorbing compounds such as mycosporine-like amino acids in response to elevated UV levels (Ryan et al., 2002).

7.5. Fate of Ice Algae

Close relationships between primary production and bacterial biomass and production have been reported for Antarctic fast ice (Archer et al., 1996; D. Delille et al., 2002). Both bacteria as well as heterotrophic protists appear to be seasonally coupled to algal biomass (Fiala et al., 2006), and ice algal primary production is fueling active microbial food webs (Martin et al., 2012). Pelagic grazers utilize ice algae as a critical early season food source, and shallow water depths associated with fast-ice occurrence help efficient export of ice algae to the seafloor resulting in tight cryo-pelagic-benthic coupling (Cripps & Clarke, 1998). Close relationships between fast-ice conditions, pelagic primary productivity and, subsequently, coastal benthic communities have been reported (e.g., Cummings et al., 2018). In McMurdo Sound, benthic microbial community composition has been shown to reflect sea-ice dynamics, with areas covered by multi-year sea ice demonstrating lower sediment

19449208, 2023, 2, Downloaded from https://agupubs.onlinelibrary.wiley.com/doi/10.1029/2022RG000770 by University of Adelaide Alumni, Wiley Online Library on [16/08/2023]. See the Terms and Conditions (https://onlinelibrary.wiley.com/terms-and-conditions) on Wiley Online Library for rules of use; OA articles are governed by the applicable Creative Commons License

carbon content and a higher contribution of chemoautotrophic bacteria, reflecting restricted benthic productivity (Currie et al., 2021). Algae released from sea ice can also serve as inoculum for pelagic phytoplankton growth (Lizotte, 2001), but the role of Antarctic fast-ice algae in seeding coastal phytoplankton blooms remains uncertain (Riaux-Gobin et al., 2011; Van Leeuwe et al., 2018). Through its influence on light availability, thick and persistent fast ice (including multiyear ice) can result in a decrease in in situ pelagic and benthic primary production, reducing the quantity and quality of phytodetritus, and thereby affecting the diversity and abundance of benthic invertebrate communities (H. Kim, Ducklow, et al., 2018).

7.6. Gaps in Understanding of Fast-Ice Primary Production

The seasonality of physical controls on algal communities has been observed in Antarctic pack ice (Arrigo et al., 2014; Meiners et al., 2017), but detailed concomitant observations of physical and biological sea-ice properties in Antarctic fast ice remain limited. These measurements are necessary to determine key physical drivers (e.g., ice and snow cover thickness) of the timing, magnitude, and duration of the ice algal spring bloom. Detailed long-term time-series observations of ice algal accumulation in Antarctic fast ice would facilitate closing this gap, which in turn would improve parameterization of ice algal dynamics in sea ice biogeochemical and productivity models. Recently established optical methods to determine ice algal biomass from transmitted under-ice irradiance measurements (e.g., Cimoli et al., 2019; Mundy et al., 2007; Wongpan, Meiners, et al., 2018) promise a step-change in the development of automated observatories to measure ice algal biomass in a non-invasive manner. Combined with ice mass balance instruments they allow for automated coupled physical-biological time-series observations of key fast-ice parameters.

8. Fast Ice as a Habitat for Micro- and Macro-Grazers

The fast-ice habitat is typified by low diversity and high abundance of biota, when compared to many other marine habitats. Organisms that are small enough to inhabit the brine system, and tolerate wide ranges in salinity and temperature, are limited to a small number of taxa, including copepods, turbellarians, acoels and one species of nudibranch mollusc (Swadling, 2014). Bigger zooplankton, including amphipods, euphausiids, pteropods and large copepods, feed on ice algae at the ice-water interface, but rarely, if ever, infiltrate the brine channel system. The underlying SIPL, which is characteristic of some fast-ice regions (Langhorne et al., 2015), also provides habitat for zooplankton and fish, notably the notothen *Trematomus borchgrevinki* and eggs and larvae of *Pleuragramma antarcticum* (Antarctic silverfish; Figure 12). Here we outline current knowledge about microzooplankton (0.002–0.2 mm), mesozooplankton (0.2–20 mm) and macrozooplankton (>20 mm) that have strong relationships with fast ice, focusing, where information exists, on distribution, physiology, life history strategies and trophic interactions. While we understand there is extensive research on ice algae as a food source for Antarctic krill (*Euphausia superba*), we have chosen to omit discussion on Antarctic krill in this review as their associations to ice are not specific to the fast-ice habitat. Furthermore, despite ice krill (*E. crystallorophias*) being common to the sea-ice habitat, the extent of their use (e.g., for feeding) of the fast-ice habitat has yet to be confirmed. We conclude by considering knowledge gaps and how this community might be affected by changing environmental conditions in the coming decades.

8.1. Vertical and Horizontal Distribution of Ice-Associated Plankton

Habitat space in the fast ice is regulated by a combination of salinity and temperature, which in turn determines the volume of the liquid portion of fast ice; that is, the brine channel system that plants and animals inhabit. The diameter of brine tubes restricts the size of animals that can live within the system, with the largest organisms, copepods, measuring <600 μm in diameter (Krembs et al., 2000). Most of the biomass in fast ice is found in the bottom 2–5 cm (Figure 12b), with both chlorophyll-*a* concentration and meiofauna abundance often reaching levels much higher than those in the underlying water column (Swadling, 2001; Swadling et al., 1997; Schnack-Schiel, Dieckmann, et al., 2001). Smaller organisms can penetrate further into the ice, or be trapped in bands as the ice grows, so there is some vertical structure in the distribution of biota (Figure 12b). Protists, such as dinoflagellates, have been observed to dominate the McMurdo Sound (165°E, 77.5°S) brine community within the upper ice brine, where chlorophyll-*a* concentrations are low and less diatom-dominated, as is also typically observed in the upper pack ice (Stoecker et al., 1992).

19449208, 2023, 2, Downloaded from https://agupubs.onlinelibrary.wiley.com/doi/10.1029/2022RG000770 by University of Adelaide Alumni, Wiley Online Library on [16/08/2023]. See the Terms and Conditions (https://onlinelibrary.wiley.com/terms-and-conditions) on Wiley Online Library for rules of use; OA articles are governed by the applicable Creative Commons License

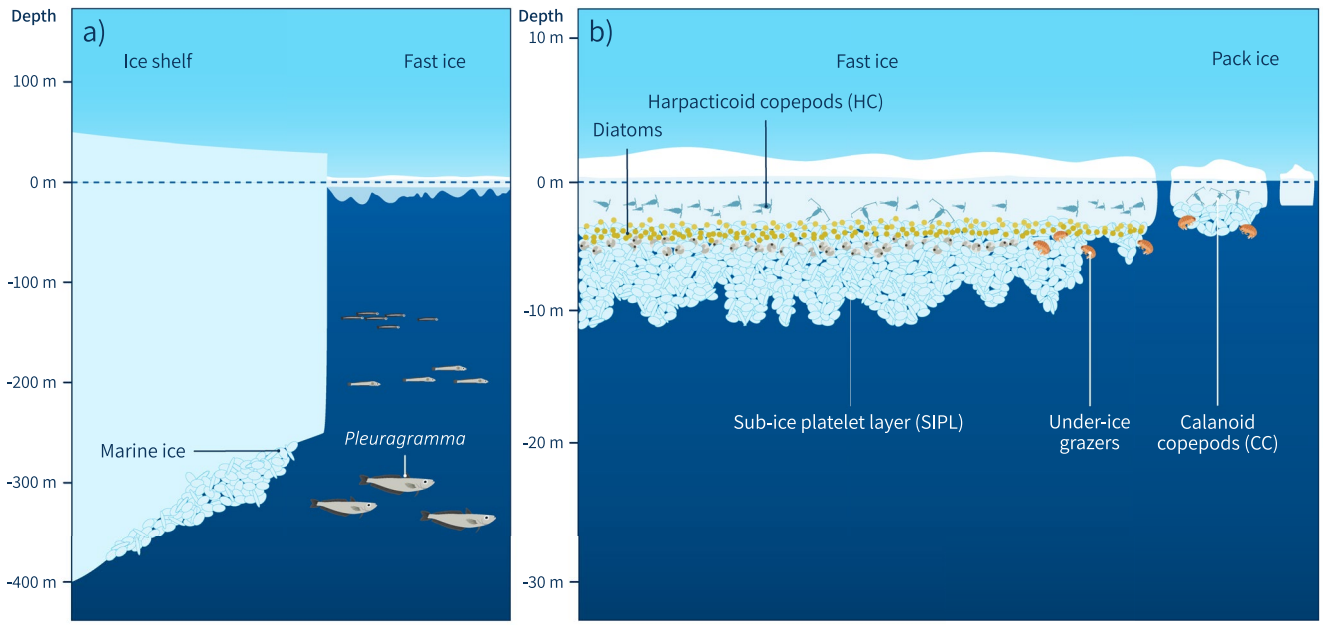

Figure 12. Schematic highlighting the important components of the fast-ice habitat for ice algae and grazers. While small organisms can inhabit the interstices of platelet and fast ice, larger species stay in proximity to the under-ice surface. Antarctic silverfish, *Pleuragramma antarcticum*, use sea ice as a nursery ground and move into deeper water as they develop. Panel (a) Schematic of the ice shelf-fast ice interface. Panel (b) A region of fast ice with a sub-ice platelet layer. Panels (a) and (b) have different vertical scales.

Although many of the species appear to be circum-Antarctic there is differential distribution between the main sectors. Notably, microzooplankton communities, which are typically comprised of ciliates, heterotrophic dinoflagellates, choanoflagellates and other heterotrophic nanoflagellates, exhibit strong patchiness in circum-Antarctic distribution (Q. Yang, Liu, et al., 2016; Scott et al., 2001). Among the mesozooplankton the copepod *Paralabidocera antarctica* can reach up to 900,000 individuals per m^2 of ice along the coastline of the Eastern Indian Ocean, though it only occurs in small numbers in the Drescher Inlet (19.3°W, 72.9°S; Schnack-Schiel et al., 2004). In Terra Nova Bay (164.5°E, 74.8°S) the dominant copepods are the calanoid *Stephos longipes* and the harpacticoid *Harpacticus furcifer* (Guglielmo et al., 2007). These four species comprise the dominant mesozooplankton inhabiting the fast ice, although the biodiversity is somewhat higher, with the presence of several other species of harpacticoids (Dahms et al., 1990) recorded. Additionally, the nudibranch mollusc *Tergipes antarcticus*, which was first observed from sea ice in the Bellingshausen Sea (see Pelseneer (1903) in Kiko, Kramer, et al., 2008), was not mentioned in the literature again until it was recorded by Kiko, Michels, et al. (2008) in sea ice from the Weddell Sea.

8.2. From Facultative to Obligate Life History Strategies

Inhabiting the fast ice requires both the physiological tolerance and the behavioral mechanisms necessary to cope with the variable salinity and temperature, and seasonal/ephemeral nature of most fast ice. Life history strategies of the best-known species occur along a spectrum from facultative, where an organism may function under more than one type of environmental conditions, to obligate, where the organism is restricted to specific conditions (in this case, the fast-ice habitat). Closer to the facultative end is *S. longipes*, which possesses sticky eggs that adhere to frazil crystals and are incorporated into the ice as it forms. Naupliar (young larval) stages of this species live in the brine channel system (Costanzo et al., 2002), but older stages are also found in the open ocean and in pack ice floes (Schnack-Schiel et al., 1995). *Stephos longipes* contain specialized proteins that support thermal hysteresis (Kiko, 2010), which enables upward penetration into the ice where temperatures fluctuate. Next along the spectrum is most likely *P. antarctica*, a species that appears to be obligate in fast ice, as the nauplii and early juvenile stages inhabit the ice in large numbers before transferring to the underlying water column as adults (Swadling et al., 2004; Tanimura et al., 1996). Eggs of *P. antarctica* undergo diapause (periods of suspended development in invertebrates) in the sediments during the period of no ice cover, and are either incorporated

19449208, 2023, 2, Downloaded from https://agupubs.onlinelibrary.wiley.com/doi/10.1029/2022RG000770 by University of Adelaide Alumni, Wiley Online Library on [16/08/2023]. See the Terms and Conditions (https://onlinelibrary.wiley.com/terms-and-conditions) on Wiley Online Library for rules of use; OA articles are governed by the applicable Creative Commons License

into the ice via active swimming to the surface by the first larval stage or, potentially, via upward transport of sediments (Ito et al., 2017). Notably, populations of this species also exist year-round in the water columns of three saline lakes in the Vestfold Hills, East Antarctica (78.25°E, 68.55°S), where they never enter the ice cover on the lakes (Swadling et al., 2004). This species does not display thermal hysteresis (Kiko, 2010) and is clearly euryhaline (broad range of salinity tolerance), as the inhabited lakes all have a salinity of less than half that of seawater.

At the obligate end of the spectrum, *Drescheriella glacialis* carries its egg sacs and lives year-round in the ice, crawling around the ice and moving into the interior. It can exist outside of the ice habitat (Loots et al., 2009), but it is not clear where the individuals live when they are not in the brine system. To survive during periods of no fast ice *D. glacialis* must be able to swim, survive in the benthos or find small floes as a refuge. The nauplii crawl rather than swim, though the later stages are good swimmers (Dahms et al., 1990) and this copepod has been found in refrozen gaps in pack ice, highlighting its affinity for the ice habitat (Schnack-Schiel, Thomas, et al., 2001). In laboratory experiments *D. glacialis* has shown temperature compensation of developmental and reproductive rates and is a clear *r*-strategist (i.e., low energetic investment toward high number of offspring) as it produces a large number of eggs, grows rapidly to small size and matures early (Bergmans et al., 1991). The presence of nudibranch *T. antarcticus* in fast ice is unusual as molluscs have not generally been recorded as ice specialists in either the Antarctic or the Arctic. Egg clutches, veliger larvae, juveniles and adults have all been collected from sea ice, highlighting that it is a true inhabitant of ice (Kiko, Kramer, et al., 2008). The egg clutches are not buoyant and the adults cannot swim actively (Kiko, Kramer, et al., 2008), pointing to a poor capacity for *T. antarcticus* to adopt a pelagic lifestyle, and perhaps making it the strongest obligate species amongst the fast-ice dwellers.

8.3. Phenology of the Microbial Community in the Ice Brine

Microbial community abundance, distribution and diversity in the brine may be a function of food availability as well as complexity in ice structure and ice history (Garcia et al., 2020; Scott et al., 2001; Stoecker et al., 1992). Given their short generation times of hours to days, the rates of development for these organisms are consequently tightly coupled to the rate of sea-ice formation. Under low light conditions in winter, grazing generally cannot be sustained, due to low phytoplankton abundance and productivity, and thus biological production in sea ice is relatively low. However, also during winter, some microheterotrophs have been shown to occasionally consume over half (ca. 54%) of the phytoplankton standing stock and >100% primary production per day (Pearce et al., 2008). By spring, the microbial community emerges in the sub-surface brine channels and both microzooplankton grazing and phytoplankton growth rates become significant. In late November to early December, chlorophyll-*a* concentrations and biomass peak, as does the biomass of photosynthetic gymnodinioid dinoflagellates in the brine (Stoecker et al., 1992). Toward January, prior to ice melt and breakout in McMurdo Sound, photosynthetic dinoflagellates form resting cysts (hypnozygotes) while the abundance of chrysophyte statocysts increases. Cyst formation is believed to be a strategy for survival in the water column. Meltwater begins to dilute the upper brine channels, consequently flushing the total autotroph and other brine community biomass into the surrounding water column. Seasonal fast ice has fully broken out by late summer (Fraser et al., 2021) and microzooplankton significantly contributes top-down control of summer phytoplankton bloom, consuming approximately 34% of primary production (Pearce et al., 2008). When sea ice begins to form in early autumn, micrograzer mortality increases, coinciding with the decline in phytoplankton biomass and chlorophyll-*a* concentration.

8.4. Macrograzers Inhabiting the Platelet Ice

The SIPL communities provide an important nutritional resource for invertebrates, including species of euphausiids and amphipods, constitute a refuge from predators, and furnish a remarkable nursery ground for many species associated with ice for only a part of their life cycle, while others appear entirely dependent upon it for reproduction and development (C. E. Arndt & Swadling, 2006; Arrigo, 2013). Two circum-Antarctic nototenoid fishes—the Antarctic silverfish (*Pleuragramma antarcticum*) and *Trematomus borchgrevinki*—play pivotal roles based on modeling of the Ross Sea food web (Pinkerton & Bradford-Grieve, 2014).

Pleuragramma antarcticum is the dominant pelagic fish in the high-Antarctic zone and plays a fundamental role in the food web of the Antarctic marine ecosystem (La Mesa & Eastman, 2012; Pinkerton, 2017; Saenz

19449208, 2023, 2, Downloaded from https://agupubs.onlinelibrary.wiley.com/doi/10.1029/2022RG000770 by University of Adelaide Alumni, Wiley Online Library on [16/08/2023]. See the Terms and Conditions (https://onlinelibrary.wiley.com/terms-and-conditions) on Wiley Online Library for rules of use; OA articles are governed by the applicable Creative Commons License

et al., 2020; Vacchi et al., 2017) and early life stages of this species are closely associated with the fast-ice environments. Similarly to other Antarctic sectors (Hubold, 1984; Kellermann, 1986), *P. antarcticum* was the dominant component in the ichthyoplankton assemblage of the western Ross Sea, constituting more than 97% of total catches (Brooks et al., 2018; Granata et al., 2009). Maximum abundances of *P. antarcticum* postlarvae were confined to Terra Nova Bay, where the northern part represents a nursery ground for the first early stages (Davis et al., 2017; Granata et al., 2002; Guglielmo et al., 1997; Vacchi et al., 2012), and where a persistent polynya could provide favorable food conditions for their development. The food composition of postlarval *P. antarcticum* collected in spring corresponds to the typical zooplankton structure found in the sea ice, platelet layer and upper water column under the sea ice (Granata et al., 2009; Guglielmo et al., 2007; Schnack-Schiel et al., 2004). The occurrence of *S. longipes* adults, *H. furcifer* adults and juvenile stages and abundant naupliar stages of *Paralabidocera antarctica*, suggests that *P. antarcticum* postlarvae actively fed on prey closely associated with the fast ice (C. E. Arndt & Swadling, 2006; Swadling et al., 1997, 2000; Tanimura et al., 1996, 2002). A different life cycle strategy was hypothesized by Swadling (2001) which supports the idea that *P. antarctica* appears to prefer first-year ice where sheltered conditions facilitate the colonization of "frazil ice" type (typical of Weddell and Ross Seas, Spindler et al., 1990) compared to "frozen ice" type. In addition, the coastal area of Terra Nova Bay is characterized by a large spatial extension of SIPL, ranging in thickness from 80 to 120 cm (Guglielmo et al., 2007; Vacchi et al., 2012). Two hatching events have been hypothesized for both populations of the Ross and Weddell Seas (Guglielmo et al., 1997; Keller, 1983), and Granata et al. (2002) indicated early-mid December, and mid-December/early January as the two hatching periods in Terra Nova Bay. Large numbers of embryonated eggs and yolk-sac larvae were found floating in the platelet ice (O'Driscoll et al., 2018; Vacchi et al., 2004), indicating that hatching starts even earlier, from mid-November onwards, and continues at least until early December. In summary, the life history of *Pleuragramma* is characterized by slow growth, late maturity, high reproductive investment and an association with coastal fast ice for spawning and larval development (Figures 12a and 12b). All those features will allow the species to weather episodic annual failures in recruitment, but not long-term change (Duan et al., 2022; Mintenbeck & Torres, 2017).

The circum-Antarctic notothenioid fish *Trematomous borchgrevinki* plays an important role in the Antarctic ecosystem and functions as food for marine mammals, birds and fish (Andriashev, 1968; La Mesa et al., 2004). *Trematomous borchgrevinki* is an abundant schooling fish commonly seen swimming near ice holes (Montgomery et al., 1989). This habitat undoubtedly protects the fish from predation, especially from seals. *Trematomus borchgrevinki* were collected from the 1.5–3 m thick layer of dense platelet ice. Gutt (2002) recorded juvenile and adult fish in the Drescher Inlet, under the ice shelf margin and fast ice, respectively. This fish is planktivorous and feeds both on zooplankton and ice fauna (Gulliksen & Lønne, 1991), with individuals found feeding in the platelet ice and in the water immediately beneath the ice, mainly consisting of amphipods (*Orchomene plebs*), pteropods (*Limacina helicina antarctica*), and small copepods (e.g., Eastman & DeVries, 1985; Foster & Montgomery, 1993). For example, 90% of the food items in the stomach contents of *Pagothenia borchgrevinki* were ice-associated copepods and their nauplii and larval stages (Hoshiai & Tamimura, 1989). Unlike *P. antarcticum* which has been found exclusively in very cold ice-shelf waters (−1.75°C to −2°C; Davis et al., 2017), the cryopelagic *T. borchgrevincki* exhibits high thermal tolerance and acclimation capacities to elevated temperatures of >4°C (E. Robinson & Davison, 2008).

8.5. Knowledge Gaps

The stability of Antarctic fast ice not only has consequences for the global climate system, but also for the ecology of the coastal regions (Hoppmann et al., 2020). The high concentration of biological matter in SIPLs has significant implications for the entire coastal Antarctic food web (Guglielmo et al., 2000, 2004; Mangoni et al., 2009).

Biogeographical patterns of macro- and micrograzers under Antarctic fast ice are based on patchy sampling efforts in both time and space (Swadling, 2014), with many regions undersampled or not sampled for ice-associated microfauna. There is also a large gap in our understanding of whether rough and smooth fast ice support the same or different communities, as no known work to date has addressed this question. There are limited seasonal data, with winter and the autumn re-freezing being particularly poorly studied. Further, observations of sea-ice fauna other than copepods are limited to a small number of studies that have occurred in the last decade. This knowledge gap highlights the need for improved sampling of the fast and platelet ice, including promoting opportunities to collect newly-forming ice as well as distant floes as they detach from the fast ice and circulate away from the

19449208, 2023, 2, Downloaded from https://agupubs.onlinelibrary.wiley.com/doi/10.1029/2022RG000770 by University of Adelaide Alumni, Wiley Online Library on [16/08/2023]. See the Terms and Conditions (https://onlinelibrary.wiley.com/terms-and-conditions) on Wiley Online Library for rules of use; OA articles are governed by the applicable Creative Commons License

continent. These latter floes are a possible mechanism for the transport of biota and associated biogeochemical pathways to deeper waters (e.g., Ojima et al., 2017). Coastal regions such as Potter Cove in the Western Antarctic Peninsula (58.65°W, 62.23°S) that experience abiotic conditions that are highly dynamic and subject to drastic change/variability on interannual timescales may provide ideal conditions for better understanding micro- to macrozooplankton responses to future sea-ice change (Garcia et al., 2020). In general, we need more information on environmental tolerances, life cycle plasticity, and food web interactions to understand the importance of these organisms in the fast-ice system and to evaluate how they might respond to changes to their habitats.

Feeding adaptations such as mixotrophy exhibited in many microzooplankton species provides flexibility between phototrophic (ie., using photosynthesis to generate energy) and phagotrophic (ie., energy is derived from engulfing particles) behaviors that enable their communities to be broadly distributed geographically and in high abundances compared to those species that use single feeding modes (Moorthi et al., 2009). Other adaptations, such as the formation of resting cysts and statocysts by brine-inhabiting dinoflagellates and chrysophytes, respectively, are temporally coupled with a decrease in brine salinity from surface melt and flushing of the ice channels, which is likely a strategy for survival in the water column (Stoecker et al., 1992; Takahashi et al., 1986).

9. Outlooks: Antarctic Fast Ice by the End of the 21st Century

Following Sections 2–8, which presented syntheses of the body of knowledge regarding specific fast-ice sub-domains, we now turn our attention to the changes likely to occur throughout the 21st Century. Although comprehensive and holistic knowledge of the drivers of Antarctic fast ice is lacking (as detailed in Sections 4 and 5 of this review), we present here a new analysis to indicate that fast ice responds rapidly to environmental change. Figure 13 presents a new, yearly time series of fast-ice extent at the time of the climatological minimum (early-mid March). These new data form an extension (to 2022) of the 2000–2018 data set of Fraser et al. (2020). Annual minimum circum-Antarctic fast ice extent reached a record low in March 2022, at 123,200 km^2 (2000–2021 mean: 208,200 km^2; range: 168,600 to 295,200 km^2). The negative fast-ice extent anomaly was spatially widespread (shown in Figure 13), with the complete loss of multi-year fast ice in the eastern Ross Sea (~140°W). A widespread loss of persistent fast ice was also found along the eastern side of the Antarctic Peninsula, and across much of East Antarctica, particularly in the Western Pacific Ocean sector. Above-average extent was only encountered in large quantities around the Amundsen Sea Embayment (~105°W) and the West Ice Shelf (~85°E). This unprecedented (in the observational record) low fast-ice extent occurred in tandem with the record low sea-ice extent minimum in 2022 (Turner et al., 2022), indicating a similar environmental response between pack and fast ice and also possible linkage between the two.

Since no global climate model currently simulates fast ice prognostically, we use Coupled Model Intercomparison Project Phase 6 (CMIP6) projections to analyze changes in several near-surface atmospheric and oceanic fields relevant to fast ice and its associated systems, including sea-surface and 2 m air temperatures, the 10 m wind field, sea-ice concentration and thickness, rainfall, snowfall and incoming shortwave radiation. We use the Shared Socioeconomic Pathway 245 (SSP245) scenario, a "middle of the road" scenario that approximately follows the CMIP5 Representative Concentration Pathway 4.5, both of which reach a radiative forcing of 4.5 W m^{-2} by the end of the 21st Century (Fricko et al., 2017).

9.1. CMIP6 Methods

Nineteen CMIP6 models on the Australian National Computational Infrastructure (NCI) Earth System Grid Federation (ESGF) replica had all requisite fields available (see Table B1 in Appendix B) for both the historical period and the scenario MIP (Eyring et al., 2016). We define the historical baseline period as 1985–2014, a 30-year period that aligns with the end of the CMIP6 historical period. Our projection period is defined as 2071–2100. We regridded all model fields to a standard 1 × 1 degree grid using bilinear interpolation with the xESMF regridder (Zhuang et al., 2020). Multi-model means have been calculated without weighting, and only the first variant for each model has been included in the ensemble so as to not bias toward modeling families with more variants. The mean change for each of the selected fields, from 1985 to 2014 to 2071–2100, has been plotted in Figures 14 and 15. Overlaid is the present-day contour of 25% fast-ice persistence (black). The spatial mean changes shown in Table 1 are calculated over the entire present-day fast-ice region (i.e., grid cells with a fast ice coverage greater than 0).

19449208, 2023, 2, Downloaded from https://agupubs.onlinelibrary.wiley.com/doi/10.1029/2022RG000770 by University of Adelaide Alumni, Wiley Online Library on [16/08/2023]. See the Terms and Conditions (https://onlinelibrary.wiley.com/terms-and-conditions) on Wiley Online Library for rules of use; OA articles are governed by the applicable Creative Commons License

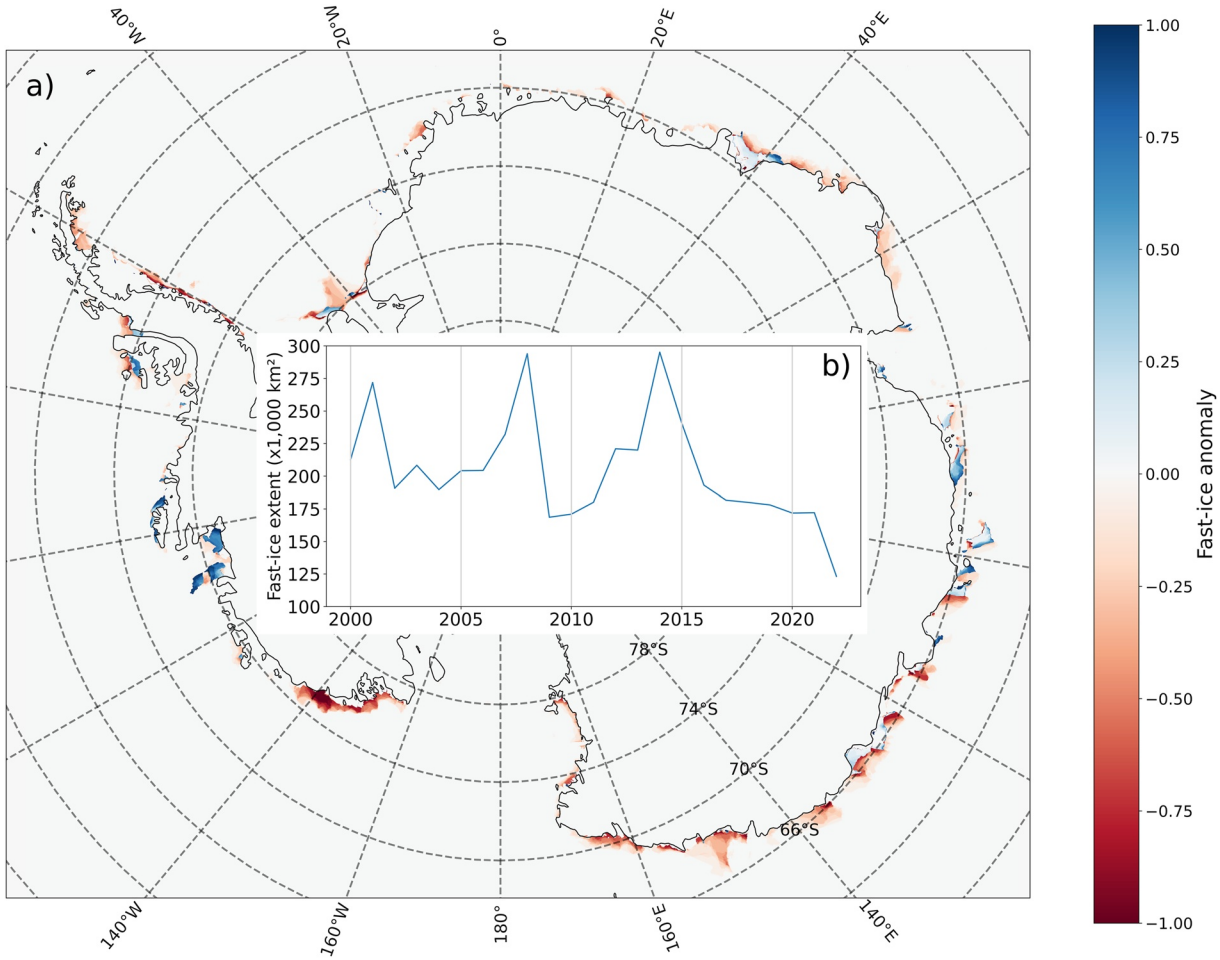

Figure 13. (a) Spatial distribution of Antarctic fast-ice extent anomaly in early-mid March 2022, obtained from cloud-free visible composite imagery after Fraser et al. (2010). Red shading indicates negative anomalies, with a value of −1.0 indicating a lack of fast ice in 2022, in a region that has had early-mid March fast-ice cover every year from 2000 to 2021. Inset, panel (b) Time series of early-mid March fast-ice extent from 2000 to 2022.

9.2. Change in Surface and Near-Surface Fields to 2100

Near-surface air temperature is projected to increase in all regions (Table 1; Figures 14a–14d), and over the (present-day) fast ice by between 1.84 K (DJF) and 3.41 K (JJA). Sea-surface temperature (Figures 14e–14h) also increases in regions where sea-ice concentration decreases but stays near the freezing point where sea-ice concentration is maintained (Figures 15m–15p). In line with an increase in the moisture capacity of a warmer atmosphere, total precipitation (i.e., snowfall plus rainfall; Figure 14 panels i–l and m–p, respectively) increases in all months, but rainfall matches snowfall in DFJ by 2100 (DJF rainfall is only half of snowfall in the baseline period). Rainfall also strongly increases in MAM (+79% compared to the baseline period). These rainfall projections are in line with those recently reported by Vignon et al. (2021), also using CMIP6 models. Snowfall increases in all seasons except DJF, where considerable moisture conversion to rainfall occurs.

Incoming surface shortwave radiation flux decreases in all regions and seasons, with the strongest decrease occurring in DJF (−12.6 W m^{-2}) when insolation is highest. This change is due to a shift toward liquid phase clouds with a higher particle density over the Southern Ocean, which reflect more shortwave radiation (Forster et al., 2021). Wind component magnitude (Figures 15a–15h) and speed (Figures 15i–15l) changes are small overall, but mean values (given in Table 1) hide regional variability. Overall, a slight reduction in the easterly and southerly components over the fast ice are suggestive of a reduction in katabatic wind outflow. Both sea-ice concentration (Figures 15m–15p) and thickness (Figures 15q–15t) are projected to experience widespread decline by 2100. Isolated pockets of minimal concentration change in JJA and SON are limited to the southwestern Weddell Sea and western-central Ross Sea.

19449208, 2023, 2, Downloaded from https://agupubs.onlinelibrary.wiley.com/doi/10.1029/2022RG000770 by University of Adelaide Alumni, Wiley Online Library on [16/08/2023]. See the Terms and Conditions (https://onlinelibrary.wiley.com/terms-and-conditions) on Wiley Online Library for rules of use; OA articles are governed by the applicable Creative Commons License

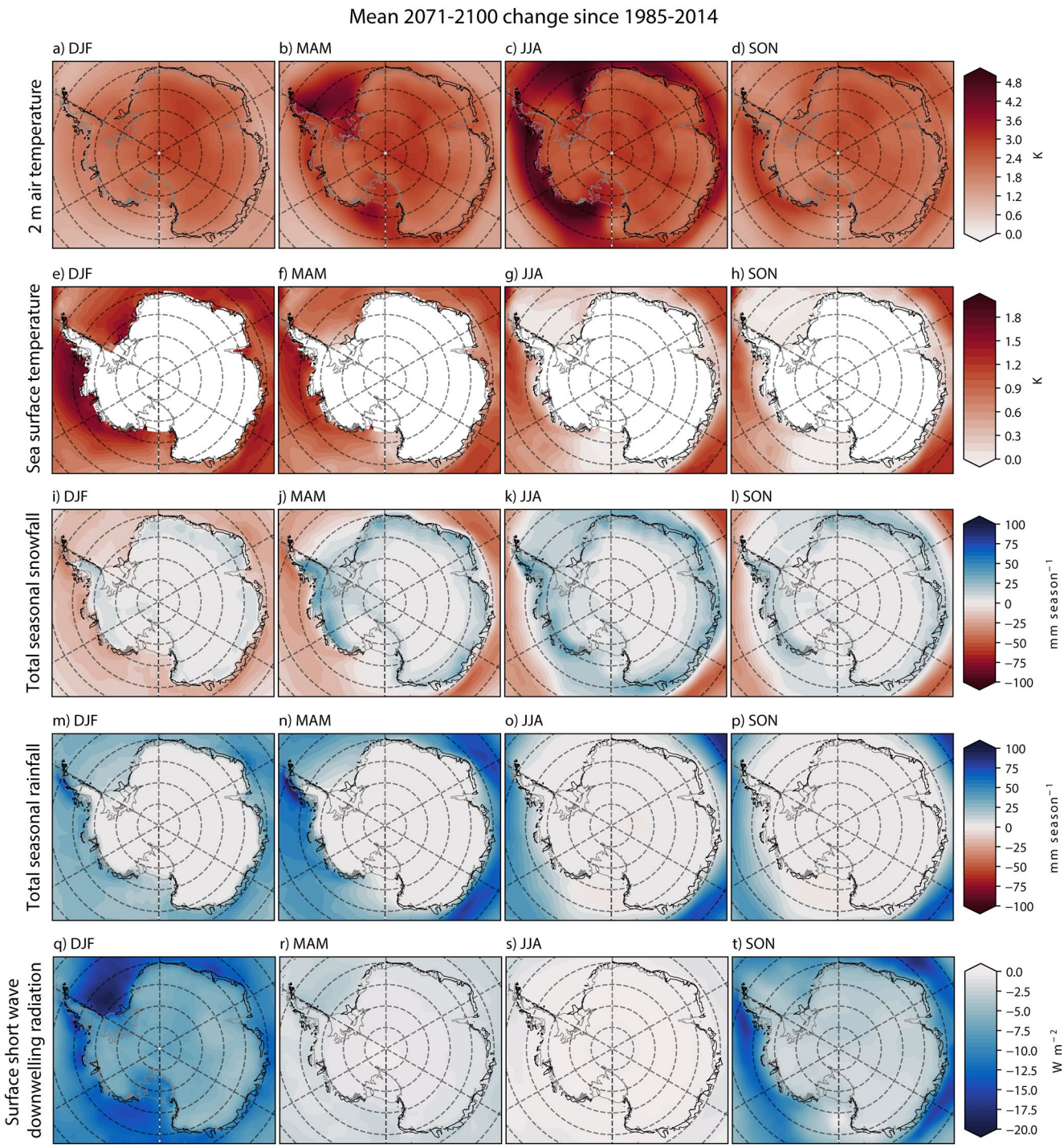

Figure 14. Multi-model mean seasonal changes (2071–2100 minus 1985–2014) in each field over the present-day fast ice extent (outlined in black). (a–d) 2 m air temperature. (e–h) Sea-surface temperature. (i–l) Total snowfall. (m–p) Total rainfall. (q–t) Shortwave radiation. Other fields are given in Figure 15.

9.3. Fast-Ice Physical Properties Outlook

We first consider the future of Antarctic fast-ice extent, in the context of the projections of its known drivers to the end of the 21st Century. In many regions, the fast-ice extent is limited in its maximum winter/springtime extent by the distribution of grounded icebergs (Fraser et al., 2012). The depth to which fast ice forms varies regionally (from around 200 m in the Bellingshausen Sea where iceberg grounding is not closely associated

19449208, 2023, 2, Downloaded from https://agupubs.onlinelibrary.wiley.com/doi/10.1029/2022RG000770 by University of Adelaide Alumni, Wiley Online Library on [16/08/2023]. See the Terms and Conditions (https://onlinelibrary.wiley.com/terms-and-conditions) on Wiley Online Library for rules of use; OA articles are governed by the applicable Creative Commons License

Table 1
Multi-Model Mean Seasonal Changes (From 1985–2014 to 2071–2100) and Baseline Mean Values (in Brackets) Averaged Over the Present-Day Fast-Ice Location for the Fields of Interest

Field	DJF	MAM	JJA	SON
2 m air temperature (°C)	1.84 (−2.14)	2.96 (−10.6)	3.41 (−18.37)	2.23 (−13.16)
Sea-surface temperature (°C)	1.25 (0.52)	0.693 (−0.79)	0.139 (−1.75)	0.0869 (−1.75)
Snowfall (mm w.e. season^{-1})	−13.5 (78.3)	6.26 (155.0)	20.0 (140.0)	9.86 (130.0)
Rainfall (mm season^{-1})	26.2 (39.5)	21.7 (27.5)	4.37 (3.63)	3.52 (4.44)
Incoming SW rad (W m^{-2})	−12.6 (253.0)	−2.1 (34.9)	−0.2 (4.9)	−6.2 (167.0)
U wind component (m s^{-1})	0.12 (−1.97)	0.12 (−2.4)	0.02 (−2.61)	0.04 (−2.21)
V wind component (m s^{-1})	−0.05 (0.82)	−0.14 (1.84)	−0.02 (1.81)	0.00 (1.16)
Mean wind speed (m s^{-1})	−0.06 (2.78)	−0.04 (4.28)	0.04 (4.34)	0.00 (3.66)
Sea-ice concentration (%)	−12.6 (32.2)	−15.7 (45.6)	−11.2 (83.1)	−7.44 (82.3)
Sea-ice thickness (m)	−0.30 (1.43)	−0.16 (0.63)	−0.22 (0.82)	−0.26 (1.1)

Note. SW rad is shortwave radiation and w.e. is water equivalent.

with fast ice formation, to around 450 m in the East Antarctic, where grounded icebergs stabilize a majority of the fast ice; Fraser et al., 2021; Li et al., 2020), depending on bathymetry and the availability of suitably deep icebergs. Projected sea-level rise by 2100 (of up to ∼1.1 m) is itself unlikely to significantly affect the distribution of grounded icebergs; however changes in ice-shelf thickness (thinning in all regions, of up to ∼100 m, after Seroussi et al., 2020) will impact the draft of icebergs and hence reduce the area of iceberg grounding zones. Using version 2 of the International Bathymetric Chart of the Southern Ocean data set (Dorschel et al., 2022) as a reference, we calculate that a reduction in maximum iceberg depth from 400 to 300 m would result in an areal reduction in potential circum-Antarctic iceberg grounding locations of ∼53.7% (from 913,000 to 423,000 km^2), highlighting the considerable sensitivity of fast-ice extent to iceberg depth.

Wholesale collapse of vulnerable ice shelves may also impact the production of suitably deep icebergs (e.g., the Thwaites Glacier which produces a multitude of icebergs which ground to form the Thwaites Iceberg Tongue, ∼74°S, 108.5°W, contributing to the extensive fast ice in that region; Scambos et al., 2017). Recent observed reduction in ice shelf area (Greene et al., 2022) is broadly consistent with projection of increased iceberg production throughout the 21st Century (Massom & Stammerjohn, 2010). This may lead to an increase in the incidence of grounded icebergs on bathymetric ridges on the continental shelf, thereby favoring fast-ice formation. The grounding (and subsequent ungrounding) of vast, tabular icebergs, such as B09B which remained grounded upstream of the MGT for several decades, is known to have profound effects on fast-ice extent (Massom, Hill, et al., 2001), but projections of the calving and subsequent grounding of such icebergs are not feasible. The marine ice cliff instability mechanism (Pollard et al., 2015) may lead to the production of icebergs with very deep drafts of (∼800 m), thus potentially leading to iceberg grounding (and fast ice forming) in new regions (Fraser et al., 2021).

In addition to changes in grounded iceberg distribution, projected changes in the climate are expected to have an effect on fast-ice stability and seasonality. An increase in air and sea-surface temperature in all seasons (Figures 14a–14h) will delay the onset of freeze-up, advance the timing of melt, and reduce thermodynamic thickening, leading to a shorter fast-ice season in regions of seasonal fast ice. Heil (2006) found a high correlation between wintertime mean air temperature and fast-ice thickness. Using the relationship from that study with a CMIP6-projected wintertime air temperature increase of 3.41°C, we project a fast-ice maximum thickness change of −0.14 m by 2100.

Changes in fast-ice physical parameters will be exacerbated by a projected increase in rainfall (Vignon et al., 2021; Figures 14m–14p), particularly in summer and autumn, which will reduce snow albedo and become a source of latent heat when refreezing (Dou et al., 2019). However, this effect may be balanced by the stabilizing effects of higher snowfall in winter and spring (Ushio, 2006). These changes are directly reflected in the projected sea-ice thinning in almost all regions (Figures 15q–15t). A reduction in adjacent pack-ice concentration

19449208, 2023, 2, Downloaded from https://agupubs.onlinelibrary.wiley.com/doi/10.1029/2022RG000770 by University of Adelaide Alumni, Wiley Online Library on [16/08/2023]. See the Terms and Conditions (https://onlinelibrary.wiley.com/terms-and-conditions) on Wiley Online Library for rules of use; OA articles are governed by the applicable Creative Commons License

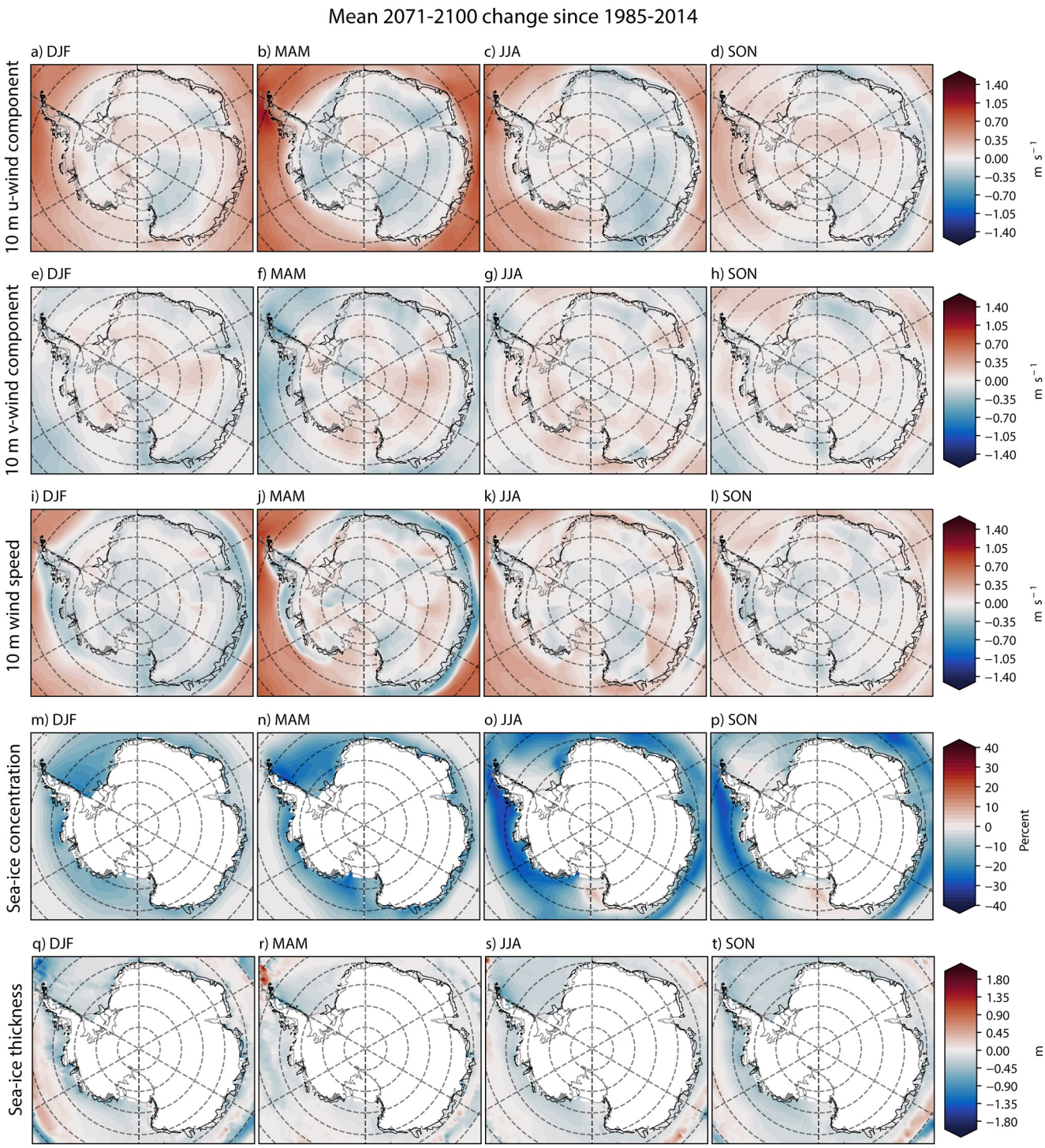

Figure 15. As for Figure 14 but for 10 m eastward wind component (Panels a–d), 10 m northward wind component (e–h), 10 m wind speed (i–l), sea-ice concentration (m–p) and sea-ice thickness (q–t).

(Figures 15m–15p), manifesting as a more open/diffuse pack-ice cover, will both permit more ocean waves within regions of fast ice and increase solar absorption in the upper ocean, potentially leading to more "mode 3" warm water incursions resulting in thinning of fast ice (S. Arndt et al., 2020). Thinner fast ice has lower tensile strength, so it is more prone to breakout (König Beatty & Holland, 2010). These changes also have the potential to change multi-year fast ice to seasonal fast ice in some regions.

19449208, 2023, 2, Downloaded from https://agupubs.onlinelibrary.wiley.com/doi/10.1029/2022RG000770 by University of Adelaide Alumni, Wiley Online Library on [16/08/2023]. See the Terms and Conditions (https://onlinelibrary.wiley.com/terms-and-conditions) on Wiley Online Library for rules of use; OA articles are governed by the applicable Creative Commons License

Near-surface wind changes throughout the 21st Century may also influence fast-ice distribution. The CMIP6 model analysis presented here indicates a trend toward reduced easterly and southerly wind components (indicative of reduced katabatic wind outflow) over fast ice, particularly around East Antarctica and in summer and autumn (Figures 15a–15l here; and Neme et al., 2022). This may modify the trajectory of near-coastal pack ice, resulting in a change in the interception of pack ice by coastal protrusions in some regions (e.g., Cape Darnley; Fraser et al., 2019), though changes are likely to be region-specific, and projections appear to be sensitive to the choice of forcing scenario (Bracegirdle et al., 2020). Based on the work of Leonard et al. (2021), the projected increase in southerly winds in autumn and winter in the western Ross Sea (Figures 15a–15l) may indicate an increase in the activation of the McMurdo Sound Polynya in these seasons, corresponding to a decrease in fast-ice extent there, although storminess (a key driver of fast-ice breakout in this region) has not been considered in our interpretation of these CMIP model projections.

Although it has yet to be studied in CMIP6 models, CMIP5-based studies agree that Southern Ocean storm tracks will intensify and move further south, potentially resulting in increased storminess in the near-coastal zone (Chemke, 2022). Recent research has also indicated that such projected changes are underestimated by CMIP5 models (Chemke et al., 2022). An increase in storminess is likely to increase ocean swell, which is recognized as a driver of fast-ice breakout (see Section 4 of this review). Reduced proximity of fast ice to cyclones will also intensify the synoptic variability in wind speed and direction as cyclonic systems transit from west to east, potentially destabilizing fast ice.

9.4. Biogeochemistry and Ecology Outlook

Prior work has demonstrated a link between increasing air temperature (Figures 14a–14d) and brine volume fraction, associated with brine drainage, particularly in the interior ice (van der Merwe et al., 2011). Therefore, fast-ice permeability is expected to increase earlier in the spring season due to warmer near-surface air temperature and thinner ice (Figures 15q–15t), leading to earlier brine drainage and decrease in sea-ice bulk salinity. Seasonally, we predict the earlier release of dissolved constituents, including Fe, from brines into underlying seawater, coincident with the earlier fast-ice breakup, extending the growing season in coastal open water. In the lower layers of fast ice, the increase in sea-ice permeability earlier in the season may lead to more nutrient exchange with underlying seawater and habitable space for ice algae within sea ice. However, the predicted increase in September-November snowfall and rainfall (Figures 14l and 14p, respectively) will have opposite impacts on snowpack thickness during the spring melt. As a result of these conflicting processes, the insulating properties of the snowpack may be variable, leading to more variability in sea-ice permeability and ice bottom layer ablation.

The greatest impact on ice algal biomass will be likely due to loss of habitat through reductions in fast- (and pack-) ice cover duration. The delayed formation and earlier breakout of seasonal fast ice will reduce the overall habitable duration for sea-ice algae, but should favor coastal phytoplankton production due to higher light availability in ice-free areas (despite slightly lower spring and summer incoming shortwave radiation; Figures 14t and 14q respectively). The shift from sea-ice algae to phytoplankton is likely to augment the exchanges of climate-active gasses between the ocean and the atmosphere, with an increase in the uptake of CO_2 and emission of DMS respectively due to derestricted ocean-atmosphere exchange. Conversely, higher (but more variable) fast-ice permeability should result in more efficient exchange with the atmosphere for the sympagic algae community that remains, but over a shorter overall season. Note that the CMIP6 models have no implementation of ice shelf cavities, and further work is thus required to establish the outlook of BGC dynamics in fast ice near ice shelves.

Other details, described in this paragraph, are likely to be second-order effects. At the end of the century, higher near-surface air temperatures (Figures 14a–14d) will likely lead to greater sea-ice porosity and permeability, probably favoring more extensive development of internal ice algal communities as well as surface communities. The predicted small decrease in downward solar radiation (Figures 14q and 14t), coupled with increases in snowfall, except for summer (Figures 14i–14l), will generally result in decreased light availability for ice algal communities and likely delay the onset of the fast-ice algal spring bloom, although increased rainfall could decrease the albedo leading to a net increase in light availability. A reduction in ice thickness will reduce the insulation capacity of the ice cover and likely negatively affect ice algal bottom communities due to higher variability in bottom ice freeze/melt cycles. The overall importance of

19449208, 2023, 2, Downloaded from https://agupubs.onlinelibrary.wiley.com/doi/10.1029/2022RG000770 by University of Adelaide Alumni, Wiley Online Library on [16/08/2023]. See the Terms and Conditions (https://onlinelibrary.wiley.com/terms-and-conditions) on Wiley Online Library for rules of use; OA articles are governed by the applicable Creative Commons License

sea-ice algae as a winter and early-spring food source for pelagic and benthic herbivores (e.g., Cummings et al., 2018) suggests that these changes will have profound flow-on ecological effects throughout coastal Antarctic food webs.

Recently, qualitative network modeling used to explore responses of micro and macrograzers showed that concentrations and abundances of pelagic algae, copepods, krill and fish will likely decrease as a response to decreasing sea-ice duration and increasing temperatures (Swadling et al., 2023). Reduced duration of fast ice due to delayed formation and earlier breakout could lead to some species being unable to complete their life cycles. As discussed in Section 8, there appears to be a spectrum along which species fall with regard to their dependency on fast ice. If the ice has a shortened duration, the nudibranch mollusc *T. antarcticus* might be the most adversely affected due to its limited ability to adopt a pelagic lifestyle. *Drescheriella glacialis* is also a weak swimmer, but its traits including fast growth, high fecundity and overlapping generations could mean that it will be able to thrive as long as any ice is present to complete its development and reproduce. The reduction in salinity of brine, as a response to increased temperature and thus permeability and drainage, could incur physiological costs for species, including microzooplankton. The microzooplankton richness in the fast-ice zone may decrease and the resulting biomass will likely be dominated by ciliates and heterotrophic dinoflagellates (Garcia et al., 2020). Haline and thermal plasticity are important for the two calanoid copepods, both of which demonstrate the capacity to survive outside of an ice cover; however the number of generations required to fully adapt to a new ice environment might be too high for them to respond effectively. Reduction in platelet ice leading to poor recruitment of the Antarctic silverfish could produce the greatest flow-on effects through the fast-ice trophic web as this fish is a vital food source for many marine predators—however a recent review of platelet ice indicated that its future is highly uncertain (Hoppmann et al., 2020). *P. antarcticum* populations have decreased substantially around the Western Antarctic Peninsula (Corso et al., 2022), where increasing incursions of warm CDW have led to the disappearance of platelet ice and loss of key nursery habitat (Hoppmann et al., 2020).

10. Summary

It should be clear by now that there is a considerable body of knowledge focusing on Antarctic fast ice. What has also emerged from compiling this review is that the majority of studies are limited either spatially (e.g., covering a small study region), temporally (e.g., a snapshot, or covering only some part of the annual cycle), or both. In this review, we have aimed to alleviate these shortcomings by synthesizing similar studies across space and time. Nevertheless, while there exist regions of concentrated studies—particularly in McMurdo Sound and Terra Nova Bay along the Victoria Land coast (162°E–170°E)—we note that there are vast tracts of fast ice which are understudied. An example of this is the fast ice lying off the coast of Marie Byrd Land at around 140°W, which is extensive and undergoing significant decline (Figure 13), but bereft of in situ observations due to its considerable distance from research stations.

It is also abundantly clear that the importance of Antarctic fast ice is paramount. A wide range of glaciological, oceanographic, biogeochemical, biological, and ecological studies have been presented here, leading to the conclusion that fast ice exerts primary control on many aspects of the Earth system—and this conclusion is clear even with our limited scope excluding trophic levels higher than macrograzers. As our understanding of the near-coastal Antarctic environment deepens, and model resolution increases, neglecting or crudely parameterizing fast ice and its multitude of interactions becomes unthinkable. Conversely, a realistic and appropriate representation of fast ice in scientific studies will pave the way to a better understanding of this crucial element of the Antarctic ice-scape, as well as its far-reaching effects.

It is worth posing the question "which is more important—the shrinkage of pack ice or the loss of fast ice into the 21st Century?" Given the fact that pack ice covers around one order of magnitude more area than fast ice at any given time of year, it is natural to assume that the loss of pack ice will be more important—however this conclusion is currently unable to be strongly supported without both (a) the ability of global coupled models to accurately represent recent trends in Antarctic sea ice (Roach et al., 2020), and (b) fast ice representation in these models. Here we have shown that fast ice "punches well above its weight" in terms of its climate impact, and its inclusion in climate models should be a focus from now.

19449208, 2023, 2, Downloaded from https://agupubs.onlinelibrary.wiley.com/doi/10.1029/2022RG000770 by University of Adelaide Alumni, Wiley Online Library on [16/08/2023]. See the Terms and Conditions (https://onlinelibrary.wiley.com/terms-and-conditions) on Wiley Online Library for rules of use; OA articles are governed by the applicable Creative Commons License

As a synthesis of the gaps presented at the end of each of the main Sections 2–8 here, we now present concluding remarks highlighting suggested future research in terms of fast-ice observations (both in situ and remote) and modeling. Taken on a circum-Antarctic scale, the present state of in situ fast-ice observation is somewhat disparate, with the AFIN (which covers only physical and basic chemical parameters) being the only attempt at measurement standardization (Heil, Gerland, & Granskog, 2011). In synthesizing chlorophyll-*a* measurements from Antarctic fast-ice cores, Meiners et al. (2018) pointed to the lack of consistent coring methodology and a highly non-uniform distribution of samples throughout space and time as major impediments to achieving a representative data set. As such, we urge the fast-ice community to develop new standardized methods for joint physical, biogeochemical and biological sampling, with a view to automated deployments in regions and time periods currently undersampled. A coordinated suite of observations would facilitate baseline characterization of key parameters as well as early identification of system changes.

Regarding remote observations of fast ice, we reiterate the fundamental importance of knowledge of large-scale fast-ice distribution. From a long-term, high-resolution data set of fast-ice distribution, many crucial baseline parameters can be obtained (e.g., the climatological cycle of fast-ice extent), as well as studies on the variability and trends in fast-ice cover. Complementary studies can then leverage such a data set, for example, the key parameters of fast-ice freeboard and roughness can be easily estimated altimetrically if its spatial distribution is known. However, accurate estimates of fast-ice density and snow density and thickness are still required for accurate conversion from freeboard to thickness using hydrostatic principles, and this requires further (and more-widespread) in situ sampling (particularly in regions of rough fast ice, where few in situ measurements exist). As such, we underscore the importance of developing an automated and accurate method for the near-real time extraction of fast-ice distribution from satellite imagery, upon which a wide range of multi-disciplinary studies can be based.

While the one-dimensional simulation of fast ice has quickly progressed toward maturity (e.g., Wongpan et al., 2021), the accurate simulation of fast ice in three dimensions has only been achieved recently for the first time (Huot et al., 2021; Van Achter, Fichefet, Goosse, Pelletier, et al., 2022), following the lead of the Arctic modeling community (König Beatty & Holland, 2010; Lemieux et al., 2016). Now that this has been demonstrated, it is hoped that many more regional sea ice-ocean models will incorporate the techniques needed to fully model fast ice, and that such an implementation paves the way for Antarctic fast-ice representation in circumpolar (and eventually global) models. The validation of these model outputs is also of crucial importance. The ability to study the formation, growth, decay and breakout of fast ice in a model not only unlocks new insights from process studies (e.g., the interaction between fast-ice extent and adjacent coastal polynya sea-ice production; Fraser et al., 2019), but also allows new understanding of fast-ice climate sensitivity and future projections.

Regarding the future of Antarctic fast ice, it is expected from the CMIP6 projections presented here that season duration will decrease, owing to a loss of adjacent protective pack ice, warming air and sea-surface temperatures, and increasing rainfall and storminess. As a consequence of the same drivers, many regions of multi-year fast ice will shift to seasonal fast ice, a process which has possibly already begun (as indicated by the loss of multi-year fast ice in early 2022, shown in Figure 13). The wintertime maximum extent of fast ice is difficult to project in the absence of prognostic representation in models: it is likely that fast-ice extent may be more resilient against change during wintertime, where the limiting factor is no longer environmental drivers but the distribution of grounded icebergs. However, its thickness may decrease in line with a shorter growth season. With so many uncertain interactions, incorporation of Antarctic fast ice into circum-Antarctic ice-ocean-atmosphere models becomes an urgent priority—an achievement which will contribute considerably to our understanding of this often overlooked but crucial component of the near-shore Antarctic system.

Appendix A: Literature Search Terms

Table A1 lists the final *Scopus* (available at https://www.scopus.com) search particulars used for each review section. Slight differences in search string format between sections were used to ensure wide coverage of relevant literature within each section.

19449208, 2023, 2, Downloaded from https://agupubs.onlinelibrary.wiley.com/doi/10.1029/2022RG000770 by University of Adelaide Alumni, Wiley Online Library on [16/08/2023]. See the Terms and Conditions (https://onlinelibrary.wiley.com/terms-and-conditions) on Wiley Online Library for rules of use; OA articles are governed by the applicable Creative Commons License

Table A1
Scopus Search Particulars for Each Review Section

Section	Date performed	Search string	Hits
2: "Growth and properties"	2021-08-04	TITLE-ABS-KEY (landfast ice OR fast ice OR land-fast ice OR landfast sea ice OR land-fast sea ice AND (antarctic OR antarctica) AND (thermodynamic OR thermodynamics OR thickness OR dimensional))	99
3: "Distribution, seasonality, remote sensing"	2021-08-05	TITLE-ABS-KEY (landfast ice OR fast ice OR fast-ice OR land-fast ice OR landfast sea ice OR land-fast sea ice AND (antarctic OR antarctica) AND (seasonality OR remote sensing OR climatology OR mapping OR break-up OR breakup OR break-out OR breakout))	98
4: "Fast ice-atmospheric interactions"	2021-07-29	TITLE-ABS-KEY (landfast ice OR fast ice OR land-fast ice OR landfast sea ice OR land-fast sea ice AND antarctic AND atmosphere OR atmospheric OR wind OR teleconnection OR climate OR breakout OR breakup OR weather)	105
5: "Fast ice-ocean interactions"	2021-07-09	TITLE-ABS-KEY (landfast ice OR fast ice OR land-fast ice OR landfast sea ice OR land-fast sea ice AND antarctic OR antarctica AND ocean)	166
6: "Biogeochemistry"	2021-08-05	TITLE-ABS-KEY (landfast ice OR fast ice OR land-fast ice OR landfast sea ice OR land-fast sea ice AND (antarctic OR antarctica) AND (nutrient OR nutrients OR metals OR carbon OR bioactive gases OR biogeochemistry OR biogeochemical))	72
7: "Primary production"	2021-07-28	TITLE-ABS-KEY (landfast ice OR fast ice OR land-fast ice OR landfast sea ice OR land-fast sea ice AND antarctic OR antarctica AND algae OR primary) Take 2: TITLE-ABS-KEY (landfast ice OR fast ice OR land-fast ice OR landfast sea ice OR land-fast sea ice AND antarctic OR antarctica AND algae OR primary OR chlorophyll)	105
8: "Grazers"	2021-07-30	TITLE-ABS-KEY (landfast ice OR fast ice OR land-fast ice OR landfast sea ice OR land-fast sea ice OR sea ice AND antarctic OR Antarctica AND copepods OR fish OR pteropods OR grazers OR grazing OR amphipods OR meiofauna AND NOT krill AND NOT penguin AND NOT seal)	183

Appendix B: CMIP6 Model Variants Used

Table B1 indicates which CMIP6 models and variants were used in Section 9 here to estimate the change in environmental parameters around the present-day fast-ice location by the end of the 21st Century.

Table B1
CMIP6 Model, Variant, and Model Reference

Model	Variant	DOI
ACCESS-CM2	r1i1p1f1	https://doi.org/10.22033/ESGF/CMIP6.2281
ACCESS-ESM1-5	r1i1p1f1	https://doi.org/10.22033/ESGF/CMIP6.2288
CMCC-ESM2	r1i1p1f1	https://doi.org/10.22033/ESGF/CMIP6.13165
CNRM-CM6-1	r1i1p1f2	https://doi.org/10.22033/ESGF/CMIP6.1375
CNRM-CM6-1-HR	r1i1p1f2	https://doi.org/10.22033/ESGF/CMIP6.1385
CNRM-ESM2-1	r1i1p1f2	https://doi.org/10.22033/ESGF/CMIP6.1391
EC-Earth3	r1i1p1f1	https://doi.org/10.22033/ESGF/CMIP6.181
EC-Earth3-CC	r1i1p1f1	https://doi.org/10.22033/ESGF/CMIP6.640
EC-Earth3-Veg	r1i1p1f1	https://doi.org/10.22033/ESGF/CMIP6.642
EC-Earth3-Veg-LR	r1i1p1f1	https://doi.org/10.22033/ESGF/CMIP6.643
GFDL-ESM4	r1i1p1f1	https://doi.org/10.22033/ESGF/CMIP6.1407
IPSL-CM6A-LR	r1i1p1f1	https://doi.org/10.22033/ESGF/CMIP6.1534
MIROC-ES2L	r1i1p1f2	https://doi.org/10.22033/ESGF/CMIP6.5602
MIROC6	r1i1p1f1	https://doi.org/10.22033/ESGF/CMIP6.881
MPI-ESM1-2-HR	r1i1p1f1	https://doi.org/10.22033/ESGF/CMIP6.741
MPI-ESM1-2-LR	r1i1p1f1	https://doi.org/10.22033/ESGF/CMIP6.6595

19449208, 2023, 2, Downloaded from https://agupubs.onlinelibrary.wiley.com/doi/10.1029/2022RG000770 by University of Adelaide Alumni, Wiley Online Library on [16/08/2023]. See the Terms and Conditions (https://onlinelibrary.wiley.com/terms-and-conditions) on Wiley Online Library for rules of use; OA articles are governed by the applicable Creative Commons License

Table B1
Continued

Model	Variant	DOI
MRI-ESM2-0	r1i1p1f1	https://doi.org/10.22033/ESGF/CMIP6.621
NESM3	r1i1p1f1	https://doi.org/10.22033/ESGF/CMIP6.2021
UKESM1-0-LL	r1i1p1f2	https://doi.org/10.22033/ESGF/CMIP6.1569

Selected Acronyms and Glossary

Acronyms

AABW	Antarctic Bottom Water
AASW	Antarctic Surface Water
ACoC	Antarctic Coastal Current
AEM	Airborne Electromagnetic
AFIN	Antarctic Fast Ice Network
AMSR	Advanced Microwave Sounding Radiometer
ASF	Antarctic Slope Front
CMIP	Coupled Model Intercomparison Project
CDW	Circumpolar Deep Water
DFe	Dissolved iron
DIC	Dissolved Inorganic Carbon
DIN	Dissolved Inorganic Nitrogen
DMSP	Dimethylsulfoniopropionate
DMS	Dimethyl sulfide
DOC	Dissolved Organic Carbon
DON	Dissolved Organic Nitrogen
DSW	Dense Shelf Water
ENSO	El Niño–Southern Oscillation
EPS	Exopolysaccharides
GLAS	Geoscience Laser Altimeter System
HH	Horizontal transmit and horizontal receive
HSSW	High Salinity Shelf Water
ICESat	Ice, Cloud and Land Elevation Satellite
InSAR	Interferometric SAR
ISW	Ice Shelf Water
MAAs	Mycosporine-like Amino Acids
mCDW	Modified Circumpolar Deep Water
MGT	Mertz Glacier Tongue
MODIS	Moderate Resolution Imaging Spectroradiometer
NPZD	Nutrient, Phytoplankton, Zooplankton and Detritus (NPZD) model
TDLs	Theoretical Dilution Lines
pCO_2	Partial pressure of CO_2
PFe	Particulate iron
POC	Particulate Organic Carbon
SAO	Semi-Annual Oscillation
SAM	Southern Annual Mode
SAR	Synthetic aperture radar
SIRAL-2	Synthetic Interferometric Radar Altimeter-2
SSP	Shared Socioeconomic Pathway
TIR	Thermal infrared
WMO	World Meteorological Organization
WW	Winter Water

19449208, 2023, 2, Downloaded from https://agupubs.onlinelibrary.wiley.com/doi/10.1029/2022RG000770 by University of Adelaide Alumni, Wiley Online Library on [16/08/2023]. See the Terms and Conditions (https://onlinelibrary.wiley.com/terms-and-conditions) on Wiley Online Library for rules of use; OA articles are governed by the applicable Creative Commons License

Acknowledgments
This project received grant funding from the Australian Government as part of the Antarctic Science Collaboration Initiative program (project ID ASCI000002), and for DL, RAM, and KMM was supported by the Australian Research Council Special Research Initiative, Australian Centre for Excellence in Antarctic Science (Project Number SR200100008). This work contributes to Australian Antarctic Science Projects 4496, 4506, 4546, 4564, 4593, and 4625. DL is funded by an Australian Research Council Future Fellowship FT190100688. PH acknowledges support through the International Space Science Institute Grant 501.
This research was undertaken with the assistance of resources and services from the National Computational Infrastructure (Project jk72), which is supported by the Australian Government. This research was supported by use of the Nectar Research Cloud and by the Tasmanian Partnership for Advanced Computing. The Nectar Research Cloud is a collaborative Australian research platform supported by the NCRIS-funded Australian Research Data Commons (ARDC). SF would like to thank the ARC Centre of Excellence for Climate Extremes for their maintenance of virtual environments and software including the Climate Finder search ESGF data at NCI. SF would also like to acknowledge the World Climate Research Programme, which, through its Working Group on Coupled Modeling, coordinated and promoted CMIP6. We thank the climate modeling groups for producing and making available their model output, the ESGF for archiving the data and providing access, and the multiple funding agencies who support CMIP6 and ESGF.
The authors would like to thank Dr. Christian Haas, one anonymous reviewer and the editor Prof. Gesine Mollenhauer for providing constructive comments which helped to improve this manuscript. We also thank Prof. Steve Warren for providing comments on the preprint during the review. The authors would also like to thank Dr. Christian Haas from Alfred Wegener Institute for Polar Research for providing aerial photographs, Dr. Stacey McCormack at Visual Knowledge for producing Figures 2 and 10–12, Mr. Dave Connell from the Australian Antarctic Data Centre for his assistance with data set hosting, and Dr. Damien Guihen, Dr. Indi Hodgson-Johnston and A/Prof. Jeffery McGee for their valuable discussion around ship tracking. We acknowledge the use of imagery from the NASA Worldview application (https://worldview.earthdata.nasa.gov/), part of the NASA Earth Observing System Data and Information System (EOSDIS).
Open access publishing facilitated by University of Tasmania, as part of the Wiley - University of Tasmania

Glossary

Chlorophyll-a (Chla) A green pigment found in plants including sea ice algae. Its concentration is a proxy of sea-ice algal biomass

Incorporated platelet ice Consolidated ice comprised of a locally grown sub-ice platelet layer and advancing interface of an established ice cover

Landfast sea ice (fast ice) Fast ice is sea ice that is fastened for a period of time (at least 2 to 3 weeks is a commonly-used range) to icebergs grounded on the continental shelf, or to the coastline itself (including ice shelves)

Pack ice Unlike fast ice, pack ice is mobile and advects with winds and currents

Pelagic Related to the water column (can be classified into zones by depth)

Primary production The creation of organic matter through photosynthesis

Polynya An open area of unfrozen seawater surrounded by sea ice

Snow ice A sea ice type formed by flooding of the upper ice surface with seawater, and freezing of the resultant slush

Sub-ice platelet layer (SIPL) A layer of unconsolidated sea ice found near Antarctic ice shelves. The sub-ice platelet layer is a highly porous, isothermal, friable layer of ice crystals and saltwater, and it can grow to a thickness of several meters

Superimposed ice A sea ice type which forms when meltwater percolating down through the snow column refreezes on contact with the ice surface into an impermeable layer of ice with a polygonal structure

Sympagic A sympagic ecosystem is one where the majority of the water is present as ice, including fast ice-associated algae

Data Availability Statement

CMIP6 data used to create Figures 14 and 15 are available on the NCI ESGF replica (see https://esgf.nci.org.au/search/cmip6-nci/) and were accessed via the Climate Finder search ESGF data at NCI (https://clef.readthedocs.io/en/stable/). The code used to create these figures is available at https://github.com/sfiddes/code_for_publications/tree/main/fast_ice_review. Data used to create Figure 4 are available at http://dx.doi.org/doi:10.26179/5d267d1ceb60c. Data used to create Figure 13 are available at http://dx.doi.org/doi:10.26179/5d267d1ceb60c and http://dx.doi.org/doi:10.26179/g5pp-z960.

References

Abrahamsson, K., Granfors, A., Ahnoff, M., Cuevas, C. A., & Saiz-Lopez, A. (2018). Organic bromine compounds produced in sea ice in Antarctic winter. *Nature Communications*, *9*(1), 5291. https://doi.org/10.1038/s41467-018-07062-8

Ackley, S. F., Buck, K. R., & Taguchi, S. (1979). Standing crop of algae in the sea ice of the Weddell Sea region. *Deep-Sea Research, Part A: Oceanographic Research Papers*, *26*(3), 269–281. https://doi.org/10.1016/0198-0149(79)90024-4

Ackley, S. F., & Sullivan, C. W. (1994). Physical controls on the development and characteristics of Antarctic sea ice biological communities—A review and synthesis. *Deep Sea Research Part I: Oceanographic Research Papers*, *41*(10), 1583–1604. https://doi.org/10.1016/0967-0637(94)90062-0

Ackley, S. F., Xie, H., & Tichenor, E. A. (2015). ocean heat flux under Antarctic sea ice in the Bellingshausen and Amundsen seas: Two case studies. *Annals of Glaciology*, *56*(69), 200–210. https://doi.org/10.3189/2015aog69a890

Ainley, D. G., Larue, M. A., Stirling, I., Stammerjohn, S., & Siniff, D. B. (2015). An apparent population decrease, or change in distribution, of Weddell seals along the Victoria Land coast. *Marine Mammal Science*, *31*(4), 1338–1361. https://doi.org/10.1111/mms.12220

Allison, I. (1989). The East Antarctic sea ice zone: Ice characteristics and drift. *Geojournal*, *18*(1), 103–115. https://doi.org/10.1007/bf00722394

Allison, I., Brandt, R. E., & Warren, S. G. (1993). East Antarctic sea ice: Albedo, thickness distribution, and snow cover. *Journal of Geophysical Research*, *98*(C7), 12417. https://doi.org/10.1029/93jc00648

Andriashev, A. (1968). The problem of the life community associated with the Antarctic fast ice. In R. Currie (Ed.), *Symposium on antarctic oceanography, scar/scor/iapo/iubs, santiago, Chile* (pp. 147–155). Scott Polar Research Institute.

Aoki, S. (2017). Breakup of land-fast sea ice in Lützow-Holm Bay, East Antarctica, and its teleconnection to tropical Pacific sea surface temperatures. *Geophysical Research Letters*, *44*(7), 3219–3227. https://doi.org/10.1002/2017gl072835

Archer, S. D., Leakey, R. J. G., Burkill, P. H., Sleigh, M. A., & Appleby, C. J. (1996). Microbial ecology of sea ice at a coastal Antarctic site: Community composition, biomass and temporal change. *Marine Ecology Progress Series*, *135*, 179–195. https://doi.org/10.3354/meps135179

Arndt, C. E., & Swadling, K. M. (2006). Crustacea in Arctic and Antarctic sea ice: Distribution, diet and life history strategies. *Advances in Marine Biology*, *51*, 197–315. https://doi.org/10.1016/s0065-2881(06)51004-1

Arndt, S., Hoppmann, M., Schmithüsen, H., Fraser, A. D., & Nicolaus, M. (2020). Seasonal and interannual variability of landfast sea ice in Atka Bay, Weddell Sea, Antarctica. *The Cryosphere*, *14*(9), 2775–2793. https://doi.org/10.5194/tc-14-2775-2020

Arrigo, K. R. (2013). Sea Ice ecosystems. *Annual Review of Marine Science*, *6*(1), 439–467. https://doi.org/10.1146/annurev-marine-010213-135103

19449208, 2023, 2, Downloaded from https://agupubs.onlinelibrary.wiley.com/doi/10.1029/2022RG000770 by University of Adelaide Alumni, Wiley Online Library on [16/08/2023]. See the Terms and Conditions (https://onlinelibrary.wiley.com/terms-and-conditions) on Wiley Online Library for rules of use; OA articles are governed by the applicable Creative Commons License

agreement via the Council of Australian University Librarians.

Arrigo, K. R. (2017). Sea ice as a habitat for primary producers. In *Sea ice* (pp. 352–369). John Wiley & Sons, Ltd. https://doi.org/10.1002/9781118778371.ch14

Arrigo, K. R., Brown, Z. W., & Mills, M. M. (2014). Sea ice algal biomass and physiology in the Amundsen Sea, Antarctica. *Elementa: Science of the Anthropocene*, *2*(1), 28. https://doi.org/10.12952/journal.elementa.000028

Arrigo, K. R., Dieckmann, G. S., Gosselin, M., Robinson, D. H., Fritsen, C. H., & Sullivan, C. W. (1995). High resolution study of the platelet ice ecosystem in McMurdo Sound, Antarctica: Biomass, nutrient, and production profiles within a dense microalgal bloom. *Marine Ecology Progress Series*, *127*, 255–268. https://doi.org/10.3354/meps127255

Arrigo, K. R., Kremer, J. N., & Sullivan, C. W. (1993). A simulated Antarctic fast ice ecosystem. *Journal of Geophysical Research*, *98*(C4), 6929–6946. https://doi.org/10.1029/93jc00141

Arrigo, K. R., Mock, T., & Lizotte, M. P. (2010). Primary producers and sea ice. In D. N. Thomas & G. S. Dieckmann (Eds.), *Sea ice* (2nd ed., pp. 283–326). Wiley-Blackwell.

Arrigo, K. R., & Sullivan, C. W. (1994). A high resolution bio-optical model of microalgal growth: Tests using sea-ice algal community time-series data. *Limnology & Oceanography*, *39*(3), 609–631. https://doi.org/10.4319/lo.1994.39.3.0609

Arrigo, K. R., Worthen, D., Schnell, A., & Lizotte, M. P. (1998). Primary production in Southern Ocean waters. *Journal of Geophysical Research*, *103*(C8), 15587–15600. https://doi.org/10.1029/98jc00930

Arrigo, K. R., Worthen, D. L., & Robinson, D. H. (2003). A coupled ocean-ecosystem model of the Ross Sea: 2. Iron regulation of phytoplankton taxonomic variability and primary production. *Journal of Geophysical Research*, *108*(C7), 3231. https://doi.org/10.1029/2001jc000856

Arthur, J. F., Stokes, C. R., Jamieson, S. S. R., Miles, B. W. J., Carr, J. R., & Leeson, A. A. (2021). The triggers of the disaggregation of Voyeykov Ice Shelf (2007), Wilkes land, East Antarctica, and its subsequent evolution. *Journal of Glaciology*, *67*(265), 1–19. https://doi.org/10.1017/jog.2021.45

Aslam, S. N., Michel, C., Niemi, A., & Underwood, G. J. C. (2016). Patterns and drivers of carbohydrate budgets in ice algal assemblages from first year Arctic sea ice. *Limnology & Oceanography*, *61*(3), 919–937. https://doi.org/10.1002/lno.10260

Aumack, C. F., Juhl, A. R., & Krembs, C. (2014). Diatom vertical migration within land-fast Arctic sea ice. *Journal of Marine Systems*, *139*, 496–504. https://doi.org/10.1016/j.jmarsys.2014.08.013

Barber, D., & Massom, R. (2007). The role of sea ice in Arctic and Antarctic polynyas (pp. 1–54). https://doi.org/10.1016/S0422-9894(06)74001-6

Barlow, R., Gosselin, M., Legendre, L., Therriault, J.-C., Demers, S., Mantoura, R., & Llewellyn, C. (1988). Photoadaptive strategies in sea-ice microalgae. *Marine Ecology Progress Series*, *45*, 145–152. https://doi.org/10.3354/meps045145

Bayer-Giraldi, M., Weikusat, I., Besir, H., & Dieckmann, G. (2011). Characterization of an antifreeze protein from the polar diatom *Fragilariopsis cylindrus* and its relevance in sea ice. *Cryobiology*, *63*(3), 210–219. https://doi.org/10.1016/j.cryobiol.2011.08.006

Belt, S. T., Smik, L., Brown, T. A., Kim, J. H., Rowland, S. J., Allen, C. S., et al. (2016). Source identification and distribution reveals the potential of the geochemical Antarctic sea ice proxy IPSO25. *Nature Communications*, *7*(1), 12655. https://doi.org/10.1038/ncomms12655

Bergmans, M., Dahms, H.-U., & Schminke, H. K. (1991). An r-strategist in Antarctic pack ice. *Oecologia*, *86*(3), 305–309. https://doi.org/10.1007/bf00317594

Bluhm, B., Swadling, K., & Gradinger, R. (2017). Sea ice as a habitat for macrograzers. In D. Thomas (Ed.), *Sea ice* (3rd ed.). John Wiley & Sons, Ltd.

Bracegirdle, T. J., Krinner, G., Tonelli, M., Haumann, F. A., Naughten, K. A., Rackow, T., et al. (2020). Twenty first century changes in Antarctic and Southern Ocean surface climate in CMIP6. *Atmospheric Science Letters*, *21*(9), e984. https://doi.org/10.1002/asl.984

Bradford, J. H., Babcock, E. L., Marshall, H.-P., & Dickins, D. F. (2016). Targeted reflection-waveform inversion of experimental ground-penetrating radar data for quantification of oil spills under sea ice. *Geophysics*, *81*(1), WA59–WA70. https://doi.org/10.1190/geo2015-0170.1

Brandt, R. E., Warren, S. G., Worby, A. P., & Grenfell, T. C. (2005). Surface albedo of the Antarctic sea ice zone. *Journal of Climate*, *18*(17), 3606–3622. https://doi.org/10.1175/jcli3489.1

Brearley, J. A., Meredith, M. P., Naveira Garabato, A. C., Venables, H. J., & Inall, M. E. (2017). Controls on turbulent mixing on the West Antarctic Peninsula shelf. *Deep Sea Research Part II: Topical Studies in Oceanography*, *139*, 18–30. https://doi.org/10.1016/j.dsr2.2017.02.011

Brett, G. M., Irvin, A., Rack, W., Haas, C., Langhorne, P. J., & Leonard, G. H. (2020). Variability in the distribution of fast ice and the sub-ice platelet layer near McMurdo ice shelf. *Journal of Geophysical Research: Oceans*, *125*(3), e2019JC015678. https://doi.org/10.1029/2019jc015678

Brooks, C. M., Caccavo, J. A., Ashford, J., Dunbar, R., Goetz, K., La Mesa, M., & Zane, L. (2018). Early life history connectivity of Antarctic silverfish (Pleuragramma Antarctica) in the Ross Sea. *Fisheries Oceanography*, *27*(3), 274–287. https://doi.org/10.1111/fog.12251

Brunt, K. M., Sergienko, O., & MacAyeal, D. R. (2006). Observations of unusual fast-ice conditions in the southwest Ross Sea, Antarctica: Preliminary analysis of iceberg and storminess effects. *Annals of Glaciology*, *44*, 183–187. https://doi.org/10.3189/172756406781811754

Budd, W. (2004). The physical environment of the Antarctic. In J. Turner & S. Pendlebury (Eds.), *The international antarctic weather forecasting handbook* (pp. 4–7). British Antarctic Survey.

Buffo, J. J., Schmidt, B. E., & Huber, C. (2018). Multiphase reactive transport and platelet ice accretion in the sea ice of McMurdo Sound, Antarctica. *Journal of Geophysical Research: Oceans*, *123*(1), 324–345. https://doi.org/10.1002/2017JC013345

Campbell, K., Mundy, C. J., Gosselin, M., Landy, J. C., Delaforge, A., & Rysgaard, S. (2017). Net community production in the bottom of first-year sea ice over the Arctic spring bloom. *Geophysical Research Letters*, *44*(17), 8971–8978. https://doi.org/10.1002/2017GL074602

Campbell, K., Mundy, C. J., Landy, J. C., Delaforge, A., Michel, C., & Rysgaard, S. (2016). Community dynamics of bottom-ice algae in Dease Strait of the Canadian Arctic. *Progress in Oceanography*, *149*, 27–39. https://doi.org/10.1016/j.pocean.2016.10.005

Caputi, S. S., Careddu, G., Calizza, E., Fiorentino, F., Maccapan, D., Rossi, L., & Costantini, M. L. (2020). Seasonal food web dynamics in the Antarctic benthos of Tethys Bay (Ross Sea): Implications for biodiversity persistence under different seasonal sea-ice coverage. *Frontiers in Marine Science*, *7*, 594454. https://doi.org/10.3389/fmars.2020.594454

Carnat, G., Zhou, J., Papakyriakou, T., Delille, B., Goossens, T., Haskell, T., et al. (2014). Physical and biological controls on DMSP dynamics in ice shelf-influenced fast ice during a winter-spring and a spring-summer transitions. *Journal of Geophysical Research: Oceans*, *119*(5), 2882–2905. https://doi.org/10.1002/2013jc009381

Charlson, R. J., Lovelock, J. E., Andreae, M. O., & Warren, S. G. (1987). Oceanic phytoplankton, atmospheric sulphur, cloud albedo and climate. *Nature*, *326*(6114), 655–661. https://doi.org/10.1038/326655a0

Chemke, R. (2022). The future poleward shift of Southern Hemisphere summer mid-latitude storm tracks stems from ocean coupling. *Nature Communications*, *13*(1), 1730. https://doi.org/10.1038/s41467-022-29392-4

Chemke, R., Ming, Y., & Yuval, J. (2022). The intensification of winter mid-latitude storm tracks in the Southern Hemisphere. *Nature Climate Change*, *12*(6), 553–557. https://doi.org/10.1038/s41558-022-01368-8

Cheng, C., Jenkins, A., Holland, P. R., Wang, Z., Liu, C., & Xia, R. (2019). Responses of sub-ice platelet layer thickening rate and frazil-ice concentration to variations in ice-shelf water supercooling in McMurdo Sound, Antarctica. *The Cryosphere*, *13*(1), 265–280. https://doi.org/10.5194/tc-13-265-2019

19449208, 2023, 2, Downloaded from https://agupubs.onlinelibrary.wiley.com/doi/10.1029/2022RG000770 by University of Adelaide Alumni, Wiley Online Library on [16/08/2023]. See the Terms and Conditions (https://onlinelibrary.wiley.com/terms-and-conditions) on Wiley Online Library for rules of use; OA articles are governed by the applicable Creative Commons License

Christie, F. D. W., Benham, T. J., Batchelor, C. L., Rack, W., Montelli, A., & Dowdeswell, J. A. (2022). Antarctic ice-shelf advance driven by anomalous atmospheric and sea-ice circulation. *Nature Geoscience*, *15*(5), 356–362. https://doi.org/10.1038/s41561-022-00938-x

Cimoli, E., Meiners, K. M., Lucieer, A., & Lucieer, V. (2019). An under-ice hyperspectral and RGB imaging system to capture fine-scale biophysical properties of sea ice. *Remote Sensing*, *11*(23), 1–35. https://doi.org/10.3390/rs11232860

Cook, A. J., & Vaughan, D. G. (2010). Overview of areal changes of the ice shelves on the Antarctic Peninsula over the past 50 years. *The Cryosphere*, *4*(1), 77–98. https://doi.org/10.5194/tc-4-77-2010

Cornett, S. (1982). Implications of ship's tracks for Inuit travel, ice thickness and ice growth acceleration. In *The Canadian Beaufort Sea (technical report)*. Dome Petroleum.

Corso, A. D., Steinberg, D. K., Stammerjohn, S. E., & Hilton, E. J. (2022). Climate drives long-term change in Antarctic Silverfish along the western Antarctic Peninsula. *Communications Biology*, *5*(1), 104. https://doi.org/10.1038/s42003-022-03042-3

Costanzo, G., Zagami, G., Crescenti, N., & Granata, A. (2002). Naupliar Development of *Stephos Longipes* (Copepoda: Calanoida) from the Annual Sea Ice of Terra Nova Bay, Antarctica. *Journal of Crustacean Biology*, *22*(4), 855–860. https://doi.org/10.1163/20021975-99990297

Cota, G. F., Legendre, L., Gosselin, M., & Ingram, R. G. (1991). Ecology of bottom ice algae: I. Environmental controls and variability. *Journal of Marine Systems*, *2*(3–4), 257–277. https://doi.org/10.1016/0924-7963(91)90036-t

Cougnon, E. A., Galton-Fenzi, B. K., Rintoul, S. R., Legrésy, B., Williams, G. D., Fraser, A. D., & Hunter, J. R. (2017). Regional changes in icescape impact shelf circulation and basal melting. *Geophysical Research Letters*, *44*(22), 519–611. https://doi.org/10.1002/2017GL074943

Cox, G., & Weeks, W. (1986). Changes in the salinity and porosity of sea-ice samples during shipping and storage. *Journal of Glaciology*, *32*(112), 371–375. https://doi.org/10.3189/S0022143000012065

Cozzi, S. (2008). High-resolution trends of nutrients, DOM and nitrogen uptake in the annual sea ice at Terra Nova Bay, Ross Sea. *Antarctic Science*, *20*(5), 441–454. https://doi.org/10.1017/S0954102008001247

Cozzi, S. (2014). Multiscale variability of ambient conditions, fast ice dynamics and biogeochemistry in the coastal zone of Victoria Land, Ross Sea. *Antarctic Science*, *26*(4), 427–444. https://doi.org/10.1017/s0954102013000813

Cozzi, S., & Cantoni, C. (2011). Stable isotope (δ^{13}C and δ^{15}N) composition of particulate organic matter, nutrients and dissolved organic matter during spring ice retreat at Terra Nova Bay. *Antarctic Science*, *23*(1), 43–56. https://doi.org/10.1017/s0954102010000611

Cripps, G. C., & Clarke, A. (1998). Seasonal variation in the biochemical composition of particulate material collected by sediment traps at Signy Island, Antarctica. *Polar Biology*, *20*(6), 414–423. https://doi.org/10.1007/s003000050323

Crocker, G. B., & Wadhams, P. (1989a). Breakup of Antarctic fast ice. *Cold Regions Science and Technology*, *17*(1), 61–76. https://doi.org/10.1016/s0165-232x(89)80016-3

Crocker, G. B., & Wadhams, P. (1989b). Modelling Antarctic Fast-Ice Growth. *Journal of Glaciology*, *35*(119), 3–8. https://doi.org/10.3189/002214389793701590

Cummings, V. J., Hewitt, J. E., Thrush, S. F., Marriott, P. M., Halliday, N. J., & Norkko, A. (2018). Linking Ross Sea coastal benthic communities to environmental conditions: Documenting baselines in a spatially variable and changing world. *Frontiers in Marine Science*, *5*(JUL), 232. https://doi.org/10.3389/fmars.2018.00232

Currie, A. A., Marshall, A. J., Lohrer, A. M., Cummings, V. J., Seabrook, S., & Cary, S. C. (2021). Sea ice dynamics drive benthic microbial communities in McMurdo Sound, Antarctica. *Frontiers in Microbiology*, *12*, 3189. https://doi.org/10.3389/fmicb.2021.745915

Curson, A. R. J., Liu, J., Bermejo Martínez, A., Green, R. T., Chan, Y., Carrión, O., et al. (2017). Dimethylsulfoniopropionate biosynthesis in marine bacteria and identification of the key gene in this process. *Nature Microbiology*, *2*(5), 17009. https://doi.org/10.1038/nmicrobiol.2017.9

Dahms, H., Bergmans, M., & Schminke, H. K. (1990). Distribution and adaptations of sea ice inhabiting Harpacticoida (Crustacea, Copepoda) of the Weddell Sea (Antarctica). *Marine Ecology*, *11*(3), 207–226. https://doi.org/10.1111/j.1439-0485.1990.tb00240.x

Dammann, D. O., Eicken, H., Mahoney, A. R., Meyer, F. J., Freymueller, J. T., & Kaufman, A. M. (2018). Evaluating landfast sea ice stress and fracture in support of operations on sea ice using SAR interferometry. *Cold Regions Science and Technology*, *149*, 51–64. https://doi.org/10.1016/j.coldregions.2018.02.001

Dammann, D. O., Eriksson, L. E. B., Mahoney, A., Eicken, H., & Meyer, F. J. (2019). Mapping pan-Arctic landfast sea ice stability using Sentinel-1 interferometry. *The Cryosphere*, *13*(2), 557–577. https://doi.org/10.5194/tc-13-557-2019

Dammann, D. O., Johnson, M. A., Fedders, E. R., Mahoney, A. R., Werner, C. L., Polashenski, C. M., et al. (2020). Ground-based radar interferometry of sea ice. *Remote Sensing*, *13*(1), 43. https://doi.org/10.3390/rs13010043

Dammann, D. O., Johnson, M. A., Mahoney, A. R., & Fedders, E. R. (2022). Observing sea ice flexural-gravity waves with ground-based radar interferometry. In *The cryosphere discussions*.

Dammert, P. B. G., Lepparanta, M., & Askne, J. (1998). SAR interferometry over Baltic Sea ice. *International Journal of Remote Sensing*, *19*(16), 3019–3037. https://doi.org/10.1080/014311698214163

Davis, L., Hofmann, E., Klinck, J., Piñones, A., & Dinniman, M. (2017). Distributions of krill and Antarctic silverfish and correlations with environmental variables in the western Ross Sea, Antarctica. *Marine Ecology Progress Series*, *584*, 45–65. https://doi.org/10.3354/meps12347

Dawson, H. M., Heal, K. R., Boysen, A. K., Carlson, L. T., Ingalls, A. E., & Young, J. N. (2020). Potential of temperature- and salinity-driven shifts in diatom compatible solute concentrations to impact biogeochemical cycling within sea ice. *Elementa: Science of the Anthropocene*, *8*, 25. https://doi.org/10.1525/elementa.421

De Jong, J., Schoemann, V., Maricq, N., Mattielli, N., Langhorne, P., Haskell, T., & Tison, J.-L. (2013). Iron in land-fast sea ice of McMurdo Sound derived from sediment resuspension and wind-blown dust attributes to primary productivity in the Ross Sea, Antarctica. *Marine Chemistry*, *157*, 24–40. https://doi.org/10.1016/j.marchem.2013.07.001

Delille, B., Jourdain, B., Borges, A. V., Tison, J.-L., & Delille, D. (2007). Biogas (CO_2, O_2, dimethylsulfide) dynamics in spring Antarctic fast ice. *Limnology & Oceanography*, *52*(4), 1367–1379. https://doi.org/10.4319/lo.2007.52.4.1367

Delille, B., Vancoppenolle, M., Geilfus, N.-X., Tilbrook, B., Lannuzel, D., Schoemann, V., et al. (2014). Southern Ocean CO_2 sink: The contribution of the sea ice. *Journal of Geophysical Research: Oceans*, *119*(9), 6340–6355. https://doi.org/10.1002/2014JC009941

Delille, D., Fiala, M., Kuparinen, J., Kuosa, H., & Plessis, C. (2002). Seasonal changes in microbial biomass in the first-year ice of the Terre Adélie area (Antarctica). *Aquatic Microbial Ecology*, *28*, 257–265. https://doi.org/10.3354/ame028257

Dempsey, D. E., Langhorne, P. J., Robinson, N. J., Williams, M. J. M., Haskell, T. G., & Frew, R. D. (2010). Observation and modeling of platelet ice fabric in McMurdo Sound, Antarctica. *Journal of Geophysical Research*, *115*(C1), C01007. https://doi.org/10.1029/2008jc005264

Dome Petroleum. (1979). *Full scale tests of the AML—X4 Canmar Kigoriak—Final report (technical report)*. Dome Petroleum.

Dorschel, B., Hehemann, L., Viquerat, S., Warnke, F., Dreutter, S., Tenberge, Y. S., et al. (2022). The international bathymetric chart of the Southern Ocean Version 2. *Scientific Data*, *9*(1), 275. https://doi.org/10.1038/s41597-022-01366-7

Dou, T., Xiao, C., Liu, J., Han, W., Du, Z., Mahoney, A. R., et al. (2019). A key factor initiating surface ablation of Arctic sea ice: Earlier and increasing liquid precipitation. *The Cryosphere*, *13*(4), 1233–1246. https://doi.org/10.5194/tc-13-1233-2019

19449208, 2023, 2, Downloaded from https://agupubs.onlinelibrary.wiley.com/doi/10.1029/2022RG000770 by University of Adelaide Alumni, Wiley Online Library on [16/08/2023]. See the Terms and Conditions (https://onlinelibrary.wiley.com/terms-and-conditions) on Wiley Online Library for rules of use; OA articles are governed by the applicable Creative Commons License

Druckenmiller, M. L., Eicken, H., Johnson, M. A., Pringle, D. J., & Williams, C. C. (2009). Toward an integrated coastal sea-ice observatory: System components and a case study at Barrow, Alaska. *Cold Regions Science and Technology*, *56*(2–3), 61–72. https://doi.org/10.1016/j.coldregions.2008.12.003

Duan, M., Zhang, C., Liu, Y., Ye, Z., Yang, J., Liu, C., & Tian, Y. (2022). Growth and early life stage of Antarctic silverfish (Pleuragramma Antarctica) in the Amundsen Sea of the Southern Ocean: Evidence for a potential new spawning/nursery ground. *Polar Biology*, *45*(2), 359–368. https://doi.org/10.1007/s00300-021-02994-2

Dunbar, R. B., Leventer, A. R., & Stockton, W. L. (1989). Biogenic sedimentation in McMurdo Sound, Antarctica. *Marine Geology*, *85*(2–4), 155–179. https://doi.org/10.1016/0025-3227(89)90152-7

Duprat, L., Kanna, N., Janssens, J., Roukaerts, A., Deman, F., Townsend, A. T., et al. (2019). Enhanced iron flux to Antarctic sea ice via dust deposition from ice-free coastal areas. *Journal of Geophysical Research: Oceans*, *124*(12), 8538–8557. https://doi.org/10.1029/2019jc015221

Eastman, J. T., & DeVries, A. L. (1985). Adaptations for cryopelagic life in the Antarctic notothenioid fish Pagothenia borchgrevinki. *Polar Biology*, *4*(1), 45–52. https://doi.org/10.1007/bf00286816

Eicken, H. (2010). Indigenous knowledge and sea ice science: What can we learn from indigenous ice users? In *Siku: Knowing our ice* (pp. 357–376). Springer. https://doi.org/10.1007/978-90-481-8587-0{_}15

Emmerson, L., & Southwell, C. (2022). Environment-triggered demographic changes cascade and compound to propel a dramatic decline of an Antarctic seabird metapopulation. *Global Change Biology*, *28*(24), 7234–7249. https://doi.org/10.1111/gcb.16437

Enomoto, H., Nishio, F., Warashina, H., & Ushio, S. (2002). Satellite observation of melting and break-up of fast ice in Lützow-Holm Bay, East Antarctica. *Polar Meteorology and Glaciology*, *16*, 1–14.

Eyring, V., Bony, S., Meehl, G. A., Senior, C. A., Stevens, B., Stouffer, R. J., & Taylor, K. E. (2016). Overview of the coupled model intercomparison project phase 6 (CMIP6) experimental design and organization. *Geoscientific Model Development*, *9*(5), 1937–1958. https://doi.org/10.5194/gmd-9-1937-2016

Fedotov, V., Cherepanov, N., & Tyshko, K. (1998). Some features of the growth, structure and metamorphism of East Antarctic landfast sea ice. In M. Jeffries (Ed.), *Antarctic research series: Antarctic sea ice: Physical processes, interactions and variability* (1st ed., Vol. 74, pp. 343–354). American Geophysical Union.

Fiala, M., Kuosa, H., Kopczýnska, E. E., Oriol, L., & Delille, D. (2006). Spatial and seasonal heterogeneity of sea ice microbial communities in the first-year ice of Terre Adélie area (Antarctica). *Aquatic Microbial Ecology*, *43*, 95–106. https://doi.org/10.3354/ame043095

Filhol, S., & Sturm, M. (2015). Snow bedforms: A review, new data, and a formation model. *Journal of Geophysical Research: Earth Surface*, *120*(9), 1645–1669. https://doi.org/10.1002/2015jf003529

Fogwill, C. J., van Sebille, E., Cougnon, E. A., Turney, C. S. M., Rintoul, S. R., Galton-Fenzi, B. K., et al. (2016). Brief communication: Impacts of a developing polynya off Commonwealth Bay, East Antarctica, triggered by grounding of iceberg B09B. *The Cryosphere*, *10*(6), 2603–2609. https://doi.org/10.5194/tc-10-2603-2016

Foldvik, A., & Kvinge, T. (1974). Conditional instability of sea-water at freezing-point. *Deep-Sea Research*, *21*(3), 169–174. https://doi.org/10.1016/0011-7471(74)90056-4

Forster, P., Storelvmo, T., Armour, K., Collins, W., Dufresne, J.-L., Frame, D., et al. (Eds.). In Climate change 2021: The physical science basis. Contribution of working group I to the sixth assessment report of the intergovernmental panel on climate change (chapter 7). Cambridge University Press.

Foster, B. A., & Montgomery, J. C. (1993). Planktivory in benthic nototheniid fish in McMurdo Sound, Antarctica. *Environmental Biology of Fishes*, *36*(3), 313–318. https://doi.org/10.1007/bf00001727

Fraser, A. D. (2011). *East Antarctic landfast sea-ice distribution and variability (unpublished doctoral dissertation)*. University of Tasmania.

Fraser, A. D., Massom, R. A., Handcock, M. S., Reid, P., Ohshima, K. I., Raphael, M. N., et al. (2021). Eighteen-year record of circum-Antarctic landfast sea ice distribution allows detailed baseline characterisation and reveals trends and variability. *The Cryosphere*, *15*(11), 5061–5077. https://doi.org/10.5194/tc-15-5061-2021

Fraser, A. D., Massom, R. A., & Michael, K. J. (2009). A method for compositing polar MODIS satellite images to remove cloud cover for landfast sea-ice detection. *IEEE Transactions on Geoscience and Remote Sensing*, *47*(9), 3272–3282. https://doi.org/10.1109/tgrs.2009.2019726

Fraser, A. D., Massom, R. A., & Michael, K. J. (2010). Generation of high-resolution East Antarctic landfast sea-ice maps from cloud-free MODIS satellite composite imagery. *Remote Sensing of Environment*, *114*(12), 2888–2896. https://doi.org/10.1016/j.rse.2010.07.006

Fraser, A. D., Massom, R. A., Michael, K. J., Galton-Fenzi, B. K., & Lieser, J. L. (2012). East Antarctic landfast sea ice distribution and variability, 2000–08. *Journal of Climate*, *25*(4), 1137–1156. https://doi.org/10.1175/jcli-d-10-05032.1

Fraser, A. D., Massom, R. A., Ohshima, K. I., Willmes, S., Kappes, P. J., Cartwright, J., & Porter-Smith, R. (2020). High-resolution mapping of circum-Antarctic landfast sea ice distribution, 2000–2018. *Earth System Science Data*, *12*(4), 2987–2999. https://doi.org/10.5194/essd-12-2987-2020

Fraser, A. D., Ohshima, K. I., Nihashi, S., Massom, R. A., Tamura, T., Nakata, K., et al. (2019). Landfast ice controls on sea-ice production in the Cape Darnley Polynya: A case study. *Remote Sensing of Environment*, *233*, 111315. https://doi.org/10.1016/j.rse.2019.111315

Freitag, J. (1999). The hydraulic properties of Arctic sea ice-implications for the small-scale particle transport. *Berichte zur Polarforschung*, *325*, 150.

Fretwell, P., Pritchard, H. D., Vaughan, D. G., Bamber, J. L., Barrand, N. E., Bell, R., et al. (2013). Bedmap2: Improved ice bed, surface and thickness datasets for Antarctica. *The Cryosphere*, *7*(1), 375–393. https://doi.org/10.5194/tc-7-375-2013

Fricko, O., Havlik, P., Rogelj, J., Klimont, Z., Gusti, M., Johnson, N., et al. (2017). The marker quantification of the Shared Socioeconomic Pathway 2: A middle-of-the-road scenario for the 21st century. *Global Environmental Change*, *42*, 251–267. https://doi.org/10.1016/j.gloenvcha.2016.06.004

Fripiat, F., Sigman, D. M., Massé, G., & Tison, J. (2015). High turnover rates indicated by changes in the fixed N forms and their stable isotopes in Antarctic landfast sea ice. *Journal of Geophysical Research: Oceans*, *120*(4), 3079–3097. https://doi.org/10.1002/2014jc010583

Galton-Fenzi, B. K., Hunter, J. R., Coleman, R., Marsland, S. J., & Warner, R. C. (2012). Modeling the basal melting and marine ice accretion of the Amery Ice Shelf. *Journal of Geophysical Research*, *117*(C9), 526. https://doi.org/10.1029/2012jc008214

Garcia, M. D., Dutto, M. S., Chazarreta, C. J., Berasategui, A. A., Schloss, I. R., & Hoffmeyer, M. S. (2020). Micro- and mesozooplankton successions in an Antarctic coastal environment during a warm year. *PLoS One*, *15*(5), e0232614. https://doi.org/10.1371/journal.pone.0232614

Genovese, C., Grotti, M., Ardini, F., Corkill, M. J., Duprat, L. P., Wuttig, K., et al. (2023). A proposed seasonal cycle of dissolved iron-binding ligands in Antarctic sea ice. *Elementa: Science of the Anthropocene*, *10*(1), 1–16. https://doi.org/10.1525/elementa.2021.00030

Gerringa, L. J. A., Alderkamp, A.-C., Laan, P., Thuróczy, C.-E., de Baar, H., Mills, M. M., et al. (2012). Iron from melting glaciers fuels the phytoplankton blooms in Amundsen Sea (Southern Ocean): Iron biogeochemistry. *Deep Sea Research Part II: Topical Studies in Oceanography*, *71–76*, 16–31. https://doi.org/10.1016/j.dsr2.2012.03.007

19449208, 2023, 2, Downloaded from https://agupubs.onlinelibrary.wiley.com/doi/10.1029/2022RG000770 by University of Adelaide Alumni, Wiley Online Library on [16/08/2023]. See the Terms and Conditions (https://onlinelibrary.wiley.com/terms-and-conditions) on Wiley Online Library for rules of use; OA articles are governed by the applicable Creative Commons License

Giannelli, V., Thomas, D. N., Haas, C., Kattner, G., Kennedy, H., & Dieckmann, G. S. (2001). Behaviour of dissolved organic matter and inorganic nutrients during experimental sea-ice formation. *Annals of Glaciology*, *33*, 317–321. https://doi.org/10.3189/172756401781818572

Giles, A. B., Massom, R. A., & Lytle, V. I. (2008). Fast-ice distribution in East Antarctica during 1997 and 1999 determined using RADARSAT data. *Journal of Geophysical Research*, *113*(C2), C02S14. https://doi.org/10.1029/2007jc004139

Gogineni, S., Chuah, T., Allen, C., Jezek, K., & Moore, R. K. (1998). An improved coherent radar depth sounder. *Journal of Glaciology*, *44*(148), 659–669. https://doi.org/10.3189/S0022143000002161

Golden, K. M., Ackley, S. F., & Lytle, V. I. (1998). The percolation phase transition in sea ice. *Science*, *282*(5397), 2238–2241. https://doi.org/10.1126/science.282.5397.2238

Gomez-Fell, R., Rack, W., Purdie, H., & Marsh, O. (2022). Parker Ice Tongue collapse, Antarctica, triggered by loss of stabilizing land-fast sea ice. *Geophysical Research Letters*, *49*(1), e2021GL096156. https://doi.org/10.1029/2021GL096156

Gough, A. J., Mahoney, A., Langhorne, P. J., Williams, M. J. M., Robinson, N. J., & Haskell, T. G. (2012). Signatures of supercooling: McMurdo Sound platelet ice. *Journal of Glaciology*, *58*(207), 38–50. https://doi.org/10.3189/2012jog10j218

Gough, A. J., Mahoney, A. R., Langhorne, P. J., & Haskell, T. G. (2013). Salinity evolution and mechanical properties of snow-loaded multiyear sea ice near an ice shelf. *Antarctic Science*, *25*(6), 821–831. https://doi.org/10.1017/S0954102013000217

Gow, A. J., Ackley, S. F., Govoni, J. W., & Weeks, W. F. (1998). Physical and structural properties of land-fast sea ice in McMurdo Sound, Antarctica. In M. O. Jeffries (Ed.), *Antarctic sea ice: Physical processes, interactions and variability* (Vol. 74, pp. 355–374). AGU. https://doi.org/10.1029/AR074p0355

Granata, A., Cubeta, A., Guglielmo, L., Sidoti, O., Greco, S., Vacchi, M., & La Mesa, M. (2002). Ichthyoplankton abundance and distribution in the Ross Sea during 1987–1996. *Polar Biology*, *25*(3), 187–202. https://doi.org/10.1007/s00300-001-0326-y

Granata, A., Zagami, G., Vacchi, M., & Guglielmo, L. (2009). Summer and spring trophic niche of larval and juvenile *Pleuragramma antarcticum* in the Western Ross Sea, Antarctica. *Polar Biology*, *32*(3), 369–382. https://doi.org/10.1007/s00300-008-0551-8

Greene, C. A., Gardner, A. S., Schlegel, N.-J., & Fraser, A. D. (2022). Antarctic calving loss rivals ice-shelf thinning. *Nature*, *609*(7929), 948–953. https://doi.org/10.1038/s41586-022-05037-w

Greene, C. A., Young, D. A., Gwyther, D. E., Galton-Fenzi, B. K., & Blankenship, D. D. (2018). Seasonal dynamics of Totten Ice Shelf controlled by sea ice buttressing. *The Cryosphere*, *12*(9), 2869–2882. https://doi.org/10.5194/tc-12-2869-2018

Grossi, S. M., & Sullivan, C. W. (1985). Sea ice microbial communities. V. The vertical donation of diatoms in an Antarctic fast ice community. *Journal of Phycology*, *21*(3), 401–409. https://doi.org/10.1111/j.0022-3646.1985.00401.x

Grotti, M., Soggia, F., Ianni, C., & Frache, R. (2005). Trace metals distributions in coastal sea ice of Terra Nova Bay, Ross Sea, Antarctica. *Antarctic Science*, *17*(2), 289–300. https://doi.org/10.1017/S0954102005002695

Guglielmo, L., Carrada, G. C., Catalano, G., Cozzi, S., Dell'Anno, A., Fabiano, M., et al. (2004). Biogeochemistry and algal communities in the annual sea ice at Terra Nova Bay (Ross Sea, Antarctica). *Chemistry and Ecology*, *20*(sup1), 43–55. https://doi.org/10.1080/02757540310001656657

Guglielmo, L., Carrada, G. C., Catalano, G., Dell'Anno, A., Fabiano, M., Lazzara, L., et al. (2000). Structural and functional properties of sympagic communities in the annual sea ice at Terra Nova Bay (Ross Sea, Antarctica). *Polar Biology*, *23*(2), 137–146. https://doi.org/10.1007/s003000050019

Guglielmo, L., Granata, A., & Greco, S. (1997). Distribution and abundance of postlarval and juvenile *Pleuragramma antarcticum* (Pisces, Nototheniidae) off Terra Nova Bay (Ross Sea, Antarctica). *Polar Biology*, *19*(1), 37–51. https://doi.org/10.1007/s003000050214

Guglielmo, L., Zagami, G., Saggiomo, V., Catalano, G., & Granata, A. (2007). Copepods in spring annual sea ice at Terra Nova Bay (Ross Sea, Antarctica). *Polar Biology*, *30*(6), 747–758. https://doi.org/10.1007/s00300-006-0234-2

Gulliksen, B., & Lønne, O. (1991). Sea ice macrofauna in the Antarctic and the Arctic. *Journal of Marine Systems*, *2*(1–2), 53–61. https://doi.org/10.1016/0924-7963(91)90013-K

Günther, S., & Dieckmann, G. S. (1999). Seasonal development of algal biomass in snow-covered fast ice and the underlying platelet layer in the Weddell Sea, Antarctica. *Antarctic Science*, *11*(3), 305–315. https://doi.org/10.1017/s0954102099000395

Gutt, J. (2002). The Antarctic ice shelf: An extreme habitat for notothenioid fish. *Polar Biology*, *25*(4), 320–322. https://doi.org/10.1007/s00300-001-0352-9

Haas, C., Langhorne, P. J., Rack, W., Leonard, G. H., Brett, G. M., Price, D., et al. (2021). Airborne mapping of the sub-ice platelet layer under fast ice in McMurdo Sound, Antarctica. *The Cryosphere*, *15*(1), 247–264. https://doi.org/10.5194/tc-15-247-2021

Haas, C., Lobach, J., Hendricks, S., Rabenstein, L., & Pfaffling, A. (2009). Helicopter-borne measurements of sea ice thickness, using a small and lightweight, digital EM system. *Journal of Applied Geophysics*, *67*(3), 234–241. https://doi.org/10.1016/j.jappgeo.2008.05.005

Han, H., & Lee, H. (2018). Glacial and tidal strain of landfast sea ice in Terra Nova Bay, East Antarctica, observed by interferometric SAR techniques. *Remote Sensing of Environment*, *209*, 41–51. https://doi.org/10.1016/j.rse.2018.02.033

Hao, G., Pirazzini, R., Yang, Q., Tian, Z., & Liu, C. (2021). Spectral albedo of coastal landfast sea ice in Prydz Bay, Antarctica. *Journal of Glaciology*, *67*(261), 126–136. https://doi.org/10.1017/jog.2020.90

Haskell, T., Robinson, W., & Langhorne, P. (1996). Preliminary results from fatigue tests on in situ sea ice beams. *Cold Regions Science and Technology*, *24*(2), 167–176. https://doi.org/10.1016/0165-232X(95)00015-4

Hassler, C., Cabanes, D., Blanco-Ameijeiras, S., Sander, S. G., & Benner, R. (2020). Importance of refractory ligands and their photodegradation for iron oceanic inventories and cycling. *Marine and Freshwater Research*, *71*(3), 311–320. https://doi.org/10.1071/MF19213

Haumann, F. A., Moorman, R., Riser, S. C., Smedsrud, L. H., Maksym, T., Wong, A. P. S., et al. (2020). Supercooled Southern Ocean waters. *Geophysical Research Letters*, *47*(20), e2020GL090242. https://doi.org/10.1029/2020GL090242

Hayashida, H., Carnat, G., Galí, M., Monahan, A. H., Mortenson, E., Sou, T., & Steiner, N. S. (2020). Spatiotemporal variability in modeled bottom ice and sea surface dimethylsulfide concentrations and fluxes in the Arctic during 1979–2015. *Global Biogeochemical Cycles*, *34*(10), e2019GB006456. https://doi.org/10.1029/2019GB006456

Heil, P. (2006). Atmospheric conditions and fast ice at Davis, East Antarctica: A case study. *Journal of Geophysical Research*, *111*(C5), C05009. https://doi.org/10.1029/2005jc002904

Heil, P., Allison, I., & Lytle, V. I. (1996). Seasonal and interannual variations of the oceanic heat flux under a landfast Antarctic sea ice cover. *Journal of Geophysical Research*, *101*(C11), 25741–25752. https://doi.org/10.1029/96JC01921

Heil, P., Gerland, S., & Granskog, M. (2011). An Antarctic monitoring initiative for fast ice and comparison with the Arctic. *The Cryosphere Discussions*, *5*, 2437–2463. https://doi.org/10.5194/tcd-5-2437-2011

Heil, P., Massom, R. A., Allison, I., & Worby, A. P. (2011). Physical attributes of sea-ice kinematics during spring 2007 off East Antarctica. *Deep Sea Research Part II: Topical Studies in Oceanography*, *58*(9–10), 1158–1171. https://doi.org/10.1016/j.dsr2.2010.12.004

Heine, A. J. (1963). Ice breakout around the Southern end of Ross Island, Antarctica. *New Zealand Journal of Geology and Geophysics*, *6*(3), 395–401. https://doi.org/10.1080/00288306.1963.10422071

19449208, 2023, 2, Downloaded from https://agupubs.onlinelibrary.wiley.com/doi/10.1029/2022RG000770 by University of Adelaide Alumni, Wiley Online Library on [16/08/2023]. See the Terms and Conditions (https://onlinelibrary.wiley.com/terms-and-conditions) on Wiley Online Library for rules of use; OA articles are governed by the applicable Creative Commons License

Hellmer, H. H. (2004). Impact of Antarctic ice shelf basal melting on sea ice and deep ocean properties. *Geophysical Research Letters*, *31*(10), L10307. https://doi.org/10.1029/2004GL019506

Henley, S. F., Cavan, E. L., Fawcett, S. E., Kerr, R., Monteiro, T., Sherrell, R. M., et al. (2020). Changing biogeochemistry of the Southern Ocean and its ecosystem implications (Vol. *7*). https://doi.org/10.3389/fmars.2020.00581

Henley, S. F., Tuerena, R. E., Annett, A. L., Fallick, A. E., Meredith, M. P., Venables, H. J., et al. (2017). Macronutrient supply, uptake and recycling in the coastal ocean of the west Antarctic Peninsula. *Deep Sea Research Part II: Topical Studies in Oceanography*, *139*, 58–76. https://doi.org/10.1016/j.dsr2.2016.10.003

Herborg, L.-M., Thomas, D. N., Kennedy, H., Haas, C., & Dieckmann, G. S. (2001). Dissolved carbohydrates in Antarctic sea ice. *Antarctic Science*, *13*(2), 119–125. https://doi.org/10.1017/s0954102001000190

Herman, A., Wenta, M., & Cheng, S. (2021). Sizes and shapes of sea ice floes broken by waves–A case study from the East Antarctic coast. *Frontiers in Earth Science*, *9*, 655977. https://doi.org/10.3389/feart.2021.655977

Herraiz-Borreguero, L., Coleman, R., Allison, I., Rintoul, S. R., Craven, M., & Williams, G. D. (2015). Circulation of modified Circumpolar Deep Water and basal melt beneath the Amery Ice Shelf, East Antarctica. *Journal of Geophysical Research: Oceans*, *120*(4), 3098–3112. https://doi.org/10.1002/2015JC010697

Hirano, D., Tamura, T., Kusahara, K., Ohshima, K. I., Nicholls, K. W., Ushio, S., et al. (2020). Strong ice-ocean interaction beneath Shirase Glacier Tongue in East Antarctica. *Nature Communications*, *11*(1), 4221. https://doi.org/10.1038/s41467-020-17527-4

Holdsworth, G., & Glynn, J. (1978). Iceberg calving from floating glaciers by a vibrating mechanism. *Nature*, *274*(5670), 464–466. https://doi.org/10.1038/274464a0

Holt, B., Kanagaratnam, P., Gogineni, S. P., Ramasami, V. C., Mahoney, A., & Lytle, V. (2009). Sea ice thickness measurements by ultrawideband penetrating radar: First results. *Cold Regions Science and Technology*, *55*(1), 33–46. https://doi.org/10.1016/j.coldregions.2008.04.007

Hoppmann, M., Nicolaus, M., Hunkeler, P. A., Heil, P., Behrens, L., König-Langlo, G., & Gerdes, R. (2015). Seasonal evolution of an ice-shelf influenced fast-ice regime, derived from an autonomous thermistor chain. *Journal of Geophysical Research: Oceans*, *120*(3), 1703–1724. https://doi.org/10.1002/2014jc010327

Hoppmann, M., Nicolaus, M., Paul, S., Hunkeler, P. A., Heinemann, G., Willmes, S., et al. (2015). Ice platelets below Weddell Sea landfast sea ice. *Annals of Glaciology*, *56*(69), 175–190. https://doi.org/10.3189/2015aog69a678

Hoppmann, M., Richter, M. E., Smith, I. J., Jendersie, S., Langhorne, P. J., Thomas, D. N., & Dieckmann, G. S. (2020). Platelet ice, the Southern Ocean's hidden ice: A review. *Annals of Glaciology*, *61*(83), 341–368. https://doi.org/10.1017/aog.2020.54

Horner, R., Ackley, S. F., Dieckmann, G. S., Gulliksen, B., Hoshiai, T., Legendre, L., et al. (1992). Ecology of sea ice biota—1. Habitat, terminology, and methodology. *Polar Biology*, *12*(3–4), 417. https://doi.org/10.1007/BF00243113

Hoshiai, T., & Tamimura, A. (1989). Copepods in the stomach of a nototheniid fish, Trematomus borchgrevinki fry at Syowa Station, Antarctica. *Memoirs of the National Institute of Polar Research Series E Biology Medical Science*, *34*, 44–48.

Hotzel, S., & Noble, P. (1979). *Study of influence of shipping on break-up and freeze-up in Lancaster Sound. Report 565C (technical report)*. Arctec Canada Limited for Petro-Canada Inc.

Howell, S. E. L., Laliberté, F., Kwok, R., Derksen, C., & King, J. (2016). Landfast ice thickness in the Canadian Arctic Archipelago from observations and models. *The Cryosphere*, *10*(4), 1463–1475. https://doi.org/10.5194/tc-10-1463-2016

Hubold, G. (1984). Spatial distribution of *Pleuragramma antarcticum* (Pisces: Nototheniidae) near the Filchner- and Larsen ice shelves (Weddell Sea/Antarctica). *Polar Biology*, *3*(4), 231–236. https://doi.org/10.1007/BF00292628

Hughes, C., Chuck, A. L., Rossetti, H., Mann, P. J., Turner, S. M., Clarke, A., et al. (2009). Seasonal cycle of seawater bromoform and dibromomethane concentrations in a coastal bay on the western Antarctic Peninsula. *Global Biogeochemical Cycles*, *23*(2), 1463–1475. https://doi.org/10.1029/2008gb003268

Hughes, K. G., Langhorne, P. J., Leonard, G. H., & Stevens, C. L. (2014). Extension of an Ice Shelf Water plume model beneath sea ice with application in McMurdo Sound, Antarctica. *Journal of Geophysical Research C: Oceans*, *119*(12), 8662–8687. https://doi.org/10.1002/2013JC009411

Huot, P.-V., Kittel, C., Fichefet, T., Jourdain, N. C., Sterlin, J., & Fettweis, X. (2021). Effects of the atmospheric forcing resolution on simulated sea ice and polynyas off Adélie Land, East Antarctica. *Ocean Modelling*, *168*, 101901. https://doi.org/10.1016/j.ocemod.2021.101901

Ichinomiya, M., Nakamachi, M., Fukuchi, M., & Taniguchi, A. (2008). Population dynamics of an ice-associated diatom, Thalassiosira australis Peragallo, under fast ice near Syowa Station, East Antarctica, during austral summer. *Polar Biology*, *31*(9), 1051–1058. https://doi.org/10.1007/s00300-008-0444-x

Inall, M., Brearley, A., Henley, S., Fraser, A. D., & Reed, S. (2021). Landfast ice controls on turbulence in Antarctic coastal seas. *Journal of Geophysical Research: Oceans*, *127*(1), e2021JC017963. https://doi.org/10.1029/2021JC017963

Ito, M., Ohshima, K. I., Fukamachi, Y., Mizuta, G., Kusumoto, Y., & Nishioka, J. (2017). Observations of frazil ice formation and upward sediment transport in the Sea of Okhotsk: A possible mechanism of iron supply to sea ice. *Journal of Geophysical Research: Oceans*, *122*(2), 788–802. https://doi.org/10.1002/2016JC012198

Jacobs, S. S., Hellmer, H., Doake, C. S. M., Jenkins, A., & Frolich, R. M. (1992). Melting of ice shelves and the mass balance of Antarctica. *Journal of Glaciology*, *38*(130), 375–387. https://doi.org/10.3189/S0022143000002252

Jacobs, S. S., Fairbanks, R. G., & Horibe, Y. G. (1985). Origin and evolution of water masses near the Antarctic continental margin: Evidence from $H_2{}^{18}O/H_2{}^{16}O$ ratios in seawater. In S. S. Jacobs (Ed.), *Oceanology of the antarctic continental shelf* (Vol. 43, pp. 59–85). American Geophysical Union. https://doi.org/10.1029/AR043p0059

Jacobs, S. S., Jenkins, A., Giulivi, C. F., & Dutrieux, P. (2011). Stronger ocean circulation and increased melting under Pine Island Glacier ice shelf. *Nature Geoscience*, *4*(8), 519–523. https://doi.org/10.1038/ngeo1188

Jeffries, M. O., & Adolphs, U. (1997). Early winter ice and snow thickness distribution, ice structure and development of the western Ross Sea pack ice between the ice edge and the Ross Ice Shelf. *Antarctic Science*, *9*(2), 188–200. https://doi.org/10.1017/S0954102097000242

Jeffries, M. O., Weeks, W. F., Shaw, R., & Morris, K. (1993). Structural characteristics of congelation and platelet ice and their role in the development of Antarctic land-fast sea ice. *Journal of Glaciology*, *39*(132), 223–238. https://doi.org/10.1017/s0022143000015884

Jezek, K. C., Kwok, R., Kaleschke, L., Belgiovane, D. J., Chen, C.-C., Bringer, A., et al. (2019). Remote sensing of sea ice thickness and salinity with 0.5–2 GHz microwave radiometry. *IEEE Transactions on Geoscience and Remote Sensing*, *57*(11), 8672–8684. https://doi.org/10.1109/TGRS.2019.2922163

Johnson, T., Tsamados, M., Muller, J.-P., & Stroeve, J. (2022). Mapping Arctic sea-ice surface roughness with multi-angle imaging spectroradiometer. *Remote Sensing*, *14*(24), 6249. https://doi.org/10.3390/rs14246249

Jones, J., Eicken, H., Mahoney, A., MV, R., Kambhamettu, C., Fukamachi, Y., et al. (2016). Landfast sea ice breakouts: Stabilizing ice features, oceanic and atmospheric forcing at Barrow, Alaska. *Continental Shelf Research*, *126*, 50–63. https://doi.org/10.1016/j.csr.2016.07.015

Kameyama, S., Otomaru, M., McMinn, A., & Suzuki, K. (2020). Ice melting can change DMSP production and photosynthetic activity of the Haptophyte *Phaeocystis antarctica*. *Journal of Phycology*, *56*(3), 761–774. https://doi.org/10.1111/jpy.12985

19449208, 2023, 2, Downloaded from https://agupubs.onlinelibrary.wiley.com/doi/10.1029/2022RG000770 by University of Adelaide Alumni, Wiley Online Library on [16/08/2023]. See the Terms and Conditions (https://onlinelibrary.wiley.com/terms-and-conditions) on Wiley Online Library for rules of use; OA articles are governed by the applicable Creative Commons License

Kaplan, D., Christiaen, D., & Arad, S. M. (1987). Chelating properties of extracellular polysaccharides from *Chlorella* spp. *Applied and Environmental Microbiology*, *53*(12), 2953–2956. https://doi.org/10.1128/aem.53.12.2953-2956.1987

Kawamura, T., Ohshima, K. I., Takizawa, T., & Ushio, S. (1997). Physical, structural, and isotopic characteristics and growth processes of fast sea ice in Lützow-Holm Bay, Antarctica. *Journal of Geophysical Research*, *102*(C2), 3345–3355. https://doi.org/10.1029/96JC03206

Kawamura, T., Takizawa, T., Ohshima, K., & Ushio, S. (1995). *Data of sea-ice cores obtained in Lützow-Holm Bay from 1990 to 1992 (JARE-31, -32) in the period of Japanese Antarctic Climate Research (Tech. Rep.)*. Japanese Antarctic Research Expedition.

Kawamura, T., Wakabayashi, H., & Ushio, S. (2006). Growth, properties and relation to radar backscatter coefficient of sea ice in Lützow-Holm Bay, Antarctica. *Annals of Glaciology*, *44*, 163–169. https://doi.org/10.3189/172756406781811655

Keller, R. (1983). Contributions to the early life history of *Pleuragramma antarcticum* Boul. 1902 (Pisces, Nototheniidae) in the Weddell Sea. *Meeresforschung*, *30*, 10–24.

Kellermann, A. (1986). Geographical distribution and abundance of postlarval and juvenile *Pleuragramma antarcticum* (Pisces, Notothenioidei) off the Antarctic Peninsula. *Polar Biology*, *6*(2), 111–119. https://doi.org/10.1007/BF00258262

Kennedy, F., Martin, A., Bowman, J. P., Wilson, R., & McMinn, A. (2019). Dark metabolism: A molecular insight into how the Antarctic sea-ice diatom *Fragilariopsis cylindrus* survives long-term darkness. *New Phytologist*, *223*(2), 675–691. https://doi.org/10.1111/nph.15843

Kharitonov, V. V., & Borodkin, V. A. (2022). Texture features of multi-year fresh ice in the Transcription bay, East Antarctica, in the period of summer melting. *Led i Sneg. Ice and Snow*, *62*(2), 275–286. https://doi.org/10.31857/S2076673422020132

Khazendar, A., & Jenkins, A. (2003). A model of marine ice formation within Antarctic ice shelf rifts. *Journal of Geophysical Research*, *108*(C7), 3235. https://doi.org/10.1029/2002jc001673

Khim, B. K., Shim, J., Yoon, H. I., Kang, Y. C., & Jang, Y. H. (2007). Lithogenic and biogenic particle deposition in an Antarctic coastal environment (Marian Cove, King George Island): Seasonal patterns from a sediment trap study. *Estuarine, Coastal and Shelf Science*, *73*(1–2), 111–122. https://doi.org/10.1016/j.ecss.2006.12.015

Kiko, R. (2010). Acquisition of freeze protection in a sea-ice crustacean through horizontal gene transfer? *Polar Biology*, *33*(4), 543–556. https://doi.org/10.1007/s00300-009-0732-0

Kiko, R., Kramer, M., Spindler, M., & Wägele, H. (2008). Tergipes antarcticus (Gastropoda, Nudibranchia): Distribution, life cycle, morphology, anatomy and adaptation of the first mollusc known to live in Antarctic sea ice. *Polar Biology*, *31*(11), 1383–1395. https://doi.org/10.1007/s00300-008-0478-0

Kiko, R., Michels, J., Mizdalski, E., Schnack-Schiel, S. B., & Werner, I. (2008). Living conditions, abundance and composition of the metazoan fauna in surface and sub-ice layers in pack ice of the western Weddell Sea during late spring. *Deep Sea Research Part II: Topical Studies in Oceanography*, *55*(8–9), 1000–1014. https://doi.org/10.1016/j.dsr2.2007.12.012

Kim, H., Ducklow, H. W., Abele, D., Barlett, E. M., Buma, A. G., Meredith, M. P., et al. (2018). Inter-decadal variability of phytoplankton biomass along the coastal West Antarctic Peninsula. *Philosophical Transactions of the Royal Society A: Mathematical, Physical & Engineering Sciences*, *376*(2122), 20170174. https://doi.org/10.1098/rsta.2017.0174

Kim, M., Im, J., Han, H., Kim, J., Lee, S., Shin, M., & Kim, H.-C. (2015). Landfast sea ice monitoring using multisensor fusion in the Antarctic. *GIScience and Remote Sensing*, *52*(2), 239–256. https://doi.org/10.1080/15481603.2015.1026050

Kim, M., Kim, H.-C., Im, J., Lee, S., & Han, H. (2020). Object-based landfast sea ice detection over West Antarctica using time series ALOS PALSAR data. *Remote Sensing of Environment*, *242*, 111782. https://doi.org/10.1016/j.rse.2020.111782

Kim, S., Saenz, B., Scanniello, J., Daly, K., & Ainley, D. (2018). Local climatology of fast ice in McMurdo Sound, Antarctica. *Antarctic Science*, *30*(2), 1–18. https://doi.org/10.1017/s0954102017000578

Kochanski, K., Tucker, G., & Anderson, R. (2021). Snow dune growth increases polar heat fluxes. *The Cryosphere Discussions*, *2021*, 1–14. https://doi.org/10.5194/tc-2021-205

Koga, S., Nomura, D., & Wada, M. (2014). Variation of dimethylsulfide mixing ratio over the Southern Ocean from 36°S to 70°S. *Polar Science*, *8*(3), 306–313. https://doi.org/10.1016/j.polar.2014.04.002

Kokubun, N., Tanabe, Y., Hirano, D., Mensah, V., Tamura, T., Aoki, S., & Takahashi, A. (2021). Shoreward intrusion of oceanic surface waters alters physical and biological ocean structures on the Antarctic continental shelf during winter: Observations from instrumented seals. *Limnology & Oceanography*, *66*(10), 3740–3753. https://doi.org/10.1002/lno.11914

König Beatty, C., & Holland, D. M. (2010). Modeling landfast sea ice by adding tensile strength. *Journal of Physical Oceanography*, *40*(1), 185–198. https://doi.org/10.1175/2009JPO4105.1

Kozlovsky, A. M., Nazintsev, Y. L., Fedotov, V. I., & Cherepanov, N. V. (1977). Fast ice of the Eastern Antarctic (in Russian). *Proceedings of the Soviet Antarctic Expedition*, *63*, 1–129.

Krembs, C., & Deming, J. W. (2008). The role of exopolymers in microbial adaptation to sea ice. In R. Margesin, F. Schinner, J.-C. Marx, & C. Gerday (Eds.), *Psychrophiles: From biodiversity to biotechnology* (pp. 247–264). Springer. https://doi.org/10.1007/978-3-540-74335-4{_}15

Krembs, C., Eicken, H., & Deming, J. W. (2011). Exopolymer alteration of physical properties of sea ice and implications for ice habitability and biogeochemistry in a warmer Arctic. *Proceedings of the National Academy of Sciences of the United States of America*, *108*(9), 3653–3658. https://doi.org/10.1073/pnas.1100701108

Krembs, C., Gradinger, R., & Spindler, M. (2000). Implications of brine channel geometry and surface area for the interaction of sympagic organisms in Arctic sea ice. *Journal of Experimental Marine Biology and Ecology*, *243*(1), 55–80. https://doi.org/10.1016/S0022-0981(99)00111-2

Kusahara, K., & Hasumi, H. (2014). Pathways of basal meltwater from Antarctic ice shelves: A model study. *Journal of Geophysical Research C: Oceans*, *119*(9), 5690–5704. https://doi.org/10.1002/2014JC009915

Kusahara, K., Hasumi, H., Fraser, A. D., Aoki, S., Shimada, K., Williams, G. D., et al. (2017). Modeling ocean–cryosphere interactions off Adélie and George V Land, East Antarctica. *Journal of Climate*, *30*(1), 163–188. https://doi.org/10.1175/JCLI-D-15-0808.1

Kusahara, K., Hasumi, H., & Tamura, T. (2010). Modeling sea ice production and dense shelf water formation in coastal polynyas around East Antarctica. *Journal of Geophysical Research*, *115*(C10), C10006. https://doi.org/10.1029/2010JC006133

Kusahara, K., Hasumi, H., & Williams, G. D. (2011). Impact of the Mertz Glacier Tongue calving on dense water formation and export. *Nature Communications*, *2*(1), 159. https://doi.org/10.1038/ncomms1156

Kusahara, K., Hirano, D., Fujii, M., Fraser, A. D., & Tamura, T. (2021). Modeling intensive ocean–cryosphere interactions in Lützow-Holm Bay, East Antarctica. *The Cryosphere*, *15*(4), 1697–1717. https://doi.org/10.5194/tc-15-1697-2021

Kuznetsov, M. (1960). Barchan snow drift in the wind belt of East Antarctica. *Sov Antarkt Eksped*, *10*, 175–179.

Kwok, R. (2004). ICESat observations of Arctic sea ice: A first look. *Geophysical Research Letters*, *31*(16), L16401. https://doi.org/10.1029/2004GL020309

Kwok, R., & Cunningham, G. F. (2008). ICESat over Arctic sea ice: Estimation of snow depth and ice thickness. *Journal of Geophysical Research*, *113*(C8), C08010. https://doi.org/10.1029/2008JC004753

19449208, 2023, 2, Downloaded from https://agupubs.onlinelibrary.wiley.com/doi/10.1029/2022RG000770 by University of Adelaide Alumni, Wiley Online Library on [16/08/2023]. See the Terms and Conditions (https://onlinelibrary.wiley.com/terms-and-conditions) on Wiley Online Library for rules of use; OA articles are governed by the applicable Creative Commons License

Kwok, R., Markus, T., Kurtz, N. T., Petty, A. A., Neumann, T. A., Farrell, S. L., et al. (2019). Surface height and sea ice freeboard of the Arctic Ocean from ICESat-2: Characteristics and early results. *Journal of Geophysical Research: Oceans*, *124*(10), 6942–6959. https://doi.org/10.1029/2019JC015486

Labrousse, S., Fraser, A. D., Sumner, M., Le Manach, F., Sauser, C., Horstmann, I., et al. (2021). Landfast ice: A major driver of reproductive success in a polar seabird. *Biology Letters*, *17*(6), 20210097. https://doi.org/10.1098/rsbl.2021.0097

Lacarra, M., Houssais, M.-N., Herbaut, C., Sultan, E., & Beauverger, M. (2014). Dense shelf water production in the Adélie Depression, East Antarctica, 2004–2012: Impact of the Mertz Glacier calving. *Journal of Geophysical Research: Oceans*, *119*(8), 5203–5220. https://doi.org/10.1002/2013JC009124

Laglera, L. M., Tovar-Sanchez, A., Sukekava, C. F., Naik, H., Naqvi, S. W. A., & Wolf-Gladrow, D. A. (2020). Iron organic speciation during the LOHAFEX experiment: Iron ligands release under biomass control by copepod grazing. *Journal of Marine Systems*, *207*, 103151. https://doi.org/10.1016/j.jmarsys.2019.02.002

La Mesa, M., & Eastman, J. T. (2012). Antarctic silverfish: Life strategies of a key species in the high-Antarctic ecosystem. *Fish and Fisheries*, *13*(3), 241–266. https://doi.org/10.1111/j.1467-2979.2011.00427.x

La Mesa, M., Eastman, J. T., & Vacchi, M. (2004). The role of notothenioid fish in the food web of the Ross Sea shelf waters: A review. *Polar Biology*, *27*(6), 321–338. https://doi.org/10.1007/s00300-004-0599-z

Landy, J. C., Bouffard, J., Wilson, C., Rynders, S., Aksenov, Y., & Tsamados, M. (2021). Improved Arctic sea ice freeboard retrieval from satellite altimetry using optimized sea surface decorrelation scales. *Journal of Geophysical Research: Oceans*, *126*(12), e2021JC017466. https://doi.org/10.1029/2021JC017466

Langhorne, P. J., Haas, C., Price, D., Rack, W., Leonard, G. H., Brett, G. M., & Urbini, S. (2023). Fast ice thickness distribution in the western Ross Sea in late spring. *Journal of Geophysical Research: Oceans*, *128*(2), e2022JC019459. https://doi.org/10.1029/2022jc019459

Langhorne, P. J., & Haskell, T. G. (2004). The flexural strength of partially refrozen cracks In Sea Ice (Vol. All Days). (ISOPE-I-04-053).

Langhorne, P. J., Hughes, K. G., Gough, A. J., Smith, I. J., Williams, M. J. M., Robinson, N. J., et al. (2015). Observed platelet ice distributions in Antarctic sea ice: An index for ocean-ice shelf heat flux. *Geophysical Research Letters*, *42*(13), 5442–5451. https://doi.org/10.1002/2015GL064508

Langhorne, P. J., Squire, V. A., Fox, C., Haskell, T., Shen, H. T., University of Auckland, N. Z., & Industrial Research, N. Z. (1999). Role of fatigue in wave-induced break-up of sea ice: A review. In *Proceedings of the international symposium on ice* (pp. 1019–1023).

Langhorne, P. J., Squire, V. A., Fox, C., & Haskell, T. G. (1998). Break-up of sea ice by ocean waves. *Annals of Glaciology*, *27*, 438–442. https://doi.org/10.3189/s0260305500017869

Langhorne, P. J., Squire, V. A., Fox, C., & Haskell, T. G. (2001). Lifetime estimation for a land-fast ice sheet subjected to ocean swell. *Annals of Glaciology*, *33*, 333–338. https://doi.org/10.3189/172756401781818419

Lannuzel, D., Grotti, M., Abelmoschi, M. L., & van der Merwe, P. (2015). Organic ligands control the concentrations of dissolved iron in Antarctic sea ice. *Marine Chemistry*, *174*, 120–130. https://doi.org/10.1016/j.marchem.2015.05.005

Lannuzel, D., Vancoppenolle, M., van der Merwe, P., Jong, J. D., Meiners, K. M., Grotti, M., et al. (2016). Iron in sea ice: Review and new insights. *Elementa*, *4*, 130. https://doi.org/10.12952/journal.elementa.000130

Larour, E., Rignot, E., Poinelli, M., & Scheuchl, B. (2021). Physical processes controlling the rifting of Larsen C Ice Shelf, Antarctica, prior to the calving of iceberg A68. *Proceedings of the National Academy of Sciences*, *118*(40), e2105080118. https://doi.org/10.1073/pnas.2105080118

Laxon, S. W., Giles, K. A., Ridout, A. L., Wingham, D. J., Willatt, R., Cullen, R., et al. (2013). CryoSat-2 estimates of Arctic sea ice thickness and volume. *Geophysical Research Letters*, *40*(4), 732–737. https://doi.org/10.1002/grl.50193

Leane, E., & Maddison, B. (2018). A biography of iceberg B09B. *Australian Humanities Review*, *63*, 99–115.

Lei, R., Li, Z., Cheng, B., Zhang, Z., & Heil, P. (2010). Annual cycle of landfast sea ice in Prydz Bay, East Antarctica. *Journal of Geophysical Research*, *115*(C2), 115. https://doi.org/10.1029/2008jc005223

Lemieux, J.–F., Lei, J., Dupont, F., Roy, F., Losch, M., Lique, C., & Laliberté, F. (2018). The impact of tides on simulated landfast ice in a Pan-Arctic ice-ocean model. *Journal of Geophysical Research: Oceans*, *123*(11), 7747–7762. https://doi.org/10.1029/2018JC014080

Lemieux, J.-F., Dupont, F., Blain, P., Roy, F., Smith, G. C., & Flato, G. M. (2016). Improving the simulation of landfast ice by combining tensile strength and a parameterization for grounded ridges. *Journal of Geophysical Research: Oceans*, *121*(10), 7354–7368. https://doi.org/10.1002/2016JC012006

Lemieux, J.–F., Tremblay, L. B., Dupont, F., Plante, M., Smith, G. C., & Dumont, D. (2015). A basal stress parameterization for modeling landfast ice. *Journal of Geophysical Research: Oceans*, *120*(4), 3157–3173. https://doi.org/10.1002/2014JC010678

Leonard, G. H., Langhorne, P. J., Williams, M. J. M., Vennell, R., Purdie, C. R., Dempsey, D. E., et al. (2011). Evolution of supercooling under coastal Antarctic sea ice during winter. *Antarctic Science*, *23*(4), 399–409. https://doi.org/10.1017/S0954102011000265

Leonard, G. H., Purdie, C. R., Langhorne, P. J., Haskell, T. G., Williams, M. J. M., & Frew, R. D. (2006). Observations of platelet ice growth and oceanographic conditions during the winter of 2003 in McMurdo Sound, Antarctica. *Journal of Geophysical Research*, *111*(C4), C04012. https://doi.org/10.1029/2005JCC002952

Leonard, G. H., Turner, K. E., Richter, M. E., Whittaker, M. S., & Smith, I. J. (2021). Brief communication: The anomalous winter 2019 sea-ice conditions in McMurdo Sound, Antarctica. *The Cryosphere*, *15*(10), 4999–5006. https://doi.org/10.5194/tc-15-4999-2021

Li, X., Hui, F.-M., Zhao, J.-C., Zhai, M.-X., & Cheng, X. (2022). Thickness simulation of landfast ice along Mawson Coast, East Antarctica based on a snow/ice high-resolution thermodynamic model. *Advances in Climate Change Research*, *13*(3), 375–384. https://doi.org/10.1016/j.accre.2022.02.005

Li, X., Shokr, M., Hui, F., Chi, Z., Heil, P., Chen, Z., et al. (2020). The spatio-temporal patterns of landfast ice in Antarctica during 2006–2011 and 2016–2017 using high-resolution SAR imagery. *Remote Sensing of Environment*, *242*, 111736. https://doi.org/10.1016/j.rse.2020.111736

Lieser, J. L., Curran, M. A. J., Bowie, A. R., Davidson, A. T., Doust, S. J., Fraser, A. D., et al. (2015). Antarctic slush-ice algal accumulation not quantified through conventional satellite imagery: Beware the ice of March. *The Cryosphere Discussions*, *9*, 6187–6222. https://doi.org/10.5194/tcd-9-6187-2015

Lim, S. M., Moreau, S., Vancoppenolle, M., Deman, F., Roukaerts, A., Meiners, K. M., et al. (2019). Field observations and physical-biogeochemical modeling suggest low silicon affinity for Antarctic fast ice diatoms. *Journal of Geophysical Research: Oceans*, *124*(11), 7837–7853. https://doi.org/10.1029/2018jc014458

Lizotte, M. P. (2001). The contributions of sea ice algae to Antarctic marine primary production. *American Zoologist*, *41*(1), 57–73. https://doi.org/10.1093/icb/41.1.57

Loots, C., Swadling, K. M., & Koubbi, P. (2009). Annual cycle of distribution of three ice-associated copepods along the coast near Dumont d'Urville, Terre Adélie (Antarctica). *Journal of Marine Systems*, *78*(4), 599–605. https://doi.org/10.1016/j.jmarsys.2009.01.003

Lubin, D., & Massom, R. A. (2006). *Polar remote sensing: Atmospheres and oceans* (1st ed., Vol. 1). Springer. https://doi.org/10.1007/3-540-30785-0

19449208, 2023, 2, Downloaded from https://agupubs.onlinelibrary.wiley.com/doi/10.1029/2022RG000770 by University of Adelaide Alumni, Wiley Online Library on [16/08/2023]. See the Terms and Conditions (https://onlinelibrary.wiley.com/terms-and-conditions) on Wiley Online Library for rules of use; OA articles are governed by the applicable Creative Commons License

Lutsenko, E. I., & Timokhov, L. A. (1977). Some characteristics of sea ice in the Antarctic in comparison with the Arctic. *Polar Geography*, *1*(1), 56–59. https://doi.org/10.1080/10889377709388613

Lythe, M., Hauser, A., & Wendler, G. (1999). Classification of sea ice types in the Ross Sea, Antarctica from SAR and AVHRR imagery. *International Journal of Remote Sensing*, *20*(15–16), 3073–3085. https://doi.org/10.1080/014311699211624

Mager, S. M., Smith, I. J., Kempema, E. W., Thomson, B. J., & Leonard, G. H. (2013). Anchor ice in polar oceans. *Progress in Physical Geography: Earth and Environment*, *37*(4), 468–483. https://doi.org/10.1177/0309133313479815

Mahoney, A. R., Eicken, H., Gaylord, A. G., & Shapiro, L. (2007). Alaska landfast sea ice: Links with bathymetry and atmospheric circulation. *Journal of Geophysical Research*, *112*(C2), C02001. https://doi.org/10.1029/2006JC003559

Mahoney, A. R., Eicken, H., & Shapiro, L. (2007). How fast is landfast sea ice? A study of the attachment and detachment of nearshore ice at Barrow, Alaska. *Cold Regions Science and Technology*, *47*(3), 233–255. https://doi.org/10.1016/j.coldregions.2006.09.005

Mahoney, A. R., Eicken, H., Shapiro, L., & Grenfell, T. C. (2004). Ice motion and driving forces during a spring ice shove on the Alaskan Chukchi coast. *Journal of Glaciology*, *50*(169), 195–207. https://doi.org/10.3189/172756504781830141

Mahoney, A. R. (2011). *Literature review of potential icebreaker impacts on sea ice as they relate to the Beaufort and Chukchi seas (technical report)*. Bureau of Ocean Energy Management, Regulation, and Enforcement.

Mahoney, A. R. (2018). Landfast sea ice in a changing Arctic. In E. Osborne, J. A. Richter-Menge, & M. O. Jeffries (Eds.), *Arctic report card 2018*. NOAA.

Mahoney, A. R., Dammann, D. O., Johnson, M. A., Eicken, H., & Meyer, F. J. (2016). Measurement and imaging of infragravity waves in sea ice using InSAR. *Geophysical Research Letters*, *43*(12), 6383–6392. https://doi.org/10.1002/2016GL069583

Mahoney, A. R., Eicken, H., Fukamachi, Y., Ohshima, K. I., Simizu, D., Kambhamettu, C., et al. (2015). Taking a look at both sides of the ice: Comparison of ice thickness and drift speed as observed from moored, airborne and shore-based instruments near Barrow, Alaska. *Annals of Glaciology*, *56*(69), 363–372. https://doi.org/10.3189/2015AoG69A565

Mahoney, A. R., Gough, A. J., Langhorne, P. J., Robinson, N. J., Stevens, C. L., Williams, M. J. M., & Haskell, T. G. (2011). The seasonal appearance of ice shelf water in coastal Antarctica and its effect on sea ice growth. *Journal of Geophysical Research*, *116*(C11), C11032. https://doi.org/10.1029/2011JC007060

Maksym, T. (2019). Arctic and Antarctic Sea Ice Change: Contrasts, Commonalities, and Causes. *Annual Review of Marine Science*, *11*(1), 187–213. https://doi.org/10.1146/annurev-marine-010816-060610

Maksym, T., & Markus, T. (2008). Antarctic sea ice thickness and snow-to-ice conversion from atmospheric reanalysis and passive microwave snow depth. *Journal of Geophysical Research*, *113*(C2), C02S12. https://doi.org/10.1029/2006jc004085

Mangoni, O., Saggiomo, M., Modigh, M., Catalano, G., Zingone, A., & Saggiomo, V. (2009). The role of platelet ice microalgae in seeding phytoplankton blooms in Terra Nova Bay (Ross Sea, Antarctica): A mesocosm experiment. *Polar Biology*, *32*(3), 311–323. https://doi.org/10.1007/s00300-008-0507-z

Martin, A., McMinn, A., Davy, S. K., Anderson, M. J., Miller, H. C., Hall, J. A., & Ryan, K. G. (2012). Preliminary evidence for the microbial loop in Antarctic sea ice using microcosm simulations. *Antarctic Science*, *24*(6), 547–553. https://doi.org/10.1017/s0954102012000491

Massom, R. A. (2003). Recent iceberg calving events in the Ninnis Glacier region, East Antarctica. *Antarctic Science*, *15*(2), 303–313. https://doi.org/10.1017/S0954102003001299

Massom, R. A., Eicken, H., Hass, C., Jeffries, M. O., Drinkwater, M. R., Sturm, M., et al. (2001). Snow on Antarctic sea ice. *Reviews of Geophysics*, *39*(3), 413–445. https://doi.org/10.1029/2000RG000085

Massom, R. A., Giles, A. B., Fricker, H. A., Warner, R. C., Legrésy, B., Hyland, G., et al. (2010). Examining the interaction between multi-year landfast sea ice and the Mertz Glacier Tongue, East Antarctica: Another factor in ice sheet stability? *Journal of Geophysical Research*, *115*(C12), C12027. https://doi.org/10.1029/2009JC006083

Massom, R. A., Giles, A. B., Warner, R. C., Fricker, H. A., Legrésy, B., Hyland, G., et al. (2015). External influences on the Mertz Glacier Tongue (East Antarctica) in the decade leading up to its calving in 2010. *Journal of Geophysical Research: Earth Surface*, *120*(3), 490–506. https://doi.org/10.1002/2014JF003223

Massom, R. A., Hill, K., Barbraud, C., Adams, N., Ancel, A., Emmerson, L., & Pook, M. J. (2009). Fast ice distribution in Adélie Land, East Antarctica: Interannual variability and implications for emperor penguins Aptenodytes forsteri. *Marine Ecology Progress Series*, *374*, 243–257. https://doi.org/10.3354/meps07734

Massom, R. A., Hill, K. L., Lytle, V. I., Worby, A. P., Paget, M., & Allison, I. (2001). Effects of regional fast-ice and iceberg distributions on the behaviour of the Mertz Glacier polynya, East Antarctica. *Annals of Glaciology*, *33*, 391–398. https://doi.org/10.3189/172756401781818518

Massom, R. A., Scambos, T. A., Bennetts, L. G., Reid, P., Squire, V. A., & Stammerjohn, S. E. (2018). Antarctic ice shelf disintegration triggered by sea ice loss and ocean swell. *Nature*, *558*(7710), 383–389. https://doi.org/10.1038/s41586-018-0212-1

Massom, R. A., & Stammerjohn, S. E. (2010). Antarctic sea ice change and variability—Physical and ecological implications. *Polar Science*, *4*(2), 149–186. https://doi.org/10.1016/j.polar.2010.05.001

Matsuoka, K., Skoglund, A., Roth, G., de Pomereu, J., Griffiths, H., Headland, R., et al. (2021). Quantarctica, an integrated mapping environment for Antarctica, the Southern Ocean, and sub-Antarctic islands. *Environmental Modelling & Software*, *140*, 105015. https://doi.org/10.1016/j.envsoft.2021.105015

Maykut, G. A., & Untersteiner, N. (1971). Some results from a time-dependent thermodynamic model of sea ice. *Journal of Geophysical Research*, *76*(6), 1550–1575. https://doi.org/10.1029/jc076i006p01550

McConville, M. J., & Wetherbee, R. (1983). The bottom-ice microalgal community from annual ice in the inshore waters of East Antarctica. *Journal of Phycology*, *19*(4), 431–439. https://doi.org/10.1111/j.0022-3646.1983.00431.x

McMinn, A. (1996). Preliminary investigation of the contribution of fast-ice algae to the spring phytoplankton bloom in Ellis Fjord, eastern Antarctica. *Polar Biology*, *16*(4), 301–307. https://doi.org/10.1007/s003000050057

McMinn, A., & Ashworth, C. (1998). The use of oxygen microelectrodes to determine the net production by an Antarctic sea ice algal community. *Antarctic Science*, *10*(1), 39–44. https://doi.org/10.1017/s0954102098000066

McMinn, A., Ashworth, C., & Ryan, K. (1999). Growth and productivity of Antarctic sea ice algae under PAR and UV Irradiances. *Botanica Marina*, *42*(4), 401–407. https://doi.org/10.1515/BOT.1999.046

McMinn, A., Ashworth, C., & Ryan, K. G. (2000). In situ net primary productivity of an Antarctic fast ice bottom algal community. *Aquatic Microbial Ecology*, *21*, 177–185. https://doi.org/10.3354/ame021177

McMinn, A., Heijnist, H., & Hodgson, D. (1994). Minimal effects of UVB radiation on Antarctic diatoms over the past 20 years. *Nature*, *370*(6490), 547–549. https://doi.org/10.1038/370547a0

McMinn, A., Liang, Y., & Wang, M. (2020). Minireview: The role of viruses in marine photosynthetic biofilms. *Marine Life Science and Technology*, *2*(3), 203–208. https://doi.org/10.1007/s42995-020-00042-2

19449208, 2023, 2, Downloaded from https://agupubs.onlinelibrary.wiley.com/doi/10.1029/2022RG000770 by University of Adelaide Alumni, Wiley Online Library on [16/08/2023]. See the Terms and Conditions (https://onlinelibrary.wiley.com/terms-and-conditions) on Wiley Online Library for rules of use; OA articles are governed by the applicable Creative Commons License

McMinn, A., & Martin, A. (2013). Dark survival in a warming world. *Proceedings of the Royal Society B: Biological Sciences*, *280*(1755), 20122909. https://doi.org/10.1098/rspb.2012.2909

McMinn, A., Müller, M. N., Martin, A., Ugalde, S. C., Lee, S., Castrisios, K., & Ryan, K. G. (2017). Effects of CO_2 concentration on a late summer surface sea ice community. *Marine Biology*, *164*(4), 87. https://doi.org/10.1007/s00227-017-3102-4

McMinn, A., Pankowski, A., & Delfatti, T. (2005). Effect of hyperoxia on the growth and photosynthesis of polar sea ice microalgae. *Journal of Phycology*, *41*(4), 732–741. https://doi.org/10.1111/j.1529-8817.2005.00095.x

McMinn, A., Pankowskii, A., Ashworth, C., Bhagooli, R., Ralph, P., & Ryan, K. (2010). In situ net primary productivity and photosynthesis of Antarctic sea ice algal, phytoplankton and benthic algal communities. *Marine Biology*, *157*(6), 1345–1356. https://doi.org/10.1007/s00227-010-1414-8

McMinn, A., Skerratt, J., Trull, T., Ashworth, C., & Lizotte, M. (1999). Nutrient stress gradient in the bottom 5 cm of fast ice, McMurdo Sound, Antarctica. *Polar Biology*, *21*(4), 220–227. https://doi.org/10.1007/s003000050356

McPhee, M. G., Stevens, C. L., Smith, I. J., & Robinson, N. J. (2016). Turbulent heat transfer as a control of platelet ice growth in supercooled under-ice ocean boundary layers. *Ocean Science*, *12*(2), 507–515. https://doi.org/10.5194/os-12-507-2016

Meiners, K. M., Arndt, S., Bestley, S., Krumpen, T., Ricker, R., Milnes, M., et al. (2017). Antarctic pack ice algal distribution: Floe-scale spatial variability and predictability from physical parameters. *Geophysical Research Letters*, *44*(14), 7382–7390. https://doi.org/10.1002/2017GL074346

Meiners, K. M., & Michel, C. (2017). Dynamics of nutrients, dissolved organic matter and exopolymers in sea ice. In *Sea ice* (pp. 415–432). John Wiley & Sons, Ltd. https://doi.org/10.1002/9781118778371.ch17

Meiners, K. M., Vancoppenolle, M., Carnat, G., Castellani, G., Delille, B., Delille, D., et al. (2018). Chlorophyll-*a* in Antarctic landfast sea ice: A first synthesis of historical ice core data. *Journal of Geophysical Research: Oceans*, *123*(11), 8444–8459. https://doi.org/10.1029/2018jc014245

Meiners, K. M., Vancoppenolle, M., Thanassekos, S., Dieckmann, G. S., Thomas, D. N., Tison, J. L., et al. (2012). Chlorophyll *a* in Antarctic sea ice from historical ice core data. *Geophysical Research Letters*, *39*(21), 1–5. https://doi.org/10.1029/2012GL053478

Melsheimer, C., Spreen, G., Ye, Y., & Shokr, M. (2022). Antarctic sea ice types from active and passive microwave remote sensing. *The Cryosphere Discussions*, *17*(1), 105–126. https://doi.org/10.5194/tc-17-105-2023

Meyer, F. J., Mahoney, A., Eicken, H., Denny, C. L., Druckenmiller, H. C., & Hendricks, S. (2011). Mapping arctic landfast ice extent using L-band synthetic aperture radar interferometry. *Remote Sensing of Environment*, *115*(12), 3029–3043. https://doi.org/10.1016/j.rse.2011.06.006

Michael, K., & Hill, K. (2003). *Sea ice Atlas from advanced very high resolution radiometer (AVHRR) imagery 1992–1999*. Australian Antarctic Data Centre.

Miles, B. W. J., Stokes, C. R., & Jamieson, S. S. R. (2017). Simultaneous disintegration of outlet glaciers in Porpoise Bay (Wilkes Land), East Antarctica, driven by sea ice break-up. *The Cryosphere*, *11*(1), 427–442. https://doi.org/10.5194/tc-11-427-2017

Miles, B. W. J., Stokes, C. R., & Jamieson, S. S. R. (2018). Velocity increases at Cook Glacier, East Antarctica, linked to ice shelf loss and a subglacial flood event. *The Cryosphere*, *12*(10), 3123–3136. https://doi.org/10.5194/tc-12-3123-2018

Miles, B. W. J., Stokes, C. R., Jenkins, A., Jordan, J. R., Jamieson, S. S. R., & Gudmundsson, G. H. (2020). Intermittent structural weakening and acceleration of the Thwaites Glacier Tongue between 2000 and 2018. *Journal of Glaciology*, *66*(257), 485–495. https://doi.org/10.1017/jog.2020.20

Miles, B. W. J., Stokes, C. R., Jenkins, A., Jordan, J. R., Jamieson, S. S. R., & Gudmundsson, G. H. (2023). Slowdown of Shirase Glacier, East Antarctica, caused by strengthening alongshore winds. *The Cryosphere*, *17*(1), 445–456. https://doi.org/10.5194/tc-17-445-2023

Miller, L. A., Fripiat, F., Else, B. G., Bowman, J. S., Brown, K. A., Collins, R. E., et al. (2015). Methods for biogeochemical studies of sea ice: The state of the art, caveats, and recommendations. *Elementa*, *3*, 000038. https://doi.org/10.12952/journal.elementa.000038

Mintenbeck, K., & Torres, J. J. (2017). Impact of climate change on the Antarctic silverfish and its consequences for the Antarctic ecosystem (pp. 253–286). https://doi.org/10.1007/978-3-319-55893-6{_}12

Montgomery, J. C., Foster, B. A., & Cargill, J. M. (1989). Stomach evacuation rate in the planktivorous Antarctic fish *Pagothenia borchgrevinki*. *Polar Biology*, *9*(6), 405–408. https://doi.org/10.1007/BF00442532

Moorthi, S., Caron, D. A., Gast, R. J., & Sanders, R. W. (2009). Mixotrophy: A widespread and important ecological strategy for planktonic and sea-ice nanoflagellates in the Ross Sea, Antarctica. *Aquatic Microbial Ecology*, *54*, 269–277. https://doi.org/10.3354/ame01276

Morales Maqueda, M. A., Willmott, A. J., & Biggs, N. R. T. (2004). Polynya dynamics: A review of observations and modeling. *Reviews of Geophysics*, *42*(1), RG1004. https://doi.org/10.1029/2002RG000116

Moreçki, V. N. (1965). Underwater sea ice. English translation by E. R. Hope, DRB Canada Report No. T497R April 1968. *Probl Arkt Antarkt*, *19*, 32–38.

Morgan-Kiss, R. M., Priscu, J. C., Pocock, T., Gudynaite-Savitch, L., & Huner, N. P. A. (2006). Adaptation and acclimation of photosynthetic microorganisms to permanently cold environments. *Microbiology and Molecular Biology Reviews*, *70*(1), 222–252. https://doi.org/10.1128/mmbr.70.1.222-252.2006

Morlighem, M., Williams, C. N., Rignot, E., An, L., Arndt, J. E., Bamber, J. L., et al. (2017). BedMachine v3: Complete bed topography and ocean bathymetry mapping of Greenland From multibeam echo sounding combined with mass conservation. *Geophysical Research Letters*, *44*(21), 11-051. https://doi.org/10.1002/2017GL074954

Mundy, C. J., Ehn, J. K., Barber, D. G., & Michel, C. (2007). Influence of snow cover and algae on the spectral dependence of transmitted irradiance through Arctic landfast first-year sea ice. *Journal of Geophysical Research*, *112*(3), 1–10. https://doi.org/10.1029/2006JC003683

Murphy, E. J., Clarke, A., Abram, N. J., & Turner, J. (2014). Variability of sea-ice in the northern Weddell Sea during the 20th century. *Journal of Geophysical Research: Oceans*, *119*(7), 4549–4572. https://doi.org/10.1002/2013jc009511

Murphy, E. J., Clarke, A., Symon, C., & Priddle, J. (1995). Temporal variation in Antarctic sea-ice: Analysis of a long term fast-ice record from the South Orkney Islands. *Deep Sea Research Part I: Oceanographic Research Papers*, *42*(7), 1045–1062. https://doi.org/10.1016/0967-0637(95)00057-d

Nakamura, K., Aoki, S., Yamanokuchi, T., & Tamura, T. (2022). Interactive movements of outlet glacier tongue and landfast sea ice in Lützow-Holm Bay, East Antarctica, detected by ALOS-2/PALSAR-2 imagery. *Science of Remote Sensing*, *6*, 100064. https://doi.org/10.1016/j.srs.2022.100064

Nakamura, K., Doi, K., & Shibuya, K. (2010). Fluctuations in the flow velocity of the Antarctic Shirase Glacier over an 11-year period. *Polar Science*, *4*(3), 443–455. https://doi.org/10.1016/j.polar.2010.04.010

Nakamura, K., Wakabayashi, H., Uto, S., Ushio, S., & Nishio, F. (2009). Observation of sea-ice thickness using Envisat data from Lützow-Holm Bay, East Antarctica. *IEEE Geoscience and Remote Sensing Letters*, *6*(2), 277–281. https://doi.org/10.1109/lgrs.2008.2011061

Nakata, K., Ohshima, K. I., & Nihashi, S. (2021). Mapping of active frazil for Antarctic Coastal Polynyas, with an estimation of sea-ice production. *Geophysical Research Letters*, *48*(6). https://doi.org/10.1029/2020GL091353

Neme, J., England, M. H., & McCHogg, A. (2022). Projected changes of surface winds over the Antarctic continental margin. *Geophysical Research Letters*, *49*(16), e2022GL098820. https://doi.org/10.1029/2022GL098820

19449208, 2023, 2, Downloaded from https://agupubs.onlinelibrary.wiley.com/doi/10.1029/2022RG000770 by University of Adelaide Alumni, Wiley Online Library on [16/08/2023]. See the Terms and Conditions (https://onlinelibrary.wiley.com/terms-and-conditions) on Wiley Online Library for rules of use; OA articles are governed by the applicable Creative Commons License

Nihashi, S., & Ohshima, K. I. (2015). Circumpolar mapping of Antarctic coastal polynyas and landfast sea ice: Relationship and variability. *Journal of Climate*, *28*(9), 3650–3670. https://doi.org/10.1175/jcli-d-14-00369.1

Nihashi, S., Ohshima, K. I., Tamura, T., Fukamachi, Y., & Saitoh, S.-I. (2009). Thickness and production of sea ice in the Okhotsk Sea coastal polynyas from AMSR-E. *Journal of Geophysical Research*, *114*(C10), C10025. https://doi.org/10.1029/2008JC005222

Nomura, D., Granskog, M. A., Assmy, P., Simizu, D., & Hashida, G. (2013). Arctic and Antarctic sea ice acts as a sink for atmospheric CO_2 during periods of snowmelt and surface flooding. *Journal of Geophysical Research: Oceans*, *118*(12), 6511–6524. Portico. https://doi.org/10.1002/2013jc009048

Nomura, D., Kasamatsu, N., Tateyama, K., Kudoh, S., & Fukuchi, M. (2011). DMSP and DMS in coastal fast ice and under-ice water of Lützow-Holm Bay, eastern Antarctica. *Continental Shelf Research*, *31*(13), 1377–1383. https://doi.org/10.1016/j.csr.2011.05.017

Nomura, D., Ooki, A., Simizu, D., & Fukuchi, M. (2011). Bromoform concentrations in slush-layer water in Antarctic fast ice. *Antarctic Science*, *23*(6), 623–628. https://doi.org/10.1017/s0954102011000459

Nomura, D., Simizu, D., Chavanich, S., Shinagawa, H., & Fukuchi, M. (2012). An artificial pool experiment in Antarctic sea ice: Effects of sea ice melting on physical and biogeochemical components of pool water. *Antarctic Science*, *24*(5), 536–544. https://doi.org/10.1017/s0954102012000284

Nowak, A., Hodson, A., & Turchyn, A. V. (2018). Spatial and temporal dynamics of dissolved organic carbon, chlorophyll, nutrients, and trace metals in maritime antarctic snow and snowmelt. *Frontiers in Earth Science*, *6*, 201. https://doi.org/10.3389/feart.2018.00201

O'Driscoll, R. L., Ladroit, Y., Parker, S. J., Vacchi, M., Canese, S., Ghigliotti, L., et al. (2018). Acoustic deployments reveal Antarctic silverfish under ice in the Ross Sea. *Antarctic Science*, *30*(6), 345–353. https://doi.org/10.1017/s0954102018000366

Ohshima, K. I. (2000). Effect of landfast sea ice on coastal currents driven by the wind. *Journal of Geophysical Research*, *105*(C7), 17133–17141. https://doi.org/10.1029/2000jc900081

Ohshima, K. I., Fukamachi, Y., Williams, G. D., Nihashi, S., Roquet, F., Kitade, Y., et al. (2013). Antarctic Bottom Water production by intense sea-ice formation in the Cape Darnley polynya. *Nature Geoscience*, *6*(3), 235–240. https://doi.org/10.1038/ngeo1738

Ohshima, K. I., Takizawa, T., Ushio, S., & Kawamura, T. (1996). Seasonal variations of the Antarctic coastal ocean in the vicinity of Lützow-Holm Bay. *Journal of Geophysical Research*, *101*(C9), 20617–20628. https://doi.org/10.1029/96JC01752

Ojima, M., Takahashi, K. T., Iida, T., Moteki, M., Miyazaki, N., Tanimura, A., & Odate, T. (2017). Variability of the fauna within drifting sea ice floes in the seasonal ice zone of the Southern Ocean during the austral summer. *Polar Science*, *12*, 19–24. https://doi.org/10.1016/j.polar.2017.02.005

Pearce, I., Davidson, A. T., Wright, S., & Enden, R. V. D. (2008). Seasonal changes in phytoplankton growth and microzooplankton grazing at an Antarctic coastal site. *Aquatic Microbial Ecology*, *50*, 157–167. https://doi.org/10.3354/ame01149

Penrose, J. D., Conde, M., & Pauly, T. J. (1994). Acoustic detection of ice crystals in Antarctic waters. *Journal of Geophysical Research*, *99*(C6), 12573. https://doi.org/10.1029/93JC03507

Perovich, D. K. (2017). Sea ice and sunlight. In *Sea ice* (pp. 110–137). John Wiley & Sons, Ltd. https://doi.org/10.1002/9781118778371.ch4

Perovich, D. K., & Polashenski, C. (2012). Albedo evolution of seasonal Arctic sea ice. *Geophysical Research Letters*, *39*(8), 8501. https://doi.org/10.1029/2012gl051432

Petrich, C., & Eicken, H. (2017). Overview of sea ice growth and properties. In *Sea ice* (pp. 1–41). John Wiley & Sons, Ltd. https://doi.org/10.1002/9781118778371.ch1

Petrich, C., Langhorne, P. J., & Haskell, T. G. (2007). Formation and structure of refrozen cracks in land-fast first-year sea ice. *Journal of Geophysical Research*, *112*(C4), C04006. https://doi.org/10.1029/2006jc003466

Petrou, K., Hill, R., Doblin, M. A., McMinn, A., Johnson, R., Wright, S. W., & Ralph, P. J. (2011). Photoprotection of sea-ice microalgal communities from the East Antarctic pack ice. *Journal of Phycology*, *47*(1), 77–86. https://doi.org/10.1111/j.1529-8817.2010.00944.x

Petrou, K., Kranz, S. A., Trimborn, S., Hassler, C. S., Ameijeiras, S. B., Sackett, O., et al. (2016). Southern Ocean phytoplankton physiology in a changing climate (Vol. *203*). https://doi.org/10.1016/j.jplph.2016.05.004

Petrov, I. (1967). Ice thickness and snow depth distribution in the coastal part of the davis sea. *Soviet Antarctic Expedition Information Bulletin*, *6*, 305–307.

Pinkerton, M. H. (2017). Diet and trophic ecology of adult Antarctic silverfish (*Pleuragramma antarctica*) (pp. 93–111). https://doi.org/10.1007/978-3-319-55893-6{_}5

Pinkerton, M. H., & Bradford-Grieve, J. M. (2014). Characterizing foodweb structure to identify potential ecosystem effects of fishing in the Ross Sea, Antarctica. *ICES Journal of Marine Science*, *71*(7), 1542–1553. https://doi.org/10.1093/icesjms/fst230

Pirazzini, R. (2004). Surface albedo measurements over Antarctic sites in summer. *Journal of Geophysical Research*, *109*(D20), D20118. https://doi.org/10.1029/2004jd004617

Pollard, D., DeConto, R. M., & Alley, R. B. (2015). Potential Antarctic Ice Sheet retreat driven by hydrofracturing and ice cliff failure. *Earth and Planetary Science Letters*, *412*, 112–121. https://doi.org/10.1016/j.epsl.2014.12.035

Porter-Smith, R., McKinlay, J., Fraser, A. D., & Massom, R. A. (2021). Coastal complexity of the Antarctic continent. *Earth System Science Data*, *13*(7), 3103–3114. https://doi.org/10.5194/essd-13-3103-2021

Powell, R. T., & Wilson-Finelli, A. (2003). Importance of organic Fe complexing ligands in the Mississippi River plume. *Estuarine, Coastal and Shelf Science*, *58*(4), 757–763. https://doi.org/10.1016/S0272-7714(03)00182-3

Prebble, M. M. (1968). Ice breakout, McMurdo Sound, Antarctica. *New Zealand Journal of Geology and Geophysics*, *11*(4), 908–921. https://doi.org/10.1080/00288306.1968.10420760

Price, D., Beckers, J., Ricker, R., Kurtz, N., Rack, W., Haas, C., et al. (2015). Evaluation of CryoSat-2 derived sea-ice freeboard over fast ice in McMurdo Sound, Antarctica. *Journal of Glaciology*, *61*(226), 285–300. https://doi.org/10.3189/2015jog14j157

Price, D., Rack, W., Langhorne, P. J., Haas, C., Leonard, G., & Barnsdale, K. (2014). The sub-ice platelet layer and its influence on freeboard to thickness conversion of Antarctic sea ice. *The Cryosphere*, *8*(3), 1031–1039. https://doi.org/10.5194/tc-8-1031-2014

Price, D., Soltanzadeh, I., Rack, W., & Dale, E. (2019). Snow-driven uncertainty in CryoSat-2-derived Antarctic sea ice thickness—Insights from McMurdo Sound. *The Cryosphere*, *13*(4), 1409–1422. https://doi.org/10.5194/tc-13-1409-2019

Pringle, D., Eicken, H., Trodahl, H., & Backstrom, L. (2007). Thermal conductivity of landfast Antarctic and Arctic sea ice. *Journal of Geophysical Research*, *112*(C4), C04017. https://doi.org/10.1029/2006jc003641

Purdie, C. R., Langhorne, P. J., Leonard, G. H., & Haskell, T. G. (2006). Growth of first-year landfast Antarctic sea ice determined from winter temperature measurements. *Annals of Glaciology*, *44*, 170–176. https://doi.org/10.3189/172756406781811853

Raymond, J. A., Sullivan, C. W., & DeVries, A. L. (1994). Release of an ice-active substance by Antarctic sea ice diatoms. *Polar Biology*, *14*(1), 71–75. https://doi.org/10.1007/bf00240276

Remy, J.-P., Becquevort, S., Haskell, T. G., & Tison, J.-L. (2007). Impact of the B-15 iceberg "stranding event" on the physical and biological properties of sea ice in McMurdo Sound, Ross Sea, Antarctica. *Antarctic Science*, *20*(6), 593–604. https://doi.org/10.1017/s0954102008001284

19449208, 2023, 2, Downloaded from https://agupubs.onlinelibrary.wiley.com/doi/10.1029/2022RG000770 by University of Adelaide Alumni, Wiley Online Library on [16/08/2023]. See the Terms and Conditions (https://onlinelibrary.wiley.com/terms-and-conditions) on Wiley Online Library for rules of use; OA articles are governed by the applicable Creative Commons License

Riaux-Gobin, C., Dieckmann, G. S., Poulin, M., Neveux, J., Labrune, C., & Vétion, G. (2013). Environmental conditions, particle flux and sympagic microalgal succession in spring before the sea-ice break-up in Adélie Land, East Antarctica. *Polar Research*, *32*(0), 19675. https://doi.org/10.3402/polar.v32i0.19675

Riaux-Gobin, C., Poulin, M., Dieckmann, G., Labrune, C., & Vétion, G. (2011). Spring phytoplankton onset after the ice break-up and sea-ice signature (Adélie Land, East Antarctica). *Polar Research*, *30*(0), 5910. https://doi.org/10.3402/polar.v30i0.5910

Riaux-Gobin, C., Poulin, M., Prodon, R., & Treguer, P. (2003). Land-fast ice microalgal and phytoplanktonic communities (Adélie Land, Antarctica) in relation to environmental factors during ice break-up. *Antarctic Science*, *15*(3), 353–364. https://doi.org/10.1017/s0954102003001378

Richter, M. E., Leonard, G. H., Smith, I. J., Langhorne, P. J., Mahoney, A. R., & Parry, M. (2022). Accuracy and precision when deriving sea-ice thickness from thermistor strings: A comparison of methods. *Journal of Glaciology*, *1*, 20. https://doi.org/10.1017/jog.2022.108

Richter-Menge, J. A., Perovich, D. K., Elder, B. C., Claffey, K., Rigor, I., & Ortmeyer, M. (2006). Ice mass-balance buoys: A tool for measuring and attributing changes in the thickness of the Arctic sea-ice cover. *Annals of Glaciology*, *44*, 205–210. https://doi.org/10.3189/172756406781811727

Roach, L. A., Dörr, J., Holmes, C. R., Massonnet, F., Blockley, E. W., Notz, D., et al. (2020). Antarctic sea ice area in CMIP6. *Geophysical Research Letters*, *47*(9), e2019GL086729. https://doi.org/10.1029/2019GL086729

Robinson, D. H., Arrigo, K. R., Iturriaga, R., & Sullivan, C. W. (1995). Microalgal light-harvesting in extreme low-light environments in McMurdo Sound, Antarctica. *Journal of Phycology*, *31*(4), 508–520. https://doi.org/10.1111/j.1529-8817.1995.tb02544.x

Robinson, D. H., Kolber, Z., & Sullivan, C. W. (1997). Photophysiology and photoacclimation in surface sea ice algae from McMurdo Sound, Antarctica. *Marine Ecology Progress Series*, *147*, 243–256. https://doi.org/10.3354/meps147243

Robinson, E., & Davison, W. (2008). The Antarctic notothenioid fish Pagothenia borchgrevinki is thermally flexible: Acclimation changes oxygen consumption. *Polar Biology*, *31*(3), 317–326. https://doi.org/10.1007/s00300-007-0361-4

Robinson, N. J., Stevens, C. L., & McPhee, M. G. (2017). Observations of amplified roughness from crystal accretion in the sub-ice ocean boundary layer. *Geophysical Research Letters*, *44*(4), 1814–1822. https://doi.org/10.1002/2016GL071491

Robinson, N. J., Williams, M. J. M., Stevens, C. L., Langhorne, P. J., & Haskell, T. G. (2014). Evolution of a supercooled Ice Shelf Water plume with an actively growing subice platelet matrix. *Journal of Geophysical Research*, *119*(6), 3425–3446. https://doi.org/10.1002/2013JC009399

Robinson, W., & Haskell, T. G. (1990). Calving of Erebus Glacier tongue. *Nature*, *346*(346), 615–616. https://doi.org/10.1038/346615b0

Roukaerts, A., Deman, F., Van der Linden, F., Carnat, G., Bratkic, A., Moreau, S., et al. (2021). The biogeochemical role of a microbial biofilm in sea ice: Antarctic landfast sea ice as a case study. *Elementa: Science of the Anthropocene*, *9*(1), 134. https://doi.org/10.1525/elementa.2020.00134

Ryan, K. G., Mcminn, A., Hegseth, E. N., & Davy, S. K. (2012). The effects of ultraviolet-B radiation on Antarctic sea-ice algae. *Journal of Phycology*, *48*(1), 74–84. https://doi.org/10.1111/j.1529-8817.2011.01104.x

Ryan, K. G., McMinn, A., Mitchel, K. A., & Trenerry, L. (2002). Mycosporine-like amino acids in Antarctic sea ice algae, and their response to UVB radiation. *Zeitschrift fur Naturforschung Section C Journal of Biosciences*, *57*(5–6), 471–477. https://doi.org/10.1515/znc-2002-5-612

Saenz, B. T., Ainley, D. G., Daly, K. L., Ballard, G., Conlisk, E., Elrod, M. L., & Kim, S. L. (2020). Drivers of concentrated predation in an Antarctic marginal-ice-zone food web. *Scientific Reports*, *10*(1), 7282. https://doi.org/10.1038/s41598-020-63875-y

Saenz, B. T., & Arrigo, K. R. (2012). Simulation of a sea ice ecosystem using a hybrid model for slush layer desalination. *Journal of Geophysical Research*, *117*(C5), C05007. https://doi.org/10.1029/2011JC007544

Saenz, B. T., & Arrigo, K. R. (2014). Annual primary production in Antarctic sea ice during 2005–2006 from a sea ice state estimate. *Journal of Geophysical Research: Oceans*, *119*(6), 3645–3678. https://doi.org/10.1002/2013JC009677

Saggiomo, M., Poulin, M., Mangoni, O., Lazzara, L., Stefano, M. D., Sarno, D., & Zingone, A. (2017). Spring-time dynamics of diatom communities in landfast and underlying platelet ice in Terra Nova Bay, Ross Sea, Antarctica. *Journal of Marine Systems*, *166*, 26–36. https://doi.org/10.1016/j.jmarsys.2016.06.007

Scambos, T., Bell, R., Alley, R., Anandakrishnan, S., Bromwich, D., Brunt, K., et al. (2017). How much, how fast?: A science review and outlook for research on the instability of Antarctica's Thwaites Glacier in the 21st century. *Global and Planetary Change*, *153*, 16–34. https://doi.org/10.1016/j.gloplacha.2017.04.008

Schnack-Schiel, S. B., Dieckmann, G. S., Gradinger, R., Melnikov, I., Spindler, M., & Thomas, D. N. (2001). Meiofauna in sea ice of the Weddell Sea (Antarctica). *Polar Biology*, *24*(10), 724–728. https://doi.org/10.1007/s003000100273

Schnack-Schiel, S. B., Dieckmann, G. S., Kattner, G., & Thomas, D. N. (2004). Copepods in summer platelet ice in the eastern Weddell Sea, Antarctica. *Polar Biology*, *27*(8), 502–506. https://doi.org/10.1007/s00300-004-0613-5

Schnack-Schiel, S. B., Thomas, D., Dieckmann, G. S., Eicken, H., Gradinger, R., Spindler, M., et al. (1995). Life cycle strategy of the Antarctic calanoid copepod Stephos longipes. *Progress in Oceanography*, *36*(1), 45–75. https://doi.org/10.1016/0079-6611(95)00014-3

Schnack-Schiel, S. B., Thomas, D. N., Haas, C., Dieckmann, G. S., & Alheit, R. (2001). The occurrence of the copepods Stephos longipes (Calanoida) and Drescheriella glacialis (Harpacticoida) in summer sea ice in the Weddell Sea, Antarctica. *Antarctic Science*, *13*(2), 150–157. https://doi.org/10.1017/s0954102001000232

Scott, F. J., Davidson, A. T., & Marchant, H. J. (2001). Grazing by the Antarctic sea-ice ciliate Pseudocohnilembus. *Polar Biology*, *24*(2), 127–131. https://doi.org/10.1007/s003000000184

Segal, R. A., Scharien, R. K., Cafarella, S., & Tedstone, A. (2020). Characterizing winter landfast sea-ice surface roughness in the Canadian Arctic Archipelago using Sentinel-1 synthetic aperture radar and the Multi-angle Imaging SpectroRadiometer. *Annals of Glaciology*, *61*(83), 284–298. https://doi.org/10.1017/aog.2020.48

Selyuzhenok, V., & Demchev, D. (2021). An application of sea ice tracking algorithm for fast ice and stamukhas detection in the Arctic. *Remote Sensing*, *13*(18), 3783. https://doi.org/10.3390/rs13183783

Semtner, A. J. (1976). A model for the thermodynamic growth of sea ice in numerical investigations of climate. *Journal of Physical Oceanography*, *6*(3), 379–389. https://doi.org/10.1175/1520-0485(1976)006⟨0379:AMFTTG⟩2.0.CO;2

Seroussi, H., Nowicki, S., Payne, A. J., Goelzer, H., Lipscomb, W. H., Abe-Ouchi, A., et al. (2020). ISMIP6 Antarctica: A multi-model ensemble of the Antarctic ice sheet evolution over the 21st century. *The Cryosphere*, *14*(9), 3033–3070. https://doi.org/10.5194/tc-14-3033-2020

Shadwick, E. H., Rintoul, S. R., Tilbrook, B., Williams, G. D., Young, N., Fraser, A. D., et al. (2013). Glacier tongue calving reduced dense water formation and enhanced carbon uptake. *Geophysical Research Letters*, *40*(5), 904–909. https://doi.org/10.1002/grl.50178

Shah, M. Y., Ayemi, K. K., & Shrivastava, P. K. (2017). GPR survey and physical measurements of sea ice in Quilty Bay, Larsemann Hills, East Antarctica and its correlation with local atmospheric parameters. *Journal of the Geological Society of India*, *90*(3), 371–377. https://doi.org/10.1007/s12594-017-0726-4

Shapiro, L., & Metzner, R. (1989). *Nearshore ice conditions from radar data, Point Barrow, Alaska, UAG R-268 (technical report). Fairbanks*. Geophysical Institute, University of Alaska Fairbanks.

Shetye, S. S., Mohan, R., Patil, S., Jawak, S., Nair, A., Warrier, A. K., et al. (2019). Hidden biogeochemical anonymities under Antarctic fast ice. *Regional Studies in Marine Science*, *31*, 100789. https://doi.org/10.1016/j.rsma.2019.100789

19449208, 2023, 2, Downloaded from https://agupubs.onlinelibrary.wiley.com/doi/10.1029/2022RG000770 by University of Adelaide Alumni, Wiley Online Library on [16/08/2023]. See the Terms and Conditions (https://onlinelibrary.wiley.com/terms-and-conditions) on Wiley Online Library for rules of use; OA articles are governed by the applicable Creative Commons License

Simons, M., & Rosen, P. (2007). Interferometric synthetic aperture radar geodesy. In *Treatise on geophysics* (pp. 391–446). Elsevier. https://doi.org/10.1016/B978-044452748-6.00059-6

Smetacek, V., Scharek, R., Gordon, L. I., Eicken, H., Fahrbach, E., Rohardt, G., & Moore, S. (1992). Early spring phytoplankton blooms in ice platelet layers of the southern Weddell Sea, Antarctica. Deep Sea Research Part A. *Oceanographic Research Papers*, *39*(2), 153–168. https://doi.org/10.1016/0198-0149(92)90102-y

Smith, A. J., Nelson, T., Ratnarajah, L., Genovese, C., Westwood, K., Holmes, T. M., et al. (2022). Identifying potential sources of iron-binding ligands in coastal Antarctic environments and the wider Southern Ocean. *Frontiers in Marine Science*, *9*, 948772. https://doi.org/10.3389/fmars.2022.948772

Smith, I. J., Langhorne, P. J., Frew, R. D., Vennell, R., & Haskell, T. G. (2012). Sea ice growth rates near ice shelves. *Cold Regions Science and Technology*, *83–84*, 57–70. https://doi.org/10.1016/j.coldregions.2012.06.005

Smith, I. J., Langhorne, P. J., Haskell, T. G., Trodahl, H. J., Frew, R., & Vennell, R. (2001). Platelet ice and the land-fast sea ice of McMurdo Sound, Antarctica. *Annals of Glaciology*, *33*, 21–27. https://doi.org/10.3189/172756401781818365

Spindler, M., Dieckmann, G. S., & Lange, M. A. (1990). Seasonal and geographic variations in sea ice community structure of the Weddell Sea, Antarctica. In *Antarctic ecosystems* (pp. 129–135). Springer. https://doi.org/10.1007/978-3-642-84074-6{_}12

Squire, V. A. (2020). Ocean wave interactions with sea ice: A reappraisal. *Annual Review of Fluid Mechanics*, *52*(1), 37–60. https://doi.org/10.1146/annurev-fluid-010719-060301

Steiner, N., Azetsu-Scott, K., Hamilton, J., Hedges, K., Hu, X., Janjua, M. Y., et al. (2015). Observed trends and climate projections affecting marine ecosystems in the Canadian Arctic. *Environmental Reviews*, *23*(2), 191–239. https://doi.org/10.1139/er-2014-0066

Stevens, C. L., Sirguey, P., Leonard, G. H., & Haskell, T. G. (2013). Brief Communication: The 2013 Erebus Glacier Tongue calving event. *The Cryosphere*, *7*(5), 1333–1337. https://doi.org/10.5194/tc-7-1333-2013

Stoecker, D. K., Buck, K. R., & Putt, M. (1992). Changes in the sea-ice brine community during the spring-summer transition, McMurdo Sound, Antarctica. I. Photosynthetic protists. *Marine Ecology Progress Series*, *84*, 265–278. https://doi.org/10.3354/meps084265

Stoecker, D. K., Gustafson, D. E., Baier, C. T., & Black, M. M. D. (2000). Primary production in the upper sea ice. *Aquatic Microbial Ecology*, *21*, 275–287. https://doi.org/10.3354/ame021275

Stoecker, D. K., Gustafson, D. E., Black, M. M. D., & Baier, C. T. (1998). Population dynamics of microalgae in the upper land-fast sea ice at a snow-free location. *Journal of Phycology*, *34*(1), 60–69. https://doi.org/10.1046/j.1529-8817.1998.340060.x

Stopa, J. E., Sutherland, P., & Ardhuin, F. (2018). Strong and highly variable push of ocean waves on Southern Ocean sea ice. *Proceedings of the National Academy of Sciences*, *115*(23), 5861–5865. https://doi.org/10.1073/pnas.1802011115

Stössel, A., Stössel, M. M., & Kim, J.-T. (2007). High-resolution sea ice in long-term global ocean GCM integrations. *Ocean Modelling*, *16*(3–4), 206–223. https://doi.org/10.1016/j.ocemod.2006.10.001

Sturges, W. T., Cota, G. F., & Buckley, P. T. (1992). Bromoform emission from Arctic ice algae. *Nature*, *358*(6388), 660–662. https://doi.org/10.1038/358660a0

Sturm, M., & Massom, R. A. (2016). Snow in the sea ice system: Friend or foe? In *Sea ice* (pp. 65–109). John Wiley & Sons, Ltd. https://doi.org/10.1002/9781118778371.ch3

Swadling, K. M. (2001). Population structure of two Antarctic ice-associated copepods, *Drescheriella glacialis* and *Paralabidocera antarctica*, in winter sea ice. *Marine Biology*, *139*(3), 597–603. https://doi.org/10.1007/s002270100610

Swadling, K. M., Constable, A. J., Fraser, A. D., Massom, R. A., Borup, M. D., Ghigliotti, L., et al. (2023). Biological responses to change in Antarctic sea ice habitats. *Frontiers in Ecology and Evolution*, *10*, 1073823. https://doi.org/10.3389/fevo.2022.1073823

Swadling, K. M. (2014). Sea-ice metazoans. In C. De Broyer, P. Koubbi, A.V.D. D'acoz, B. Danis, B. David, S. Grant, et al. (Eds.), *Biogeographic atlas of the southern ocean* (pp. 321–325). Scientific Committee on Antarctic Research, Scott Polar Research Institute.

Swadling, K. M., Gibson, J. A. E., Ritz, D. A., & Nichols, P. D. (1997). Horizontal patchiness in sympagic organisms of the Antarctic fast ice. *Antarctic Science*, *9*(4), 399–406. https://doi.org/10.1017/s0954102097000515

Swadling, K. M., McKinnon, A. D., De'ath, G., & Gibson, J. A. E. (2004). Life cycle plasticity and differential growth and development in marine and lacustrine populations of an Antarctic copepod. *Limnology & Oceanography*, *49*(3), 644–655. https://doi.org/10.4319/lo.2004.49.3.0644

Swadling, K. M., Nichols, P. D., Gibson, J. A. E., & Ritz, D. A. (2000). Role of lipid in the life cycles of ice-dependent and ice-independent populations of the copepod Paralabidocera Antarctica. *Marine Ecology Progress Series*, *208*, 171–182. https://doi.org/10.3354/meps208171

Takahashi, E., Watanabe, K., & Satoh, H. (1986). Siliceous cysts from Kita-no-seto Strait, north of Syowa Station, Antarctica. *Memoirs of National Institute of Polar Research Special Issue*, *40*, 84–95.

Tamura, T., Ohshima, K. I., Enomoto, H., Tateyama, K., Muto, A., Ushio, S., & Massom, R. A. (2006). Estimation of thin sea-ice thickness from NOAA AVHRR data in a polynya off the Wilkes Land coast, East Antarctica. *Annals of Glaciology*, *44*, 269–274. https://doi.org/10.3189/172756406781811745

Tamura, T., Ohshima, K. I., Fraser, A. D., & Williams, G. D. (2016). Sea ice production variability in Antarctic coastal polynyas. *Journal of Geophysical Research: Oceans*, *121*(5), 2967–2979. https://doi.org/10.1002/2015JC011537

Tamura, T., Ohshima, K. I., Markus, T., Cavalieri, D. J., Nihashi, S., & Hirasawa, N. (2007). Estimation of thin ice thickness and detection of fast ice from SSM/I data in the Antarctic Ocean. *Journal of Atmospheric and Oceanic Technology*, *24*(10), 1757–1772. https://doi.org/10.1175/jtech2113.1

Tamura, T., Williams, G. D., Fraser, A. D., & Ohshima, K. I. (2012). Potential regime shift in decreased sea ice production after the Mertz Glacier calving. *Nature Communications*, *3*(1), 826. https://doi.org/10.1038/ncomms1820

Tang, S., Qin, D., Ren, J., Kang, J., & Li, Z. (2007). Structure, salinity and isotopic composition of multi-year landfast sea ice in Nella Fjord, Antarctica. *Cold Regions Science and Technology*, *49*(2), 170–177. https://doi.org/10.1016/j.coldregions.2007.03.005

Tanimura, A., Hoshiai, T., & Fukuchi, M. (1996). The life cycle strategy of the ice-associated copepod, Paralabidocera Antarctica (Calanoida, Copepoda), at Syowa Station, Antarctica. *Antarctic Science*, *8*(3), 257–266. https://doi.org/10.1017/s0954102096000363

Tanimura, A., Hoshiai, T., & Fukuchi, M. (2002). Change in habitat of the sympagic copepod Paralabidoceraantarctica from fast ice to seawater. *Polar Biology*, *25*(9), 667–671. https://doi.org/10.1007/s00300-002-0394-7

Teder, N. J., Bennetts, L. G., Reid, P. A., & Massom, R. A. (2022). Sea ice-free corridors for large swell to reach Antarctic ice shelves. *Environmental Research Letters*, *17*(4), 045026. https://doi.org/10.1088/1748-9326/ac5edd

Thomas, D. N., & Dieckmann, G. S. (2002). Biogeochemistry of Antarctic sea ice. *Oceanography and Marine Biology*, *40*, 143–170.

Thomas, D. N., Kennedy, H., Kattner, G., Gerdes, D., Gough, C., & Dieckmann, G. S. (2001). Biogeochemistry of platelet ice: Its influence on particle flux under fast ice in the Weddell Sea, Antarctica. *Polar Biology*, *24*(7), 486–496. https://doi.org/10.1007/s003000100243

Thompson, A. F., Stewart, A. L., Spence, P., & Heywood, K. J. (2018). The Antarctic slope current in a changing climate. *Reviews of Geophysics*, *56*(4), 741–770. https://doi.org/10.1029/2018RG000624

19449208, 2023, 2, Downloaded from https://agupubs.onlinelibrary.wiley.com/doi/10.1029/2022RG000770 by University of Adelaide Alumni, Wiley Online Library on [16/08/2023]. See the Terms and Conditions (https://onlinelibrary.wiley.com/terms-and-conditions) on Wiley Online Library for rules of use; OA articles are governed by the applicable Creative Commons License

Thompson, L., Smith, M., Thomson, J., Stammerjohn, S., Ackley, S., & Loose, B. (2020). Frazil ice growth and production during katabatic wind events in the Ross Sea, Antarctica. *The Cryosphere*, *14*(10), 3329–3347. https://doi.org/10.5194/tc-14-3329-2020

Tian-Kunze, X., Kaleschke, L., Maaß, N., Mäkynen, M., Serra, N., Drusch, M., & Krumpen, T. (2014). SMOS-derived thin sea ice thickness: Algorithm baseline, product specifications and initial verification. *The Cryosphere*, *8*(3), 997–1018. https://doi.org/10.5194/tc-8-997-2014

Timco, G., & O'Brien, S. (1994). Flexural strength equation for sea ice. *Cold Regions Science and Technology*, *22*(3), 285–298. https://doi.org/10.1016/0165-232X(94)90006-X

Timco, G., & Weeks, W. (2010). A review of the engineering properties of sea ice. *Cold Regions Science and Technology*, *60*(2), 107–129. https://doi.org/10.1016/j.coldregions.2009.10.003

Tison, J.-L., Lorrain, R. D., Bouzette, A., Dini, M., Bondesan, A., & Stiévenard, M. (1998). Linking landfast sea ice variability to marine ice accretion at Hells Gate Ice Shelf, Ross Sea. In M. O. Jeffries (Ed.), *Antarctic sea ice: Physical processes, interactions and variability* (Vol. 74, pp. 375–407). AGU. https://doi.org/10.1029/AR074p0375

Trenerry, L. J., McMinn, A., & Ryan, K. G. (2002). In situ oxygen microelectrode measurements of bottom-ice algal production in McMurdo Sound, Antarctica. *Polar Biology*, *25*(1), 72–80. https://doi.org/10.1007/s003000100314

Trevena, A. J., Jones, G. B., Wright, S. W., & van den Enden, R. L. (2000). Profiles of DMSP, algal pigments, nutrients and salinity in pack ice from eastern Antarctica. *Journal of Sea Research*, *43*(3–4), 265–273. https://doi.org/10.1016/S1385-1101(00)00012-5

Trevena, A. J., & Jones, G. B. (2006). Dimethylsulphide and dimethylsulphoniopropionate in Antarctic sea ice and their release during sea ice melting. *Marine Chemistry*, *98*(2–4), 210–222. https://doi.org/10.1016/j.marchem.2005.09.005

Trevena, A. J., & Jones, G. B. (2012). DMS flux over the Antarctic sea ice zone. *Marine Chemistry*, *134*, 47–58. https://doi.org/10.1016/j.marchem.2012.03.001

Trevena, A. J., Jones, G. B., Wright, S. W., & Enden, R. L. V. D. (2003). Profiles of dimethylsulphoniopropionate (DMSP), algal pigments, nutrients, and salinity in the fast ice of Prydz Bay, Antarctica. *Journal of Geophysical Research*, *108*(C5), 3145. https://doi.org/10.1029/2002jc001369

Trodahl, H. J., McGuinness, M. J., Langhorne, P. J., Collins, K., Pantoja, A. E., Smith, I. J., & Haskell, T. G. (2000). Heat transport in McMurdo Sound first-year fast ice. *Journal of Geophysical Research*, *105*(C5), 11347–11358. https://doi.org/10.1029/1999jc000003

Turner, J., Holmes, C., Caton Harrison, T., Phillips, T., Jena, B., Reeves-Francois, T., et al. (2022). Record low Antarctic sea ice cover in February 2022. *Geophysical Research Letters*, *49*(12), e2022GL098904. https://doi.org/10.1029/2022GL098904

Urabe, N., & Inoue, M. (1988). Mechanical properties of Antarctic sea ice. *Journal of Offshore Mechanics and Arctic Engineering*, *110*(4), 403–408. https://doi.org/10.1115/1.3257079

Ushio, S. (2006). Factors affecting fast-ice break-up frequency in Lützow-Holm Bay, Antarctica. *Annals of Glaciology*, *44*, 177–182. https://doi.org/10.3189/172756406781811835

Uto, S., Shimoda, H., & Ushio, S. (2006). Characteristics of Sea-ice thickness and snow-depth distributions of the summer landfast ice in Lützow-Holm Bay, East Antarctica. *Annals of Glaciology*, *44*, 281–287. https://doi.org/10.3189/172756406781811240

Vacchi, M., DeVries, A. L., Evans, C. W., Bottaro, M., Ghigliotti, L., Cutroneo, L., & Pisano, E. (2012). A nursery area for the Antarctic silverfish *Pleuragramma antarcticum* at Terra Nova Bay (Ross Sea): First estimate of distribution and abundance of eggs and larvae under the seasonal sea-ice. *Polar Biology*, *35*(10), 1573–1585. https://doi.org/10.1007/s00300-012-1199-y

Vacchi, M., La Mesa, M., Dalu, M., & MacDonald, J. (2004). Early life stages in the life cycle of Antarctic silverfish, *Pleuragramma antarcticum* in Terra Nova Bay, Ross Sea. *Antarctic Science*, *16*(3), 299–305. https://doi.org/10.1017/S0954102004002135

Vacchi, M., Pisano, E., & Ghigliotti, L. (Eds.). (2017). *The antarctic Silverfish: A keystone species in a changing ecosystem* (Vol. 3). Springer International Publishing. https://doi.org/10.1007/978-3-319-55893-6

van der Linden, F. C., Tison, J., Champenois, W., Moreau, S., Carnat, G., Kotovitch, M., et al. (2020). Sea ice CO_2 dynamics across seasons: Impact of processes at the interfaces. *Journal of Geophysical Research: Oceans*, *125*(6), e2019JC015807. https://doi.org/10.1029/2019jc015807

van der Merwe, P., Lannuzel, D., Bowie, A. R., & Meiners, K. M. (2011). High temporal resolution observations of spring fast ice melt and seawater iron enrichment in East Antarctica. *Journal of Geophysical Research*, *116*(G3), G03017. https://doi.org/10.1029/2010jg001628

van der Merwe, P., Lannuzel, D., Nichols, C. A. M., Meiners, K., Heil, P., Norman, L., et al. (2009). Biogeochemical observations during the winter–spring transition in East Antarctic sea ice: Evidence of iron and exopolysaccharide controls. *Marine Chemistry*, *115*(3–4), 163–175. https://doi.org/10.1016/j.marchem.2009.08.001

Van Achter, G., Fichefet, T., Goosse, H., & Moreno-Chamarro, E. (2022). Influence of fast ice on future ice shelf melting in the Totten Glacier area, East Antarctica. *The Cryosphere*, *16*(11), 4745–4761. https://doi.org/10.5194/tc-16-4745-2022

Van Achter, G., Fichefet, T., Goosse, H., Pelletier, C., Sterlin, J., Huot, P. V., et al. (2022). Modelling landfast sea ice and its influence on ocean–ice interactions in the area of the Totten Glacier, East Antarctica. *Ocean Modelling*, *169*, 101920. https://doi.org/10.1016/j.ocemod.2021.101920

Vancoppenolle, M., Goosse, H., de Montety, A., Fichefet, T., Tremblay, B., & Tison, J.-L. (2010). Modeling brine and nutrient dynamics in Antarctic sea ice: The case of dissolved silica. *Journal of Geophysical Research*, *115*(C2), C02005. https://doi.org/10.1029/2009JC005369

van Leeuwe, M. A., & Stefels, J. (2007). Photosynthetic responses in Phaeocystis Antarctica towards varying light and iron conditions. In M. A. van Leeuwe, J. Stefels, S. Belviso, C. Lancelot, P. G. Verity, & W. W. C. Gieskes (Eds.), *Phaeocystis, major link in the biogeochemical cycling of climate-relevant elements* (pp. 61–70). Springer Netherlands. https://doi.org/10.1007/978-1-4020-6214-8{_}6

Van Leeuwe, M. A., Tedesco, L., Arrigo, K. R., Assmy, P., Campbell, K., Meiners, K. M., et al. (2018). Microalgal community structure and primary production in Arctic and Antarctic sea ice: A synthesis. *Elementa*, *6*, 4. https://doi.org/10.1525/elementa.267

van Tiggelen, M., Smeets, P. C. J. P., Reijmer, C. H., Wouters, B., Steiner, J. F., Nieuwstraten, E. J., et al. (2021). Mapping the aerodynamic roughness of the Greenland Ice Sheet surface using ICESat-2: Evaluation over the K-transect. *The Cryosphere*, *15*(6), 2601–2621. https://doi.org/10.5194/tc-15-2601-2021

Veazey, A., Jeffries, M., & Morris, K. (1994). Small-scale variability of physical properties and structural characteristics of Antarctic fast ice. *Annals of Glaciology*, *20*, 61–66. https://doi.org/10.3189/1994AoG20-1-61-66

Velasquez, I., Nunn, B. L., Ibisanmi, E., Goodlett, D. R., Hunter, K. A., & Sander, S. G. (2011). Detection of hydroxamate siderophores in coastal and sub-Antarctic waters off the South Eastern Coast of New Zealand. *Marine Chemistry*, *126*(1), 97–107. https://doi.org/10.1016/j.marchem.2011.04.003

Verdugo, P., Alldredge, A. L., Azam, F., Kirchman, D. L., Passow, U., & Santschi, P. H. (2004). The oceanic gel phase: A bridge in the DOM–POM continuum. *Marine Chemistry*, *92*(1–4), 67–85. https://doi.org/10.1016/j.marchem.2004.06.017

Vignon, E., Roussel, M., Gorodetskaya, I. V., Genthon, C., & Berne, A. (2021). Present and future of rainfall in Antarctica. *Geophysical Research Letters*, *48*(8), e2020GL092281. https://doi.org/10.1029/2020GL092281

Vihma, T., Johansson, M. M., & Launiainen, J. (2009). Radiative and turbulent surface heat fluxes over sea ice in the western Weddell Sea in early summer. *Journal of Geophysical Research*, *114*(C4), C04019. https://doi.org/10.1029/2008jc004995

Voermans, J. J., Liu, Q., Marchenko, A., Rabault, J., Filchuk, K., Ryzhov, I., et al. (2021). Wave dispersion and dissipation in landfast ice: Comparison of observations against models. *The Cryosphere*, *15*(12), 5557–5575. https://doi.org/10.5194/tc-15-5557-2021

19449208, 2023, 2, Downloaded from https://agupubs.onlinelibrary.wiley.com/doi/10.1029/2022RG000770 by University of Adelaide Alumni, Wiley Online Library on [16/08/2023]. See the Terms and Conditions (https://onlinelibrary.wiley.com/terms-and-conditions) on Wiley Online Library for rules of use; OA articles are governed by the applicable Creative Commons License

Wang, C., Negrel, J., Gerland, S., Divine, D. V., Dodd, P., & Granskog, M. A. (2020). Thermodynamics of fast ice off the northeast coast of Greenland (79°N) over a full year (2012–2013). *Journal of Geophysical Research: Oceans*, *125*(7), e2019JC015823. https://doi.org/10.1029/2019JC015823

Wang, Q., Li, Z., Lu, P., Xu, Y., & Li, Z. (2022). Flexural and compressive strength of the landfast sea ice in the Prydz Bay, East Antarctic. *The Cryosphere*, *16*(5), 1941–1961. https://doi.org/10.5194/tc-16-1941-2022

Wang, X., Cheng, X., Hui, F., Cheng, C., Fok, H. S., & Liu, Y. (2014). Xuelong navigation in fast ice near the Zhongshan station, Antarctica. *Marine Technology Society Journal*, *48*(1), 84–91. https://doi.org/10.4031/mtsj.48.1.5

Wang, Z., Turner, J., Sun, B., Li, B., & Liu, C. (2014). Cyclone-induced rapid creation of extreme Antarctic sea ice conditions. *Scientific Reports*, *4*(1), 5317. https://doi.org/10.1038/srep05317

Weeks, W. (2010). *On sea ice*. University of Alaska Press.

Weiss, A. I., King, J. C., Lachlan-Cope, T. A., & Ladkin, R. S. (2012). Albedo of the ice covered Weddell and Bellingshausen seas. *The Cryosphere*, *6*(2), 479–491. https://doi.org/10.5194/tc-6-479-2012

Wille, J. D., Favier, V., Jourdain, N. C., Kittel, C., Turton, J. V., Agosta, C., et al. (2022). Intense atmospheric rivers can weaken ice shelf stability at the Antarctic Peninsula. *Communications Earth & Environment*, *3*(1), 90. https://doi.org/10.1038/s43247-022-00422-9

Williams, G. D., Aoki, S., Jacobs, S. S., Rintoul, S. R., Tamura, T., & Bindoff, N. L. (2010). Antarctic Bottom Water from the Adélie and George V Land coast, East Antarctica (140–149°E). *Journal of Geophysical Research*, *115*(C4), C04027. https://doi.org/10.1029/2009JC005812

Wing, S. R., Leichter, J. J., Wing, L. C., Stokes, D., Genovese, S. J., McMullin, R. M., & Shatova, O. A. (2018). Contribution of sea ice microbial production to Antarctic benthic communities is driven by sea ice dynamics and composition of functional guilds. *Global Change Biology*, *24*(8), 3642–3653. https://doi.org/10.1111/gcb.14291

Wongpan, P., Hughes, K. G., Langhorne, P. J., & Smith, I. J. (2018). Brine convection, temperature fluctuations, and permeability in winter Antarctic land-fast sea ice. *Journal of Geophysical Research: Oceans*, *123*(1), 216–230. https://doi.org/10.1002/2017jc012999

Wongpan, P., Meiners, K. M., Langhorne, P. J., Heil, P., Smith, I. J., Leonard, G. H., et al. (2018). Estimation of antarctic land-fast sea ice algal biomass and snow thickness from under-ice radiance spectra in two contrasting areas. *Journal of Geophysical Research: Oceans*, *123*(3), 1907–1923. https://doi.org/10.1002/2017jc013711

Wongpan, P., Vancoppenolle, M., Langhorne, P. J., Smith, I. J., Madec, G., Gough, A. J., et al. (2021). Sub-ice platelet layer physics: Insights from a mushy-layer sea ice model. *Journal of Geophysical Research: Oceans*, *126*(6), e2019JC015918. https://doi.org/10.1029/2019JC015918

Wright, C. S., & Priestley, R. E. (1922). *British (Terra Nova) antarctic expedition 1910–1913: Glaciology*. Harrison and Sons. Retrieved from https://books.google.com.au/books?id=txtLwAEACAAJ

Wuite, J. (2006). *Spatial and temporal dynamics of three East Antarctic outlet glaciers and their floating ice tongues. Ph.D. Thesis*. Ohio State University.

Yang, Q., Liu, J., Leppäranta, M., Sun, Q., Li, R., Zhang, L., et al. (2016). Albedo of coastal landfast sea ice in Prydz Bay, Antarctica: Observations and parameterization. *Advances in Atmospheric Sciences*, *33*(5), 535–543. https://doi.org/10.1007/s00376-015-5114-7

Yang, Q., Liu, J., Sun, Q., Lei, R., Zhang, L., & Meng, S. (2013). Surface albedo variation and its influencing factors over coastal fast ice around Zhongshan Station, Antarctica in austral spring of 2010. *Chinese Journal of Geophysics*, *56*(7), 2177–2184. https://doi.org/10.6038/cjg20130705

Yang, Y., Zhijun, L., Leppäranta, M., Cheng, B., Shi, L., & Lei, R. (2016). Modelling the thickness of landfast sea ice in Prydz Bay, East Antarctica. *Antarctic Science*, *28*(1), 59–70. https://doi.org/10.1017/s0954102015000449

Yu, L., Yang, Q., Zhou, M., Lenschow, D. H., Wang, X., Zhao, J., et al. (2017). The variability of surface radiation fluxes over landfast sea ice near Zhongshan station, east Antarctica during austral spring. *International Journal of Digital Earth*, *12*(8), 1–18. https://doi.org/10.1080/17538947.2017.1304458

Yu, Y., Stern, H., Fowler, C., Fetterer, F., & Maslanik, J. (2014). Interannual variability of Arctic landfast ice between 1976 and 2007. *Journal of Climate*, *27*(1), 227–243. https://doi.org/10.1175/JCLI-D-13-00178.1

Zatko, M. C., & Warren, S. G. (2015). East Antarctic sea ice in spring: Spectral albedo of snow, nilas, frost flowers and slush, and light-absorbing impurities in snow. *Annals of Glaciology*, *56*(69), 53–64. https://doi.org/10.3189/2015AoG69A574

Zemmelink, H. J., Dacey, J. W. H., Houghton, L., Hintsa, E. J., & Liss, P. S. (2008). Dimethylsulfide emissions over the multi-year ice of the western Weddell Sea. *Geophysical Research Letters*, *35*(6), L06603. https://doi.org/10.1029/2007GL031847

Zemmelink, H. J., Houghton, L., Dacey, J. W. H., Worby, A. P., & Liss, P. S. (2005). Emission of dimethylsulfide from Weddell Sea leads. *Geophysical Research Letters*, *32*(23), L23610. https://doi.org/10.1029/2005GL024242

Zemmelink, H. J., Houghton, L., Frew, N. M., & Dacey, J. W. H. (2006). Dimethylsulfide and major sulfur compounds in a stratified coastal salt pond. *Limnology & Oceanography*, *51*(1), 271–279. https://doi.org/10.4319/lo.2006.51.1.0271

Zhai, M., Zhao, T., Hui, F., Cheng, X., Liu, A., Yuan, J., et al. (2019). Anomalous extensive landfast sea ice in the vicinity of inexpressible Island, Antarctica. *Adv Polar Sci*, *30*(4), 406–411. https://doi.org/10.13679/j.advps.2018.0044

Zhao, J., Cheng, B., Vihma, T., Heil, P., Hui, F., Shu, Q., et al. (2020). Fast Ice Prediction System (FIPS) for land-fast sea ice at Prydz Bay, East Antarctica: An operational service for CHINARE. *Annals of Glaciology*, *61*(83), 271–283. https://doi.org/10.1017/aog.2020.46

Zhao, J., Cheng, B., Vihma, T., Lu, P., Han, H., & Shu, Q. (2022). The internal melting of landfast sea ice in Prydz Bay, East Antarctica. *Environmental Research Letters*, *17*(7), 074012. https://doi.org/10.1088/1748-9326/ac76d9

Zhao, J., Cheng, B., Vihma, T., Yang, Q., Hui, F., Zhao, B., et al. (2019). Observation and thermodynamic modeling of the influence of snow cover on landfast sea ice thickness in Prydz Bay, East Antarctica. *Cold Regions Science and Technology*, *168*, 102869. https://doi.org/10.1016/j.coldregions.2019.102869

Zhao, J., Cheng, B., Yang, Q., Vihma, T., & Zhang, L. (2017). Observations and modelling of first-year ice growth and simultaneous second-year ice ablation in the Prydz Bay, East Antarctica. *Annals of Glaciology*, *58*(75pt1), 59–67. https://doi.org/10.1017/aog.2017.33

Zhao, J., Yang, Q., Cheng, B., Leppäranta, M., Hui, F., Xie, S., et al. (2019). Spatial and temporal evolution of landfast ice near Zhongshan Station, East Antarctica, over an annual cycle in 2011/2012. *Acta Oceanologica Sinica*, *38*(5), 51–61. https://doi.org/10.1007/s13131-018-1339-5

Zhuang, J., Dussin, R., Jüling, A., & Rasp, S. (2020). Jiaweizhuang/xesmf: V0.3.0 adding esmf.locstream capabilities. *Zenodo*. https://doi.org/10.5281/ZENODO.3700105

19449208, 2023, 2, Downloaded from https://agupubs.onlinelibrary.wiley.com/doi/10.1029/2022RG000770 by University of Adelaide Alumni, Wiley Online Library on [16/08/2023]. See the Terms and Conditions (https://onlinelibrary.wiley.com/terms-and-conditions) on Wiley Online Library for rules of use; OA articles are governed by the applicable Creative Commons License